Title: Spectral variation of the WMAP 5-year degree scale anisotropy

Date: Jun 08, 2009 11:00 AM

URL: http://pirsa.org/09060008

Abstract: The black body nature of the first acoustic peak of the cosmic microwave background (CMB) was tested using foreground reduced WMAP 5-year data, by producing subtraction maps between pairs of cosmological bands, viz. the Q, V, and W bands, for masked sky areas that avoid the Galactic disk. The resulting maps revealed a non black body signal that has three main properties. (a) It fluctuates on the degree scale preferentially in one half of the sky, producing an extra {\it random} noise there of amplitude $\approx$ 3.5 μK, which is $\gtrsim$ 10 σ above the pixel noise even after beam size differences between bands are taken into account. (b) The signal exhibits large scale asymmetry in the form of a dipole ($\approx$ 3 μK) in the Q-V and Q-W maps; and (c) a quadrupole ($\approx$ 1.5 μK) in the Q-V, Q-W, and V-W maps. While (b) is due most probably to cross-band calibration residuals of the CMB COBE dipole, the amplitude of (c) is well beyond systematics of the kind, and in any case no {\it a priori} quadrupole in the CMB exists to leave behind such a residual. The axes of symmetry of (a), (b), and (c) are tilted towards the same general direction of the ecliptic plane. This strongly suggests that foreground emission contaminates the CMB signatures at the 4 -- 5 % level even on the angular scale of the first acoustic peak.

TESTING WHAT WMAP ACTUALLY OBSERVES

Richard Lieu
Physics Dept., U. Alabama Huntsville
Jonathan Mittaz
Climatology Center, U. Maryland
Bizhu Jiang
Physics Dept., Tsinghua U. Beijing

MAP map of
ne "edge of
the
observable
universe"
lotted as a
sphere

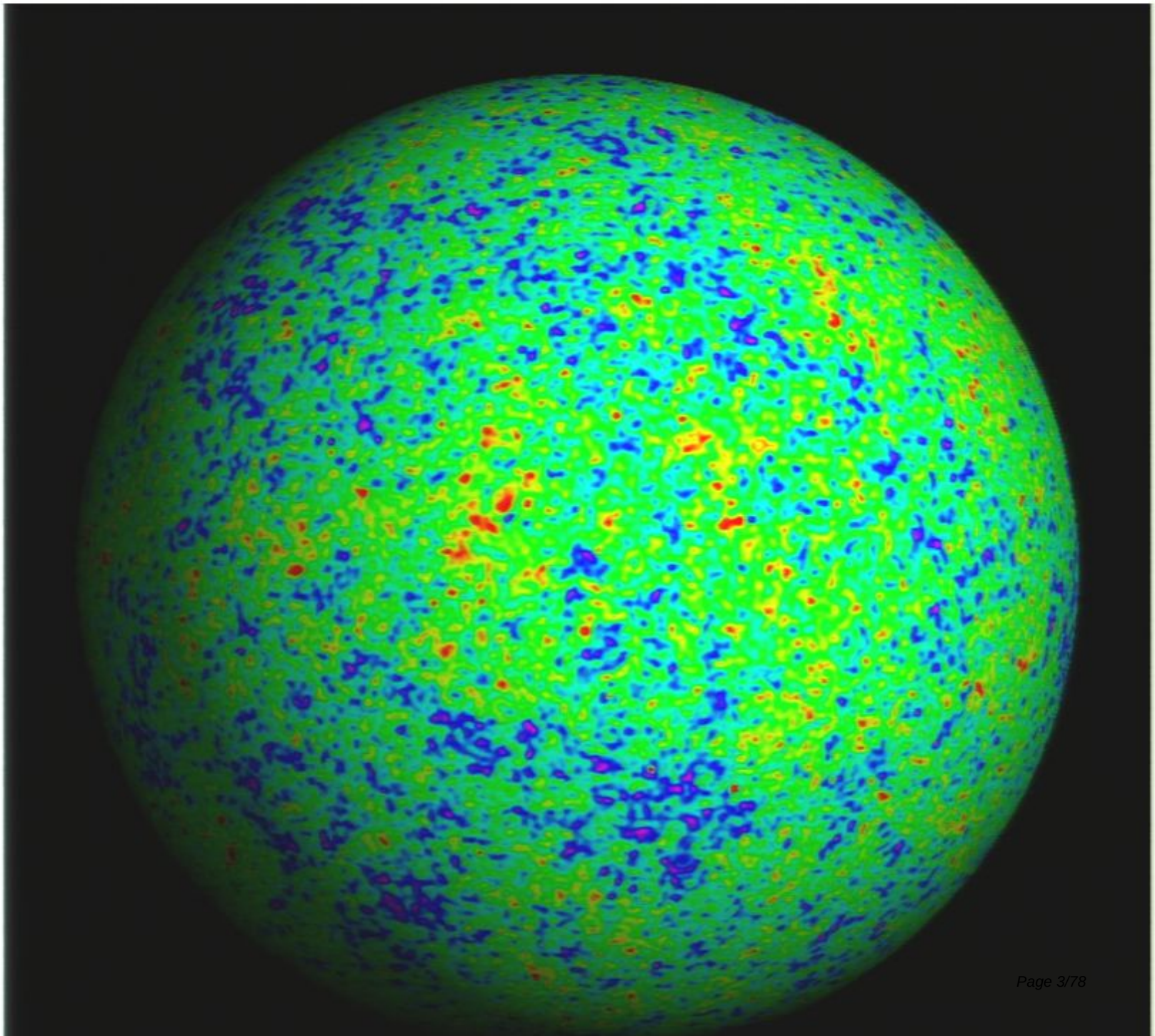

The first point detected on the CMB black body spectrum

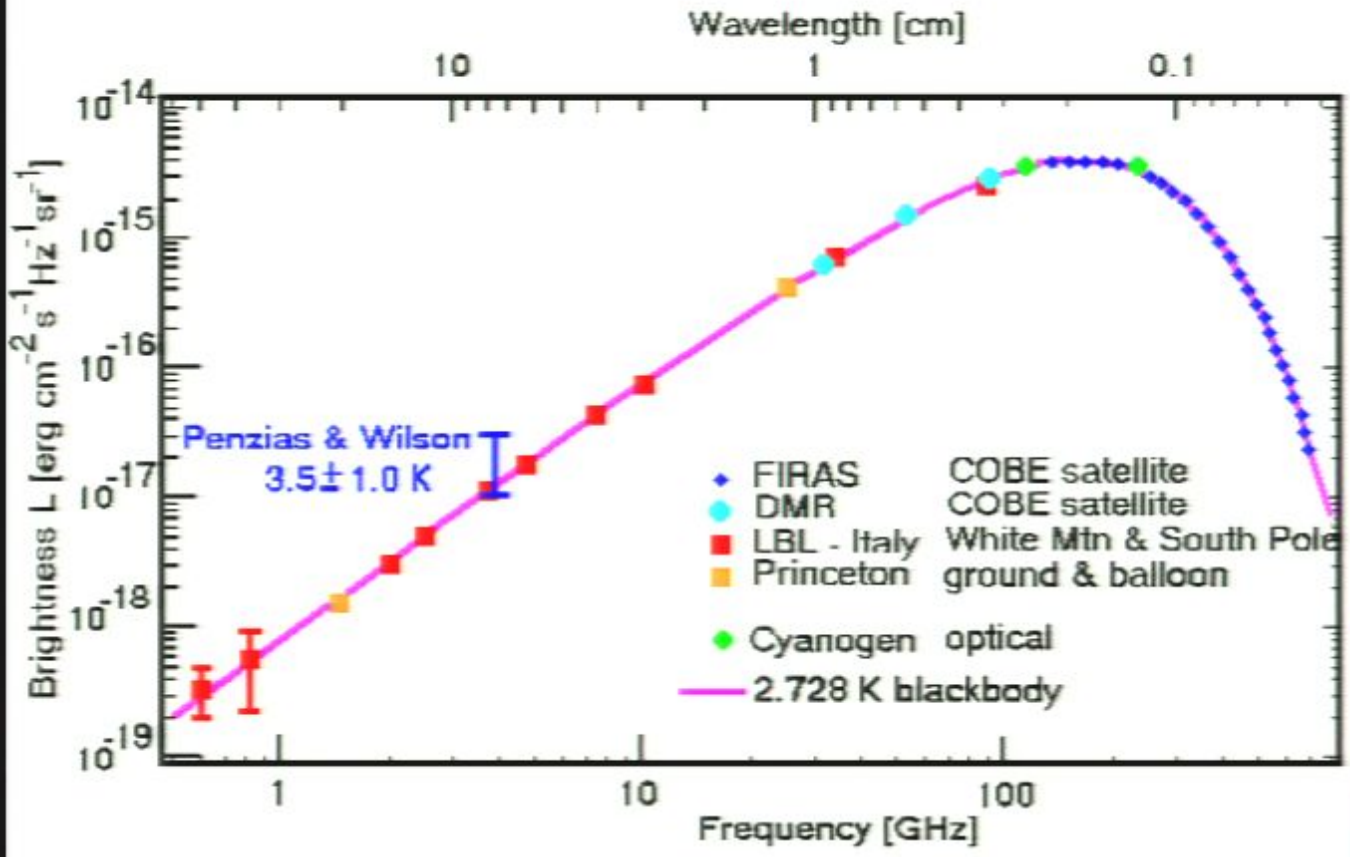

1965, 4080 MHz, Penzias & Wilson

1978 Nobel Prize in Physics

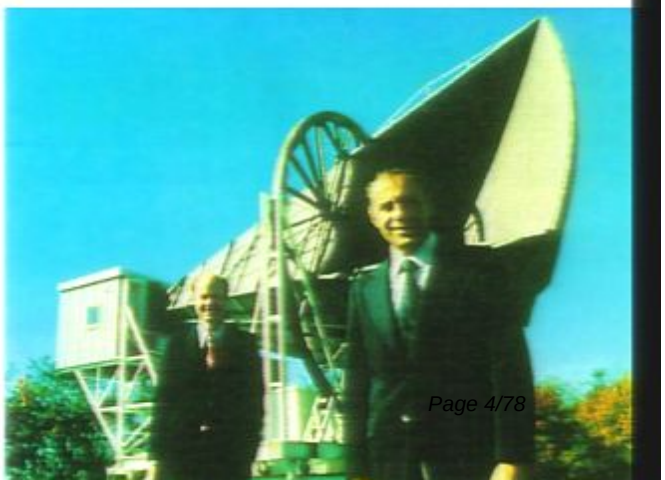

MAP map of
ne "edge of
the
observable
universe"
lotted as a
sphere

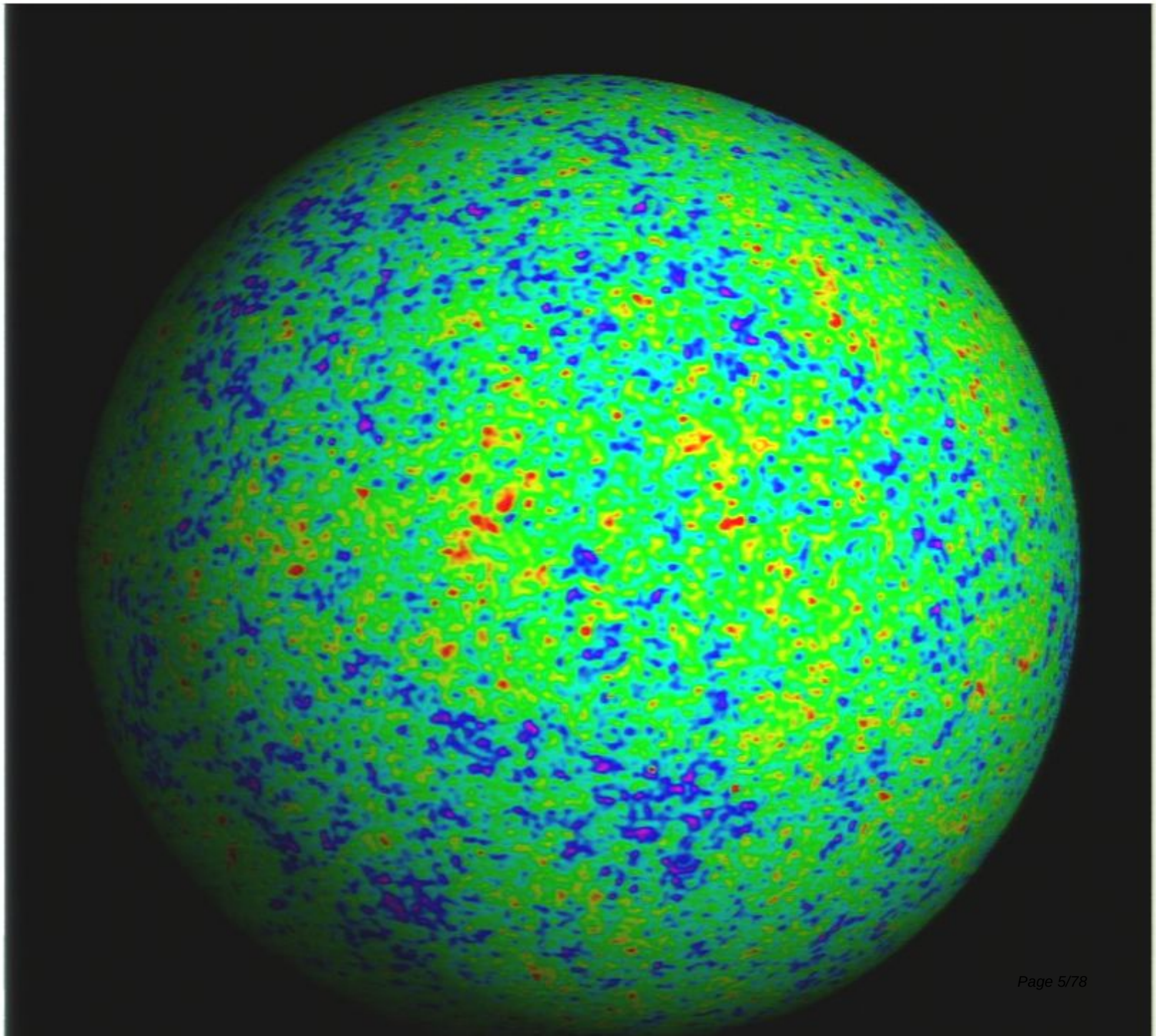

The first point detected on the CMB black body spectrum

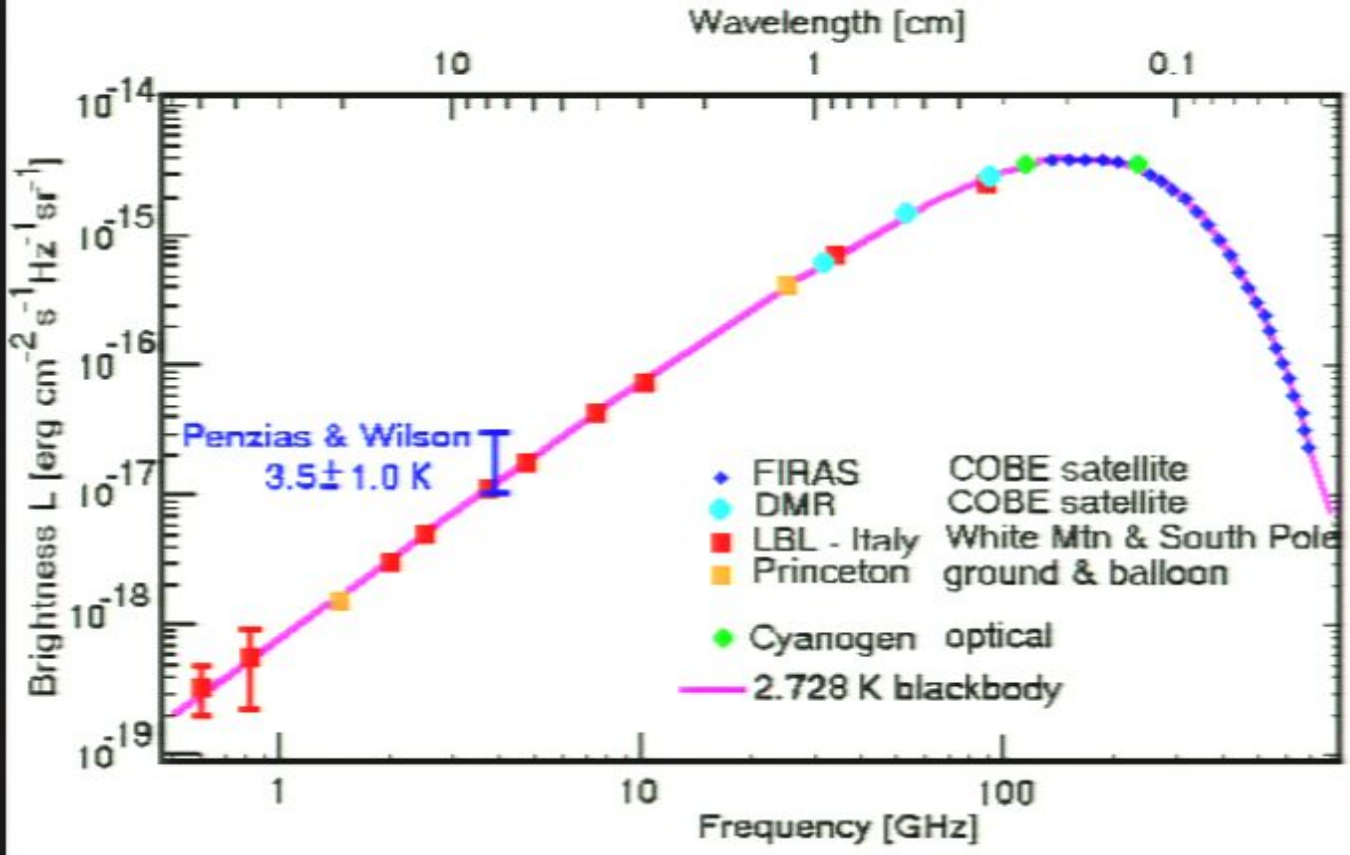

1965, 4080 MHz, Penzias & Wilson

1978 Nobel Prize in Physics

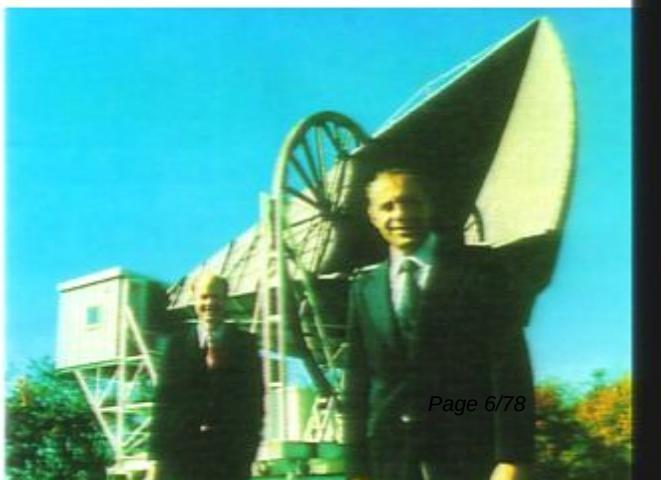

SOLAR SPECTRUM VS. BLACK BODY SPECTRUM

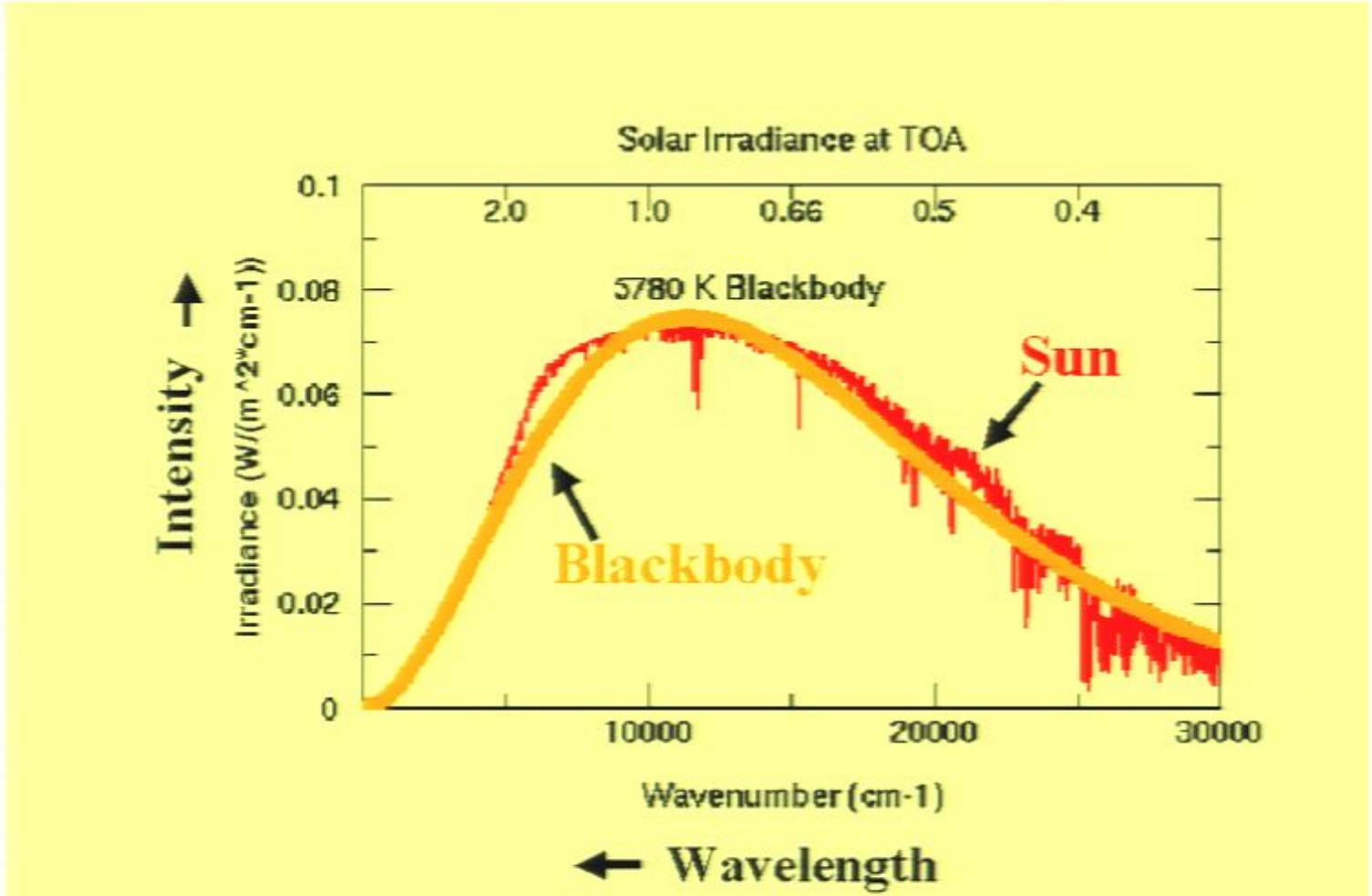

Peering into the origins of space and time

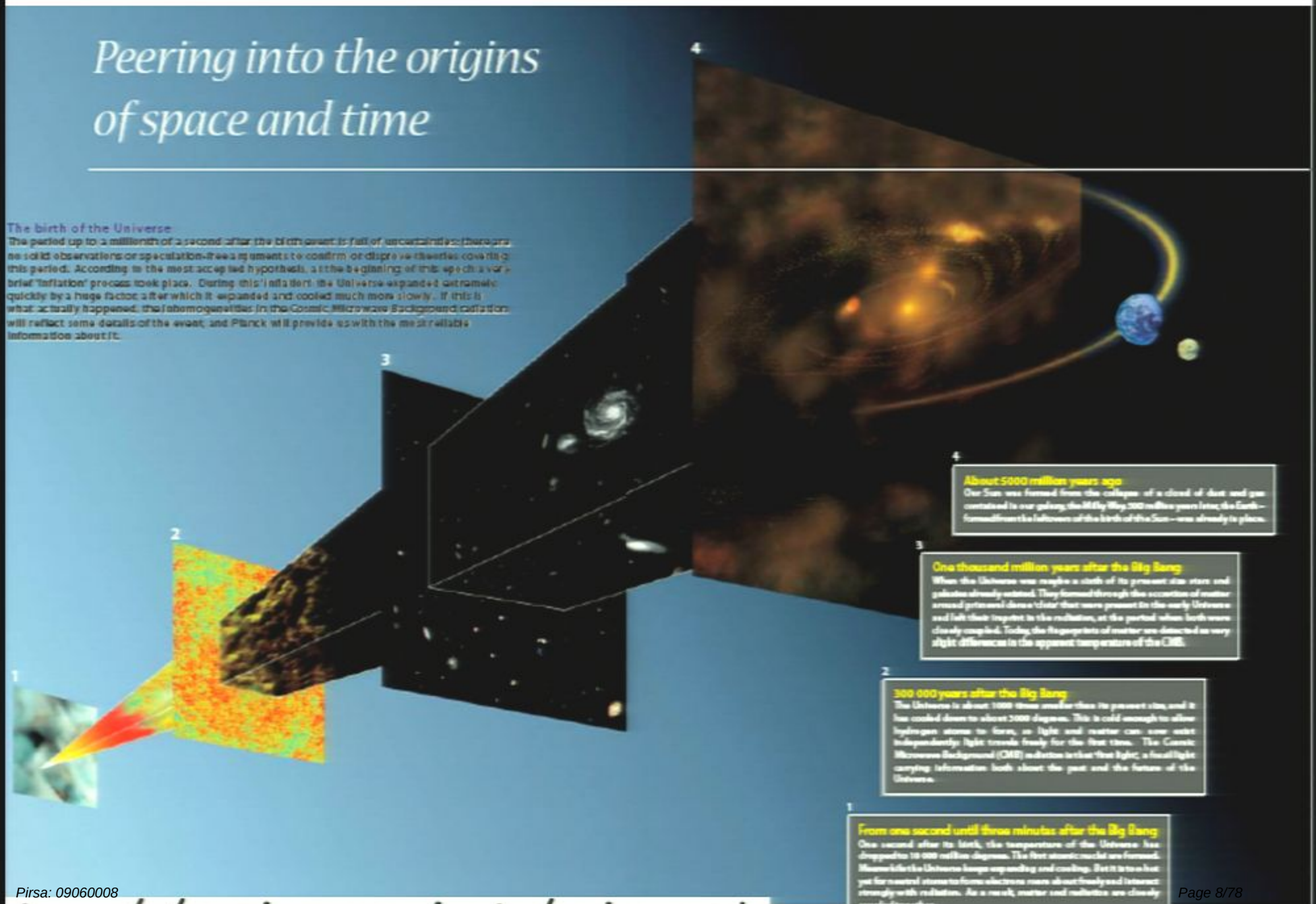

The birth of the Universe

The period up to a millionth of a second after the birth event is full of uncertainties: there are no solid observations or speculation-free arguments to confirm or disprove theories covering this period. According to the most accepted hypothesis, at the beginning of this epoch a very brief 'inflation' process took place. During this 'inflation' the Universe expanded extremely quickly by a huge factor, after which it expanded and cooled much more slowly. If this is what actually happened, the inhomogeneities in the Cosmic Microwave Background radiation will reflect some details of the event, and Planck will provide us with the most reliable information about it.

4

About 5000 million years ago

Our Sun was formed from the collapse of a cloud of dust and gas contained in our galaxy, the Milky Way. 500 million years later, the Earth – formed from the leftovers of the birth of the Sun – was already in place.

3

One thousand million years after the Big Bang

When the Universe was maybe a sixth of its present size stars and galaxies already existed. They formed through the accretion of matter around primordial dense 'clots' that were present in the early Universe and left their imprint in the radiation, at the period when both were closely coupled. Today, the fingerprints of matter are detected as very slight differences in the apparent temperature of the CMB.

2

300 000 years after the Big Bang

The Universe is about 1000 times smaller than its present size, and it has cooled down to about 3000 degrees. This is cold enough to allow hydrogen atoms to form, so light and matter can now exist independently: light travels freely for the first time. The Cosmic Microwave Background (CMB) radiation is that light, a fossil light carrying information both about the past and the future of the Universe.

1

From one second until three minutes after the Big Bang

One second after its birth, the temperature of the Universe has dropped to 10 000 million degrees. The first atomic nuclei are formed. Meanwhile the Universe keeps expanding and cooling. But it is a hot, yet for neutral atoms to form: electrons roam about freely and interact strongly with radiation. As a result, matter and radiation are closely coupled together.

http://sci.esa.int/planck

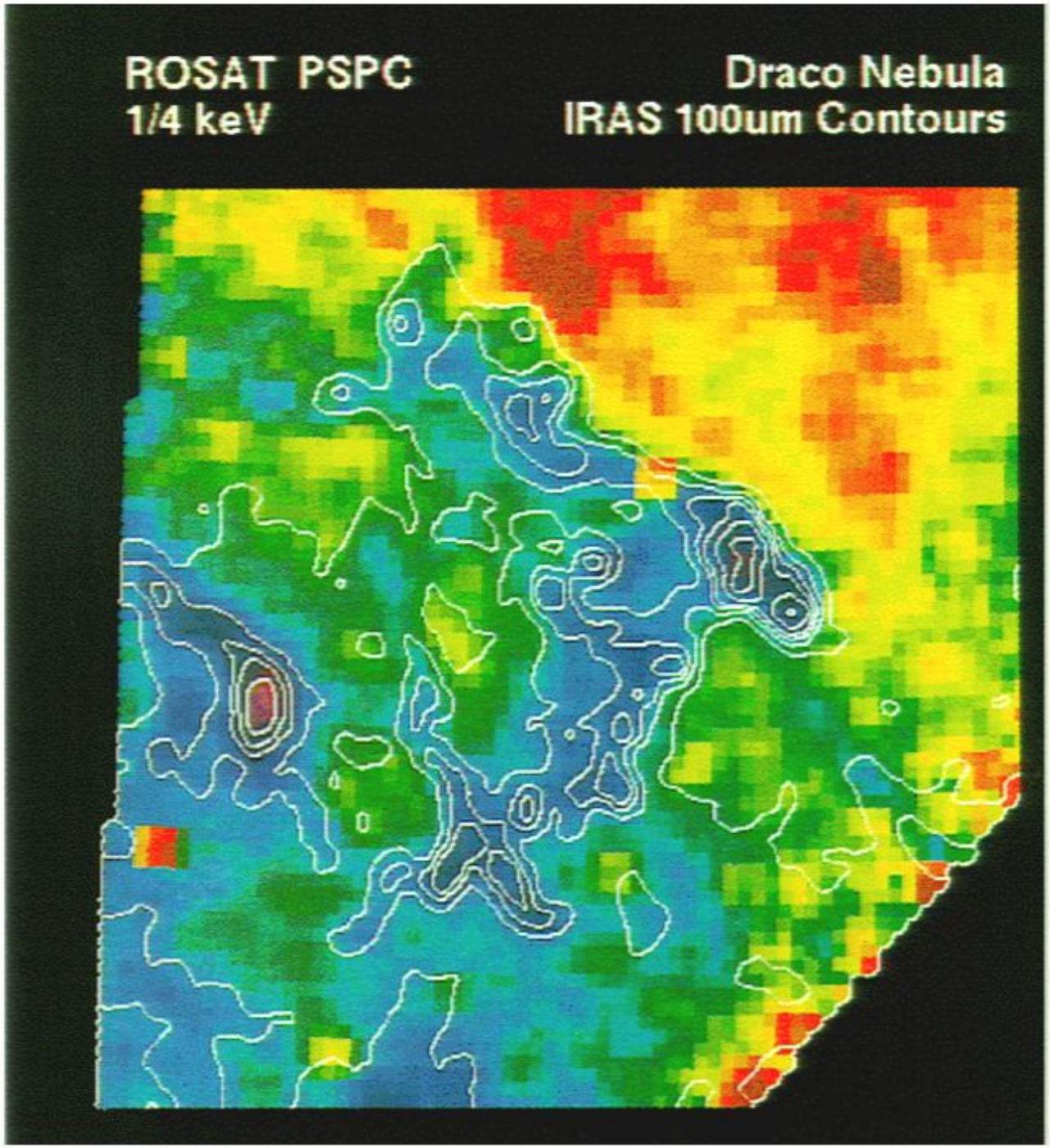
ROSAT PSPC
1/4 keV
Draco Nebula
IRAS 100um Contours

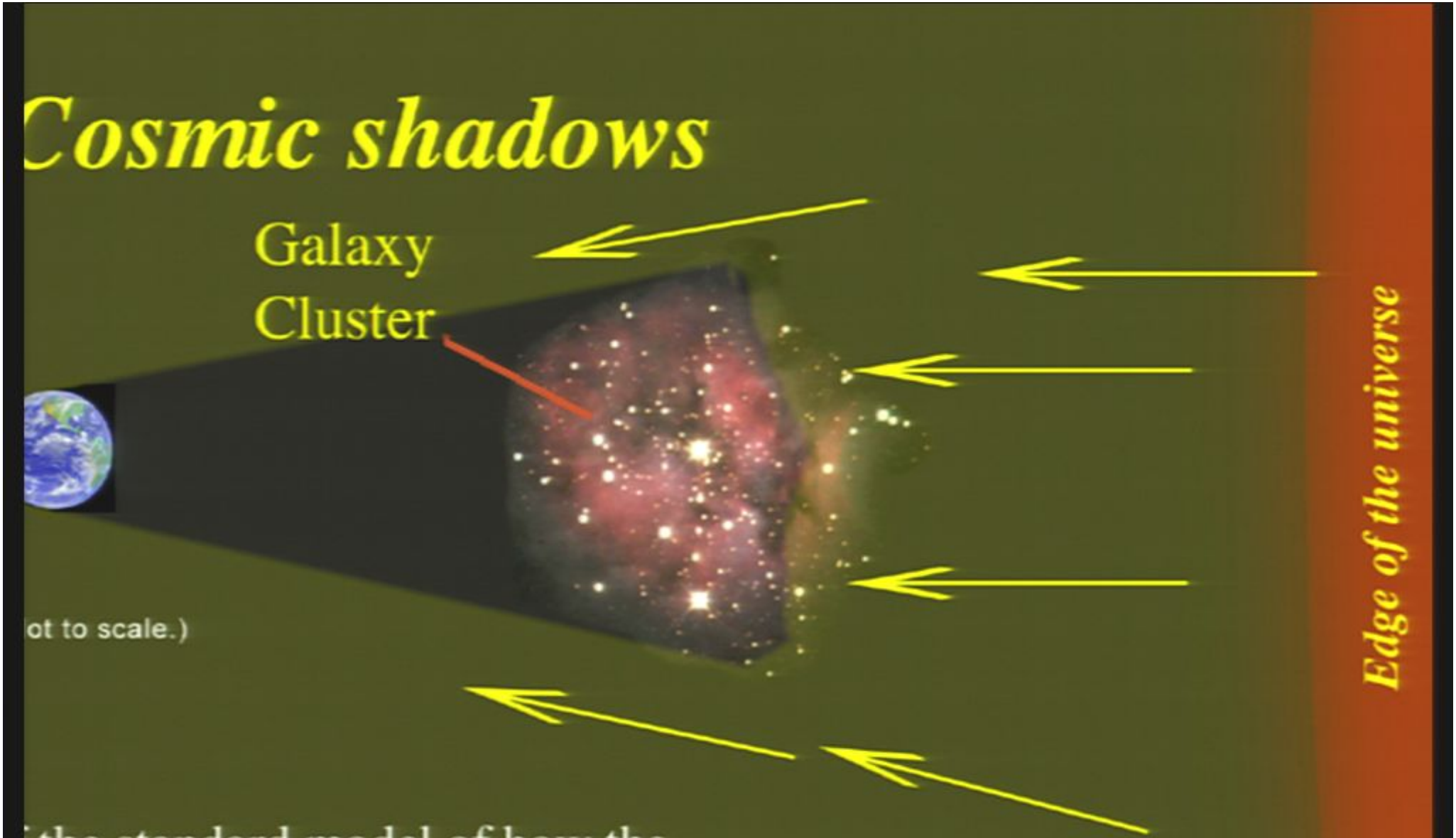

the standard model of how the
niverse was formed is correct, microwave radiation from
e edges of the universe would be blocked by clusters of
alaxies, causing ‘shadows’ in the microwave background.

Basics of the Sunyaev-Zeldovich Effect

$$\frac{\Delta T(\theta)}{T_{CMB}} = -\frac{kT}{m_e c^2}\sigma_T \int dl\, n_e \left[\frac{x(e^x+1)}{e^x-1} - 4\right]$$

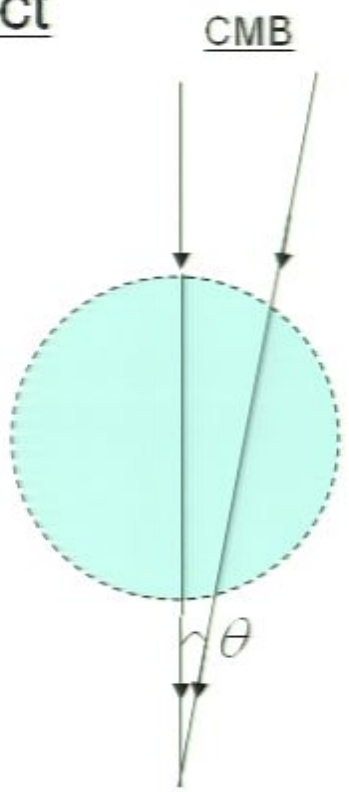

The electron density of the hot gas is obtained by fitting ROSAT X-ray surface brightness profiles $I_X(\theta)$ with the 2 parameter isothermal β-model ignoring the central cooling flow

$$n_e(r) = n_0\left[1+\left(\frac{r}{r_e}\right)^2\right]^{-3\beta/2} \Rightarrow I_X(\theta) \propto n_0^2\left[1+\left(\frac{\theta}{\theta_C}\right)^2\right]^{-3\beta+\frac{1}{2}}$$

The decrement in T_{CMB} is then given by

$$T_{SZ}(\theta) = \Delta T_{SZ}(0)\left[1+\left(\frac{\theta}{\theta_C}\right)^2\right]^{-\frac{3\beta}{2}+\frac{1}{2}} \quad \text{where } \Delta T_{SZ}(0) = -38.8\mu K\left(\frac{n}{10^{-3}cm^{-3}}\right)\left(\frac{kT}{keV}\right)\left(\frac{r_C}{Mpc}\right)\left[\frac{j(x)}{-2}\right]\frac{\Gamma\left(\frac{3\beta}{2}-\frac{1}{2}\right)}{\Gamma\left(\frac{3\beta}{2}\right)}$$

$$\text{with } j(x) = \frac{x(e^x+1)}{e^x-1} - 4$$

Name	Galactic (2000) Long.	Lat.	Redshift	kT (keV)	n_0 $\times 10^{-3}$ cm^{-3}	β	R_{core} (arcmin)	$\Delta T0_Q$ mK	$\Delta T0_V$ mK	$\Delta T0_W$ mK
Abell 85	115.053	-72.064	0.055	7.0	$14.64^{+0.33}_{-0.34}$	$0.58^{+0.03}_{-0.03}$	$1.7^{+0.6}_{-0.8}$	$-0.92^{+0.43}_{-0.32}$	$-0.87^{+0.40}_{-0.30}$	$-0.75^{+0.35}_{-0.26}$
Abell 133	149.761	-84.233	0.057	5.0	$2.98^{+0.13}_{-0.11}$	$0.72^{+0.09}_{-0.07}$	$3.4^{+0.8}_{-0.8}$	$-0.19^{+0.05}_{-0.06}$	$-0.18^{+0.05}_{-0.05}$	$-0.16^{+0.04}_{-0.05}$
Abell 665	149.735	34.673	0.1816	7.0	$3.19^{+0.19}_{-0.22}$	$0.64^{+0.10}_{-0.10}$	$1.3^{+0.1}_{-0.1}$	$-0.38^{+0.08}_{-0.14}$	$-0.36^{+0.07}_{-0.13}$	$-0.31^{+0.06}_{-0.11}$
Abell 1068	179.100	60.130	0.139	5.0	$7.80^{+0.46}_{-0.42}$	$0.90^{+0.17}_{-0.13}$	$1.6^{+0.5}_{-0.5}$	$-0.41^{+0.15}_{-0.15}$	$-0.39^{+0.14}_{-0.14}$	$-0.33^{+0.12}_{-0.12}$
Abell 1302	134.668	48.904	0.116	4.8	$2.88^{+0.19}_{-0.15}$	$0.64^{+0.12}_{-0.08}$	$1.4^{+0.4}_{-0.3}$	$-0.17^{+0.05}_{-0.07}$	$-0.16^{+0.05}_{-0.06}$	$-0.14^{+0.04}_{-0.05}$
Abell 1314	151.828	63.567	0.0341	5.0	$1.00^{+0.27}_{-0.26}$	$0.35^{+0.21}_{-0.10}$	$2.6^{+3.2}_{-2.4}$	$-0.44^{+0.58}_{nan}$	$-0.42^{+0.55}_{nan}$	$-0.36^{+0.47}_{nan}$
Abell 1361	153.292	66.581	0.1167	4.0	$2.34^{+nan}_{-0.61}$	$1.79^{+19.04}_{-1.09}$	$5.2^{+43.8}_{-4.2}$	$-0.16^{+0.18}_{nan}$	$-0.15^{+0.17}_{nan}$	$-0.13^{+0.15}_{nan}$
Abell 1367	234.799	73.030	0.0276	3.5	$1.63^{+0.03}_{-0.03}$	$0.52^{+0.02}_{-0.02}$	$8.6^{+0.5}_{-0.6}$	$-0.16^{+0.02}_{-0.02}$	$-0.15^{+0.02}_{-0.02}$	$-0.13^{+0.01}_{-0.02}$
Abell 1413	226.182	76.787	0.143	6.0	$13.65^{+0.77}_{-0.92}$	$0.68^{+0.11}_{-0.11}$	$1.1^{+0.1}_{-0.1}$	$-0.90^{+0.17}_{-0.29}$	$-0.85^{+0.16}_{-0.27}$	$-0.73^{+0.14}_{-0.24}$
Abell 1689	313.387	61.097	0.181	7.0	$13.79^{+0.75}_{-0.89}$	$0.75^{+0.12}_{-0.12}$	$1.0^{+0.0}_{-0.0}$	$-1.00^{+0.17}_{-0.27}$	$-0.94^{+0.16}_{-0.26}$	$-0.81^{+0.14}_{-0.22}$
Abell 1795	33.788	77.155	0.061	7.0	$3.05^{+0.04}_{-0.06}$	$0.99^{+0.04}_{-0.06}$	$5.2^{+0.3}_{-0.4}$	$-0.33^{+0.03}_{-0.03}$	$-0.32^{+0.03}_{-0.03}$	$-0.27^{+0.02}_{-0.02}$
Abell 1914	67.196	67.453	0.171	9.0	$11.21^{+0.19}_{-0.17}$	$0.85^{+0.04}_{-0.04}$	$1.4^{+0.1}_{-0.1}$	$-1.23^{+0.10}_{-0.10}$	$-1.17^{+0.09}_{-0.10}$	$-1.01^{+0.08}_{-0.09}$
Abell 1991	22.762	60.497	0.0586	4.0	$3.14^{+0.56}_{-0.34}$	$0.82^{+0.54}_{-0.22}$	$2.8^{+2.8}_{-8.4}$	$-0.12^{+0.36}_{-0.13}$	$-0.11^{+0.34}_{-0.13}$	$-0.10^{+0.30}_{-0.11}$
Abell 2029	6.505	50.547	0.0767	9.0	$12.07^{+0.19}_{-0.82}$	$0.67^{+0.03}_{-0.11}$	$1.9^{+0.3}_{-0.3}$	$-1.13^{+0.20}_{-0.40}$	$-1.07^{+0.19}_{-0.37}$	$-0.92^{+0.16}_{-0.32}$
Abell 2142	44.213	48.701	0.09	9.0	$7.17^{+0.41}_{-0.49}$	$0.67^{+0.11}_{-0.11}$	$2.3^{+0.2}_{-0.2}$	$-0.97^{+0.20}_{-0.33}$	$-0.92^{+0.19}_{-0.31}$	$-0.79^{+0.16}_{-0.27}$
Abell 2199	62.897	43.697	0.0302	4.5	$7.35^{+0.11}_{-0.19}$	$0.64^{+0.02}_{-0.04}$	$2.8^{+0.7}_{-1.8}$	$-0.23^{+0.15}_{-0.06}$	$-0.22^{+0.14}_{-0.06}$	$-0.19^{+0.12}_{-0.05}$
Abell 2218	97.745	38.124	0.171	6.0	$2.73^{+0.04}_{-0.18}$	$0.72^{+0.03}_{-0.12}$	$1.5^{+0.1}_{-0.1}$	$-0.25^{+0.02}_{-0.07}$	$-0.24^{+0.02}_{-0.07}$	$-0.20^{+0.02}_{-0.06}$
Abell 2219	72.597	41.472	0.228	7.0	$5.32^{+0.12}_{-0.11}$	$0.78^{+0.05}_{-0.04}$	$1.8^{+0.2}_{-0.1}$	$-0.77^{+0.08}_{-0.09}$	$-0.72^{+0.08}_{-0.08}$	$-0.63^{+0.07}_{-0.07}$
Abell 2241	54.784	36.643	0.0635	3.1	$10.94^{+0.45}_{-0.41}$	$0.74^{+0.09}_{-0.07}$	$1.0^{+0.2}_{-0.2}$	$-0.14^{+0.03}_{-0.03}$	$-0.13^{+0.03}_{-0.03}$	$-0.12^{+0.02}_{-0.03}$
Abell 2255	93.975	34.948	0.08	7.0	$2.25^{+0.05}_{-0.04}$	$0.76^{+0.04}_{-0.04}$	$4.6^{+0.4}_{-0.3}$	$-0.36^{+0.03}_{-0.04}$	$-0.34^{+0.03}_{-0.04}$	$-0.29^{+0.03}_{-0.03}$
Abell 2256	111.096	31.738	0.06	7.0	$3.70^{+0.19}_{-0.23}$	$0.85^{+0.14}_{-0.14}$	$5.5^{+0.9}_{-0.9}$	$-0.48^{+0.10}_{-0.13}$	$-0.45^{+0.10}_{-0.13}$	$-0.39^{+0.09}_{-0.11}$
Abell 2597	65.363	-64.836	0.085	4.0	$14.58^{+0.52}_{-0.68}$	$0.71^{+0.07}_{-0.08}$	$1.4^{+0.6}_{-3.3}$	$-0.45^{+1.10}_{-0.21}$	$-0.43^{+1.04}_{-0.20}$	$-0.37^{+0.90}_{-0.17}$
Abell 2670	81.318	-68.516	0.076	3.0	$3.88^{+0.16}_{-0.16}$	$0.64^{+0.07}_{-0.06}$	$1.9^{+0.7}_{-0.8}$	$-0.13^{+0.06}_{-0.05}$	$-0.12^{+0.05}_{-0.05}$	$-0.11^{+0.05}_{-0.04}$
Abell 2717	349.076	-76.390	0.049	3.0	$8.89^{+0.20}_{-0.18}$	$0.64^{+0.04}_{-0.03}$	$1.5^{+0.2}_{-0.1}$	$-0.16^{+0.02}_{-0.02}$	$-0.15^{+0.02}_{-0.02}$	$-0.13^{+0.02}_{-0.02}$
Abell 2744	8.898	-81.241	0.308	11.0	$3.13^{+0.23}_{-0.17}$	$1.60^{+0.44}_{-0.27}$	$3.3^{+0.6}_{-0.4}$	$-0.87^{+0.19}_{-0.22}$	$-0.82^{+0.18}_{-0.21}$	$-0.71^{+0.15}_{-0.18}$
Abell 3301	242.415	-37.409	0.054	7.0	$4.20^{+0.19}_{-0.18}$	$0.49^{+0.05}_{-0.04}$	$1.8^{+0.5}_{-0.4}$	$-0.38^{+0.11}_{-0.14}$	$-0.36^{+0.10}_{-0.14}$	$-0.31^{+0.09}_{-0.12}$
Abell 3558	311.978	30.738	0.048	5.0	$2.58^{+0.04}_{-0.04}$	$0.78^{+0.04}_{-0.03}$	$5.9^{+0.4}_{-0.4}$	$-0.23^{+0.02}_{-0.02}$	$-0.22^{+0.02}_{-0.02}$	$-0.19^{+0.02}_{-0.02}$
Abell 3560	312.578	28.890	0.04	2.0	$4.62^{+0.22}_{-0.20}$	$0.49^{+0.05}_{-0.04}$	$2.6^{+0.6}_{-0.5}$	$-0.12^{+0.03}_{-0.05}$	$-0.12^{+0.03}_{-0.04}$	$-0.10^{+0.03}_{-0.04}$
Abell 3562	313.308	30.349	0.04	4.5	$6.85^{+0.48}_{-0.60}$	$0.47^{+0.08}_{-0.08}$	$1.3^{+0.1}_{-0.1}$	$-0.25^{+0.08}_{-0.24}$	$-0.23^{+0.07}_{-0.23}$	$-0.20^{+0.06}_{-0.20}$
Abell 3571	316.317	28.545	0.04	7.0	$11.92^{+0.29}_{-0.29}$	$0.65^{+0.04}_{-0.04}$	$3.6^{+0.7}_{-0.8}$	$-0.97^{+0.22}_{-0.21}$	$-0.91^{+0.21}_{-0.20}$	$-0.79^{+0.18}_{-0.17}$
Abell 4059	356.833	-76.061	0.046	4.5	$4.95^{+0.42}_{-0.35}$	$1.00^{+0.29}_{-0.19}$	$6.1^{+2.1}_{-1.8}$	$-0.31^{+0.11}_{-0.13}$	$-0.29^{+0.10}_{-0.12}$	$-0.25^{+0.09}_{-0.11}$
Coma	58.080	87.958	0.023	8.2	$4.38^{+0.24}_{-0.29}$	$0.71^{+0.11}_{-0.11}$	$9.8^{+1.6}_{-1.6}$	$-0.59^{+0.14}_{-0.20}$	$-0.56^{+0.13}_{-0.18}$	$-0.48^{+0.11}_{-0.16}$

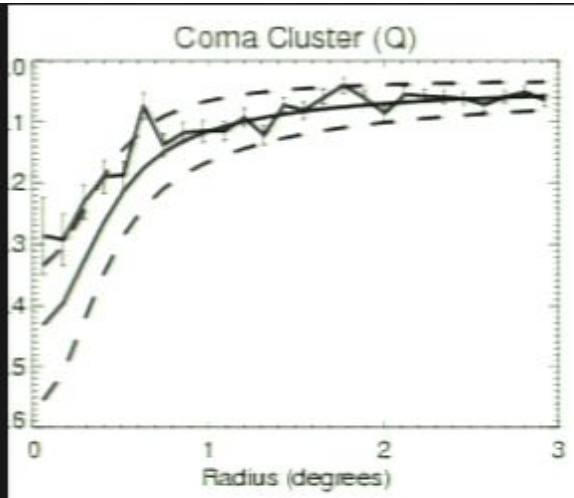
Coma Cluster (Q)
Radius (degrees)

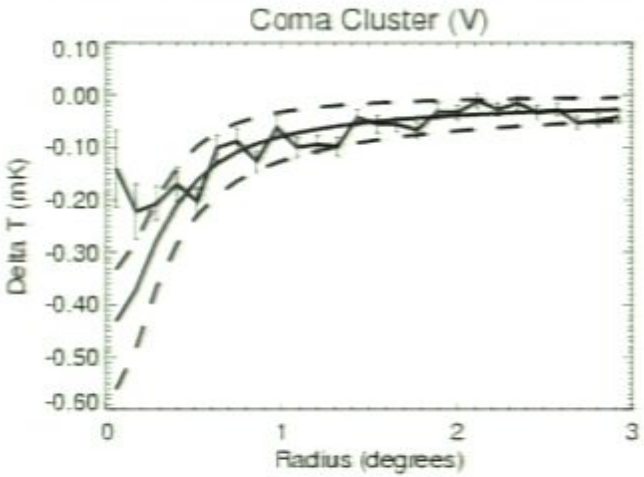
Coma Cluster (V)
Delta T (mK)
0.10
0.00
-0.10
-0.20
-0.30
-0.40
-0.50
-0.60
0
1
2
3
Radius (degrees)

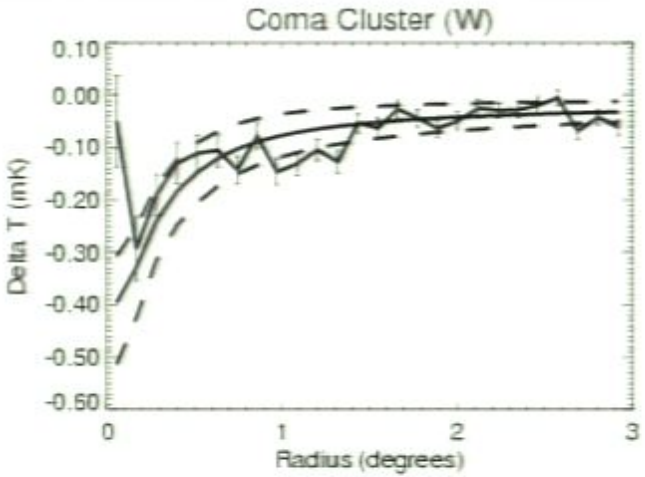
Coma Cluster (W)
Delta T (mK)
0.10
0.00
-0.10
-0.20
-0.30
-0.40
-0.50
-0.60
0
1
2
3
Radius (degrees)

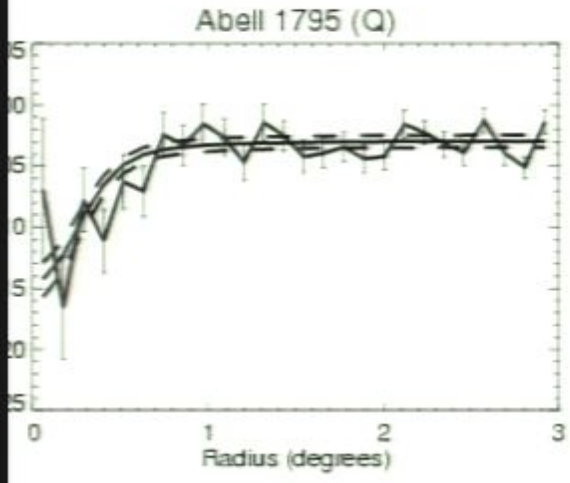
Abell 1795 (Q)
Radius (degrees)

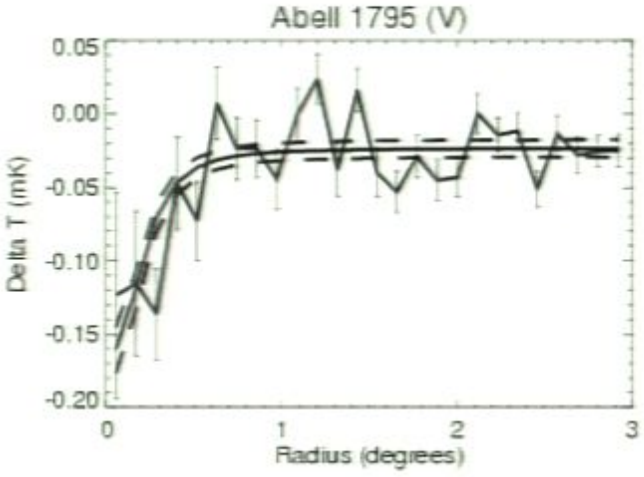
Abell 1795 (V)
Delta T (mK)
0.05
0.00
-0.05
-0.10
-0.15
-0.20
0
1
2
3
Radius (degrees)

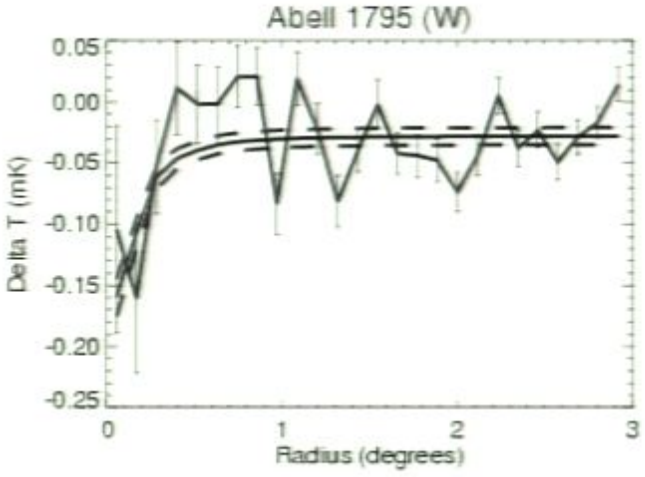
Abell 1795 (W)
Delta T (mK)
0.05
0.00
-0.05
-0.10
-0.15
-0.20
-0.25
0
1
2
3
Radius (degrees)

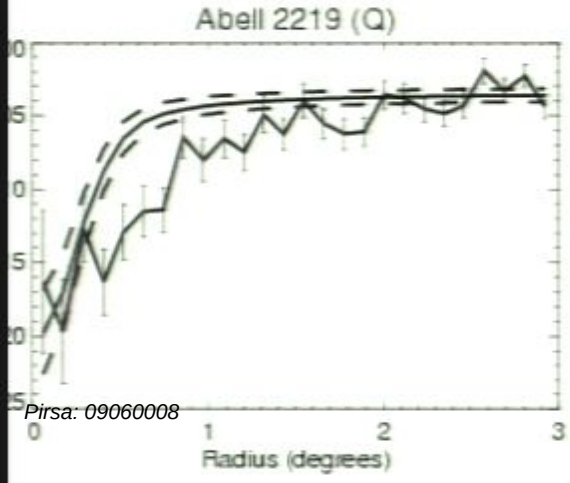
Abell 2219 (Q)
Radius (degrees)

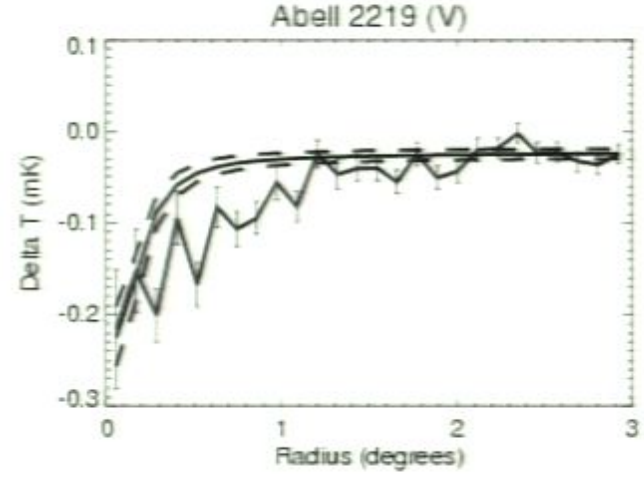
Abell 2219 (V)
Delta T (mK)
0.1
0.0
-0.1
-0.2
-0.3
0
1
2
3
Radius (degrees)

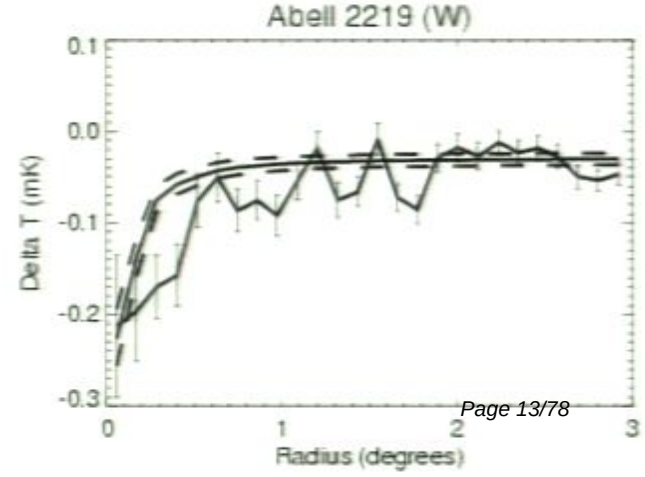
Abell 2219 (W)
Delta T (mK)
0.1
0.0
-0.1
-0.2
-0.3
0
1
2
3
Radius (degrees)

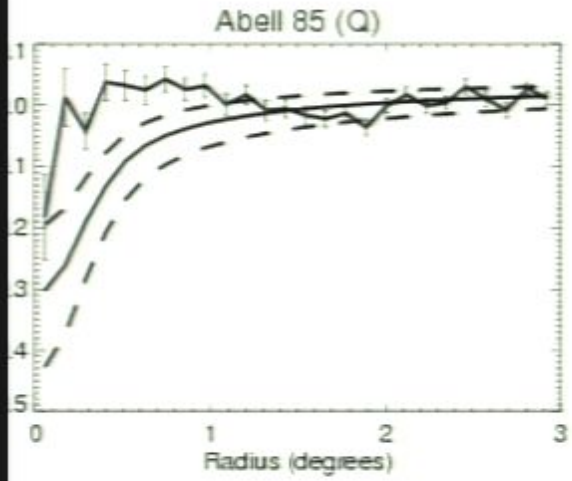
Abell 85 (Q)
Radius (degrees)

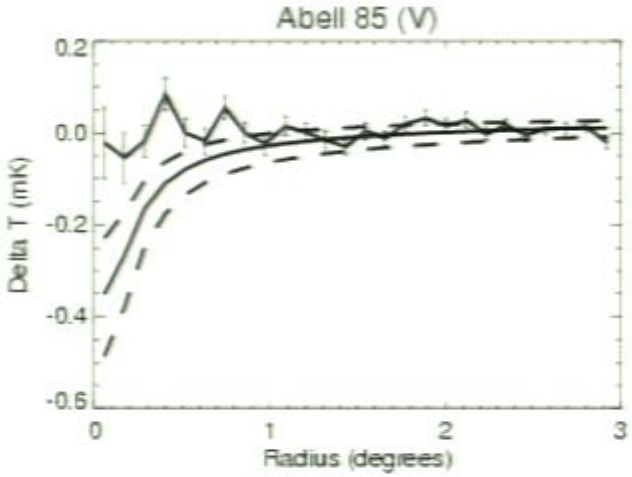
Abell 85 (V)
Delta T (mK)
Radius (degrees)

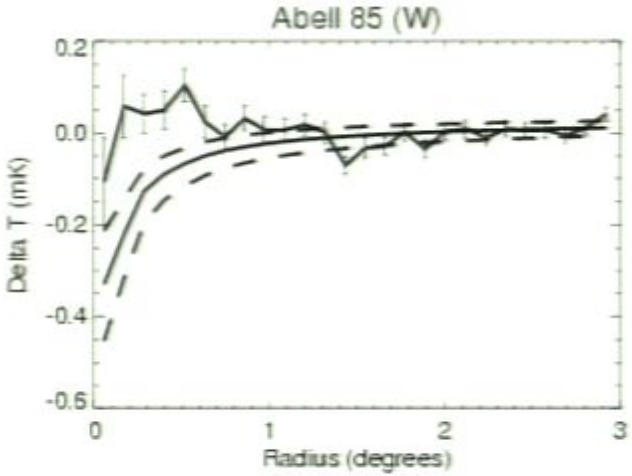
Abell 85 (W)
Delta T (mK)
Radius (degrees)

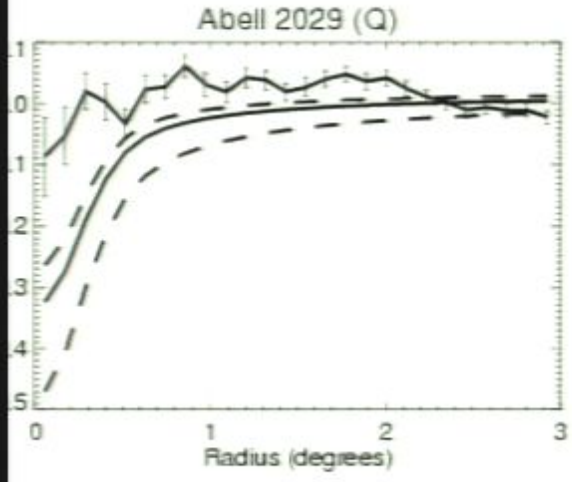
Abell 2029 (Q)
Radius (degrees)

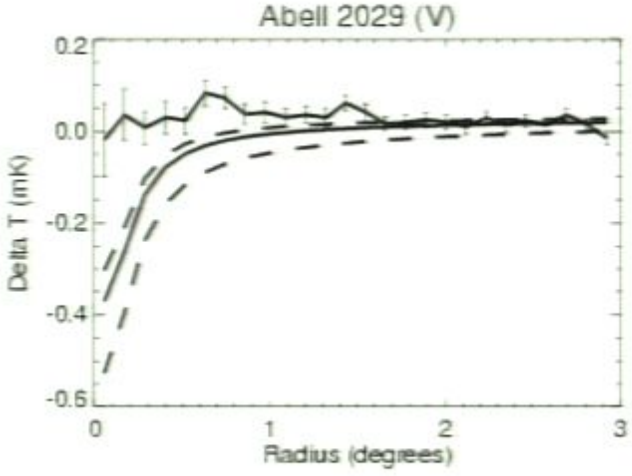
Abell 2029 (V)
Delta T (mK)
Radius (degrees)

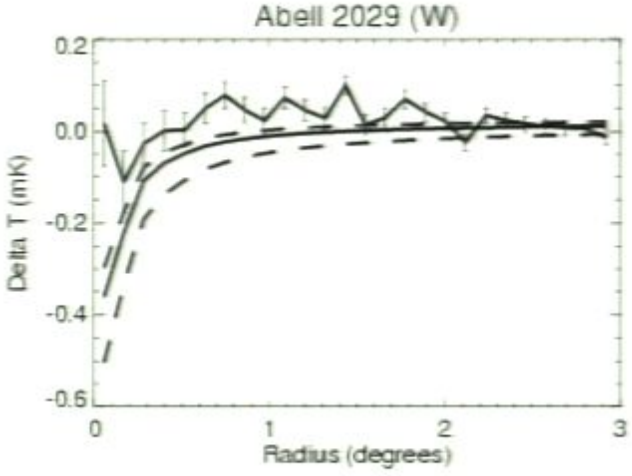
Abell 2029 (W)
Delta T (mK)
Radius (degrees)

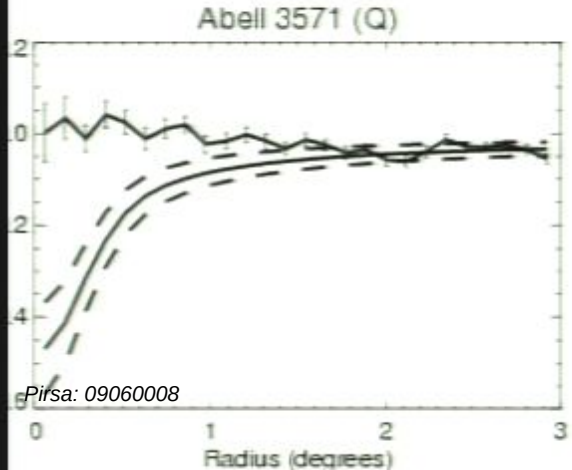
Abell 3571 (Q)
Radius (degrees)

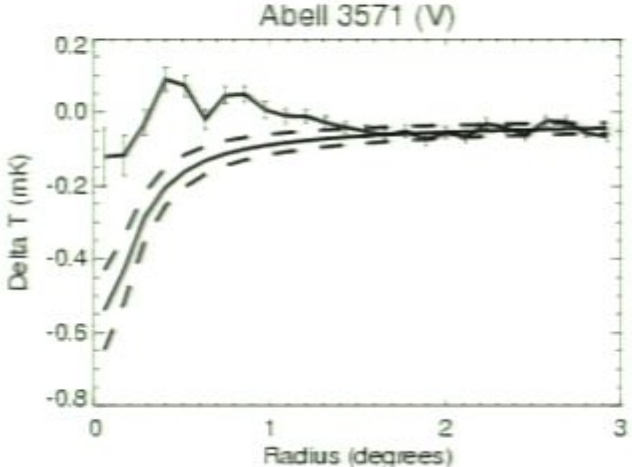
Abell 3571 (V)
Delta T (mK)
Radius (degrees)

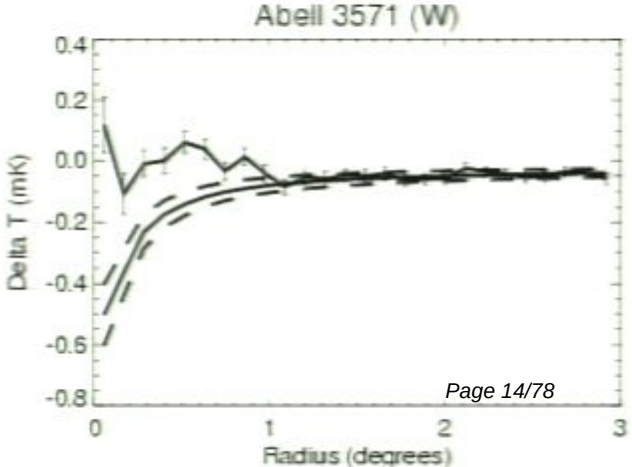
Abell 3571 (W)
Delta T (mK)
Radius (degrees)

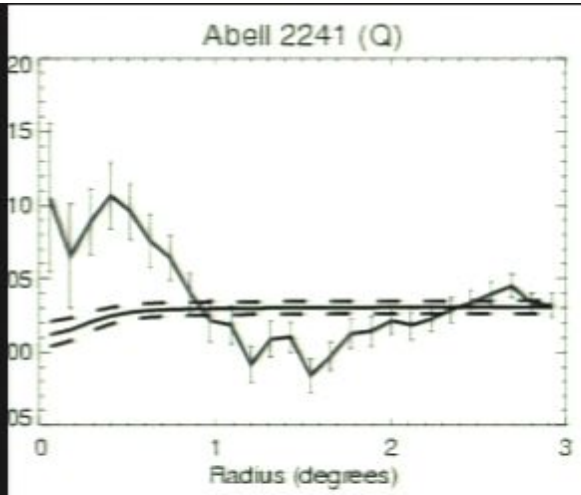
Abell 2241 (Q)
Radius (degrees)

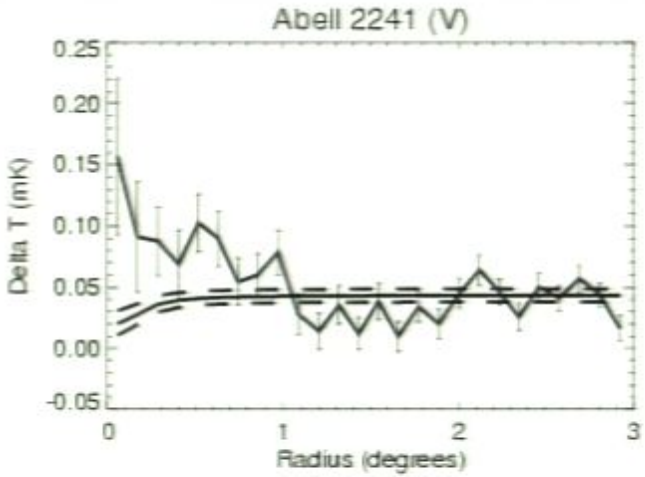
Abell 2241 (V)
Delta T (mK)
Radius (degrees)

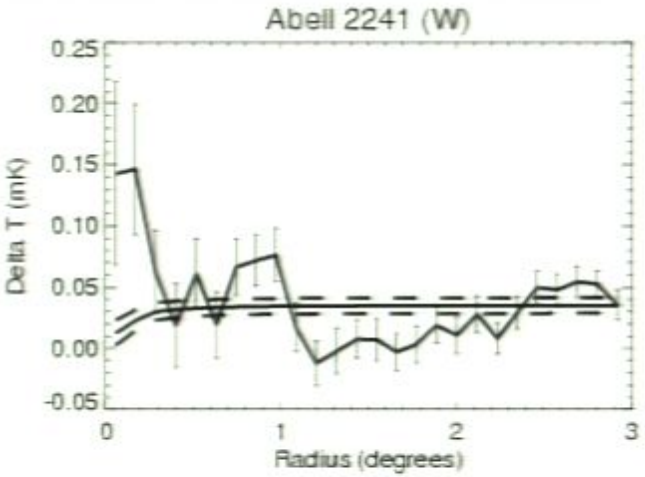
Abell 2241 (W)
Delta T (mK)
Radius (degrees)

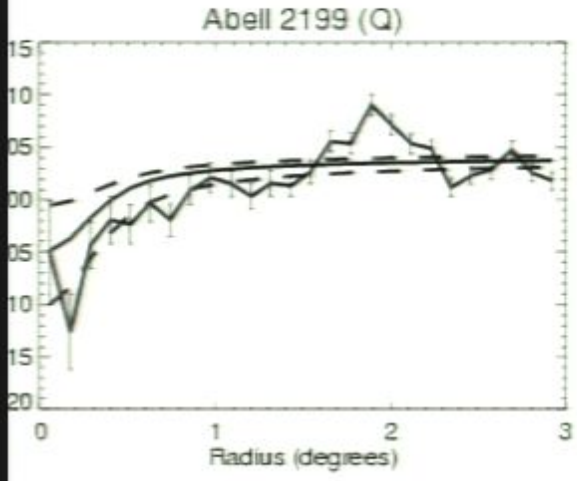
Abell 2199 (Q)
Radius (degrees)

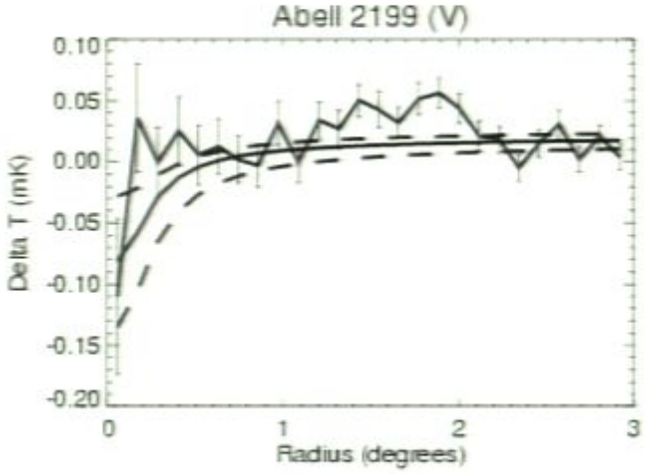
Abell 2199 (V)
Delta T (mK)
Radius (degrees)

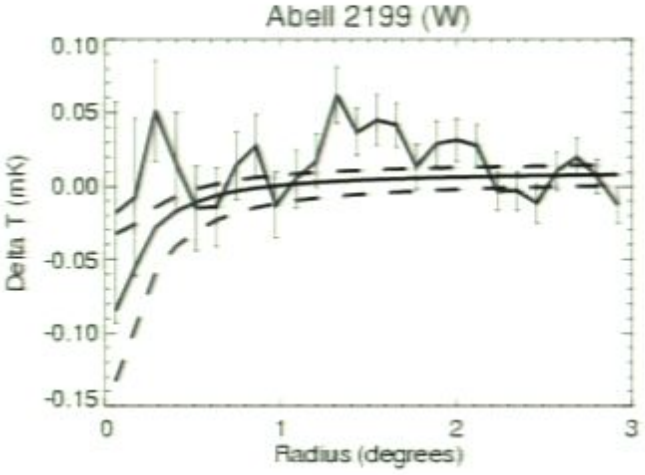
Abell 2199 (W)
Delta T (mK)
Radius (degrees)

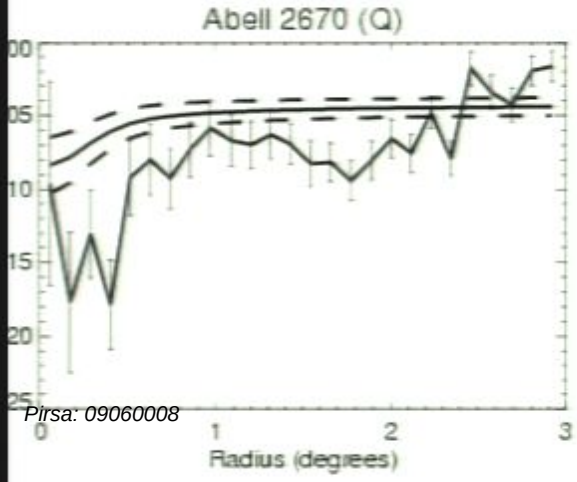
Abell 2670 (Q)
Radius (degrees)

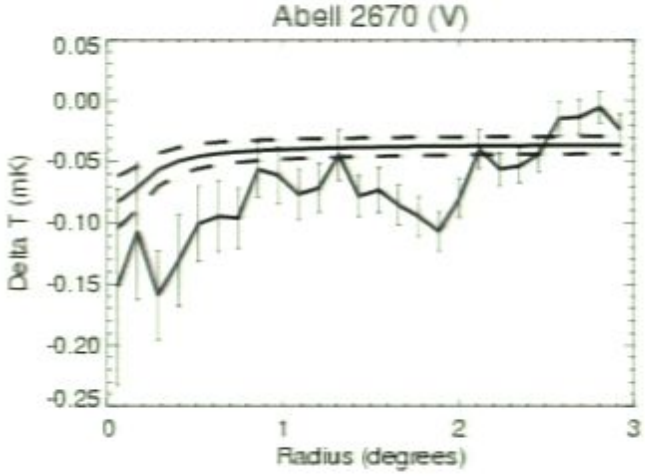
Abell 2670 (V)
Delta T (mK)
Radius (degrees)

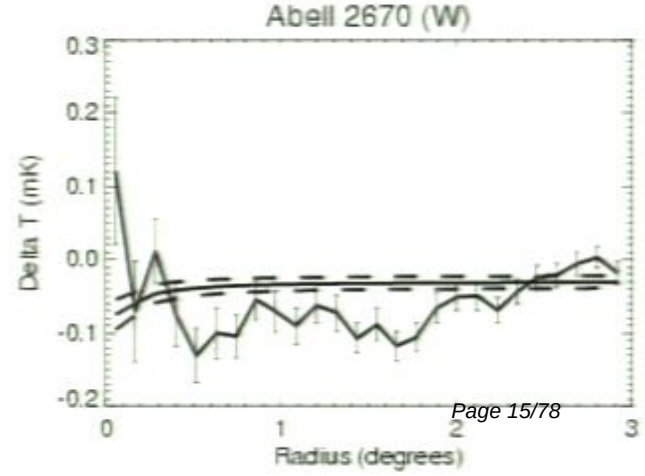
Abell 2670 (W)
Delta T (mK)
Radius (degrees)

nyaev-Zel'dovich `shadow test': composite shadow profile of 31 rich nearby clusters

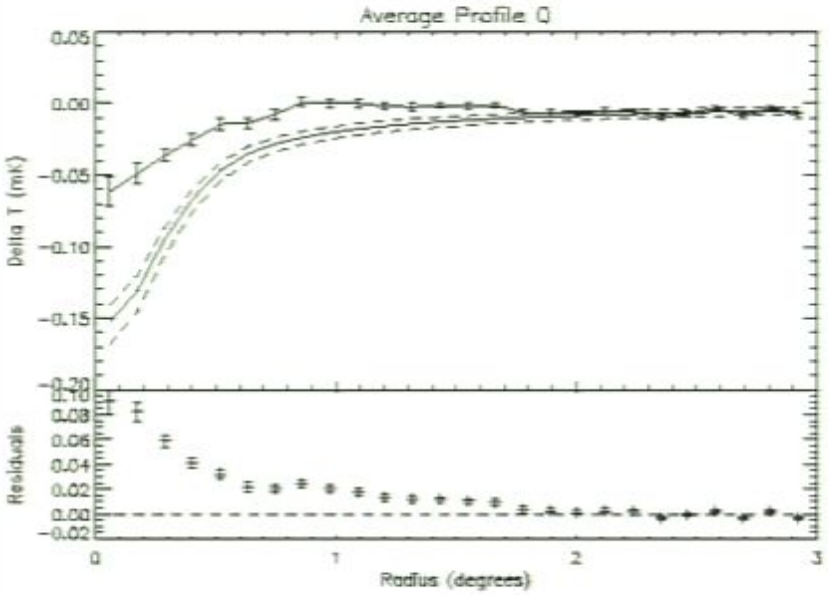

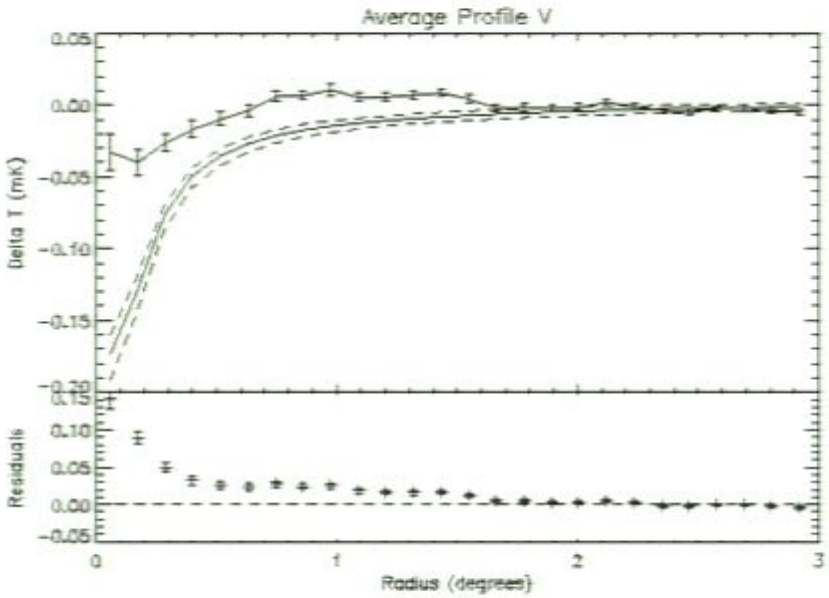

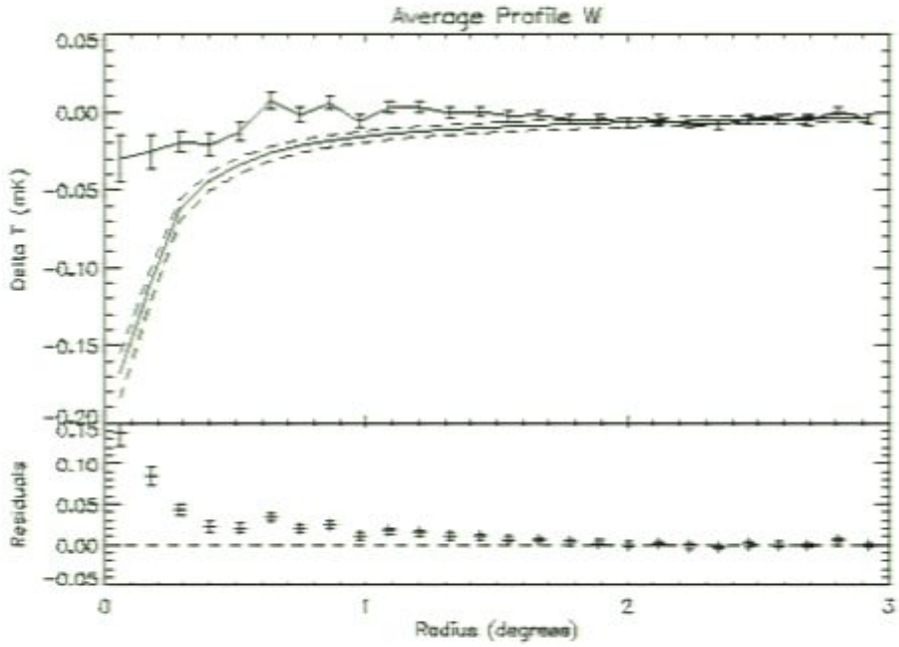

Bielby & Shanks 2007 MNRAS submitted

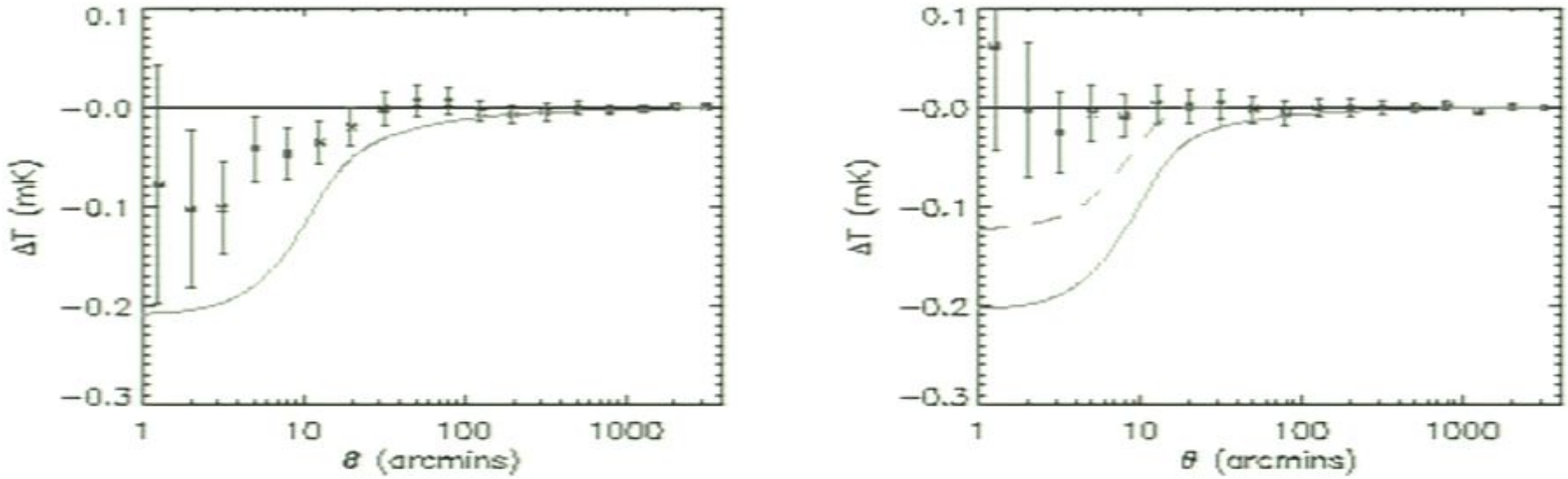

Figure 4. Average ΔT (from WMAP W-band data) plots for 0 clusters from the ROSAT sample (left) and 39 clusters from he Chandra sample (right). In both figures, the points show our ross-correlation results, whilst the curves show average SZ mod-ls (based on the parameters taken from Lieu et al. 2006 and Bonamente et al. 2006) convolved with a Gaussian representing he WMAP beam profile. For the Chandra sample, we plot the ull isothermal model (solid line) and the same model limited to $< 2'$ (dashed line).

The problem cannot be WMAP's angular resolution. The clusters used as test bed are all nearby and (hence) large. Their angular size is on average between the first and second acoustic peaks.

If WMAP cannot see them it will not be able to chart the acoustic peaks either.

The problem may be with the clusters themselves

Coma cluster 0.2-0.5 keV (ROSAT PSPC R2 band sky survey

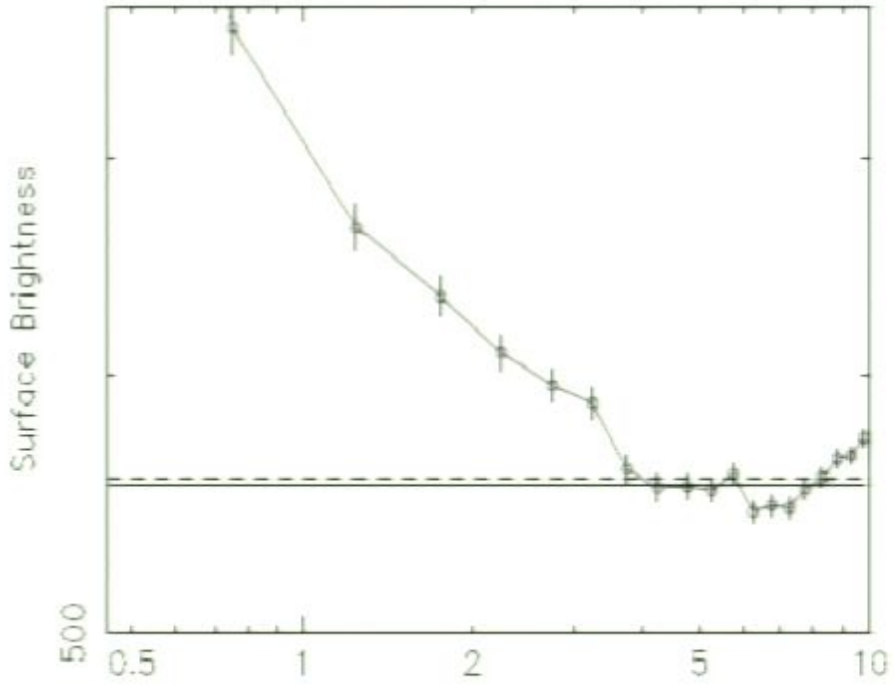

Coma cluster 1.0 – 2.0 keV ROSAT PSPC R7 band sky survey

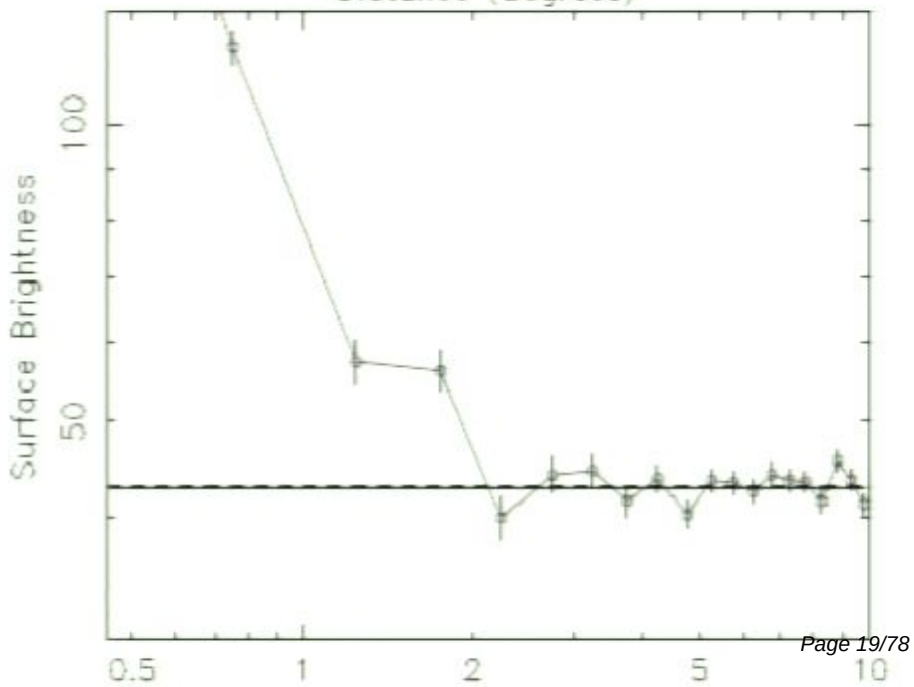

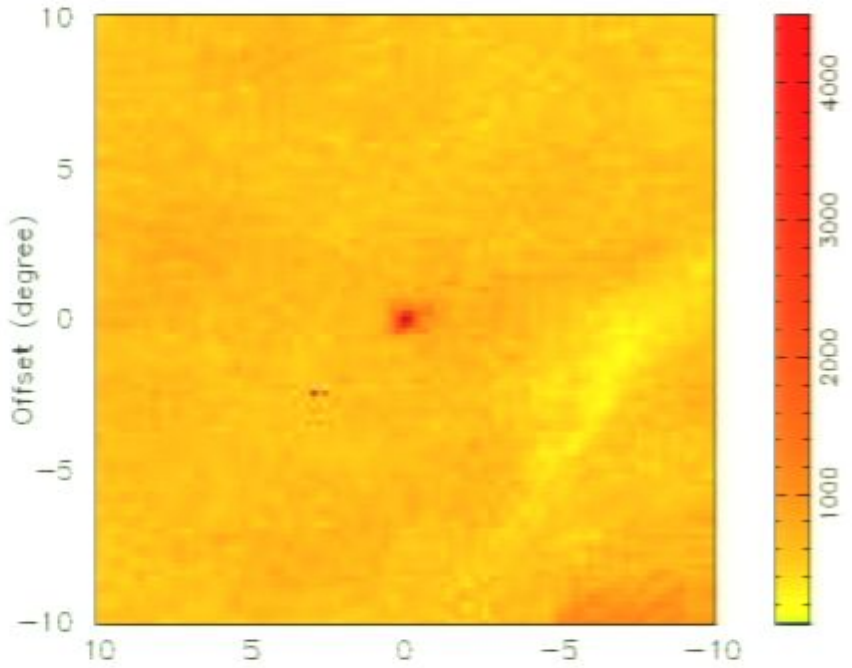

R2 band image
(0.2 – 0.5 keV)

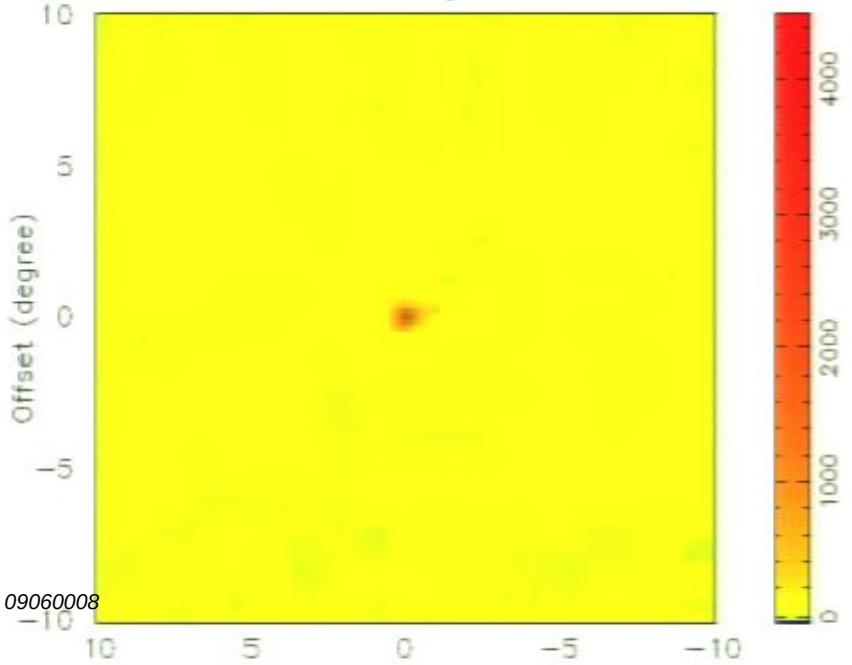

R7 band image
(1.0 – 2.0 keV)

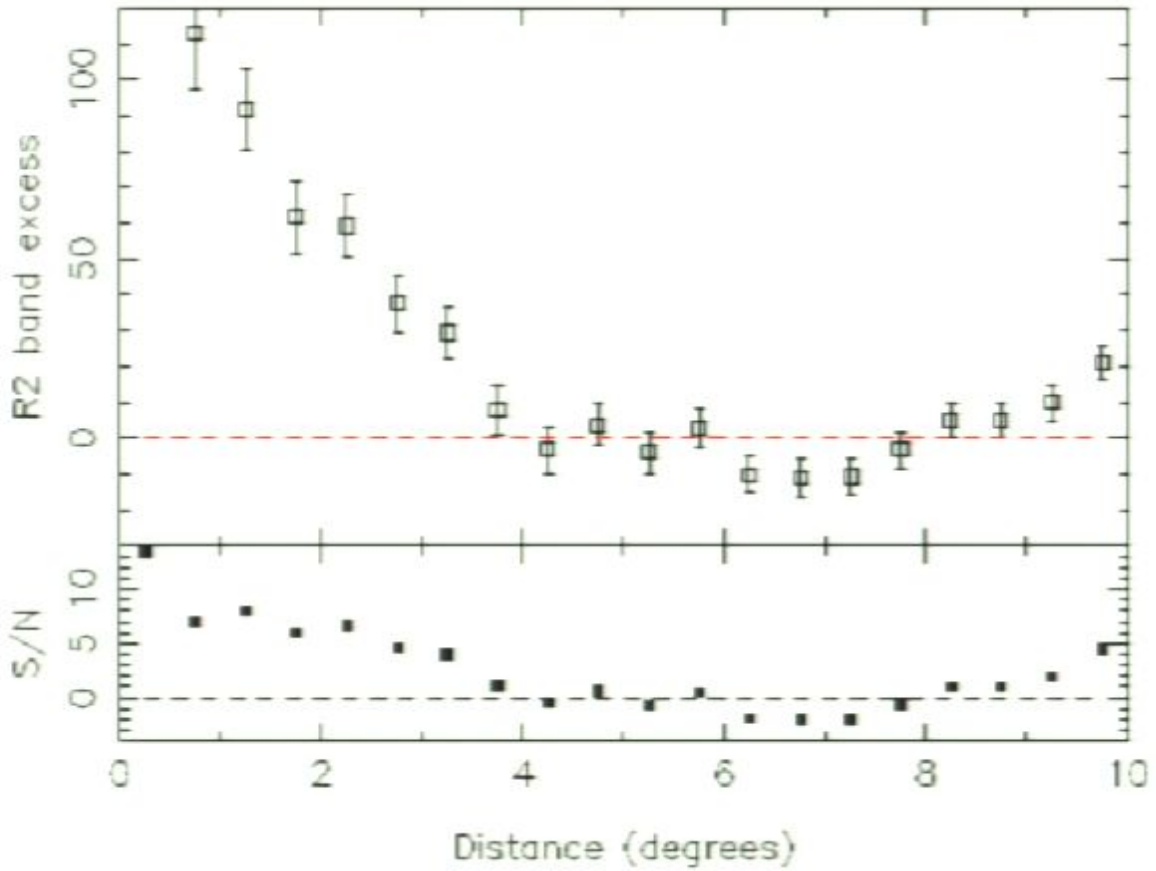
R2 band excess
100
50
0
S/N
0 5 10
0
2
4
6
8
10
Distance (degrees)

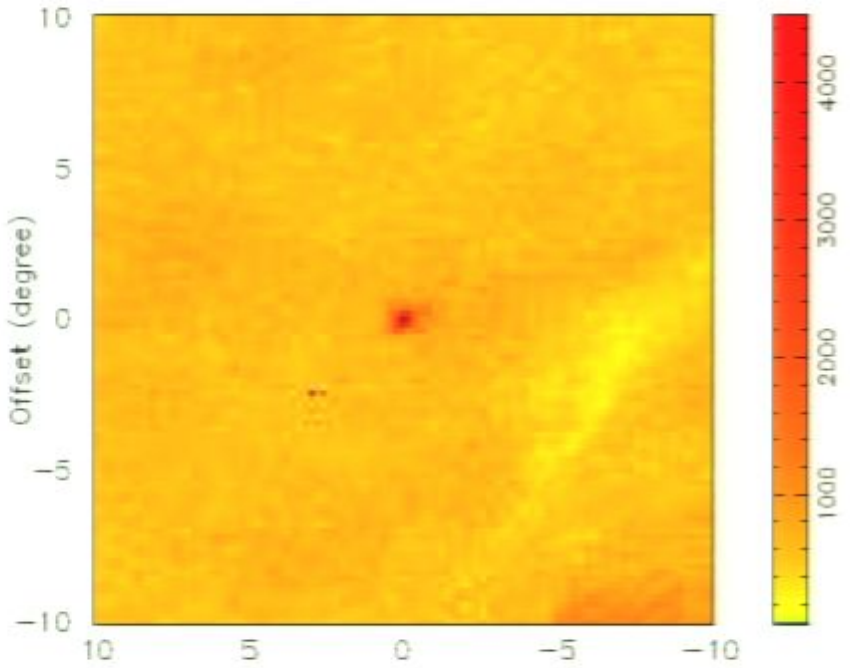

R2 band image
(0.2 – 0.5 keV)

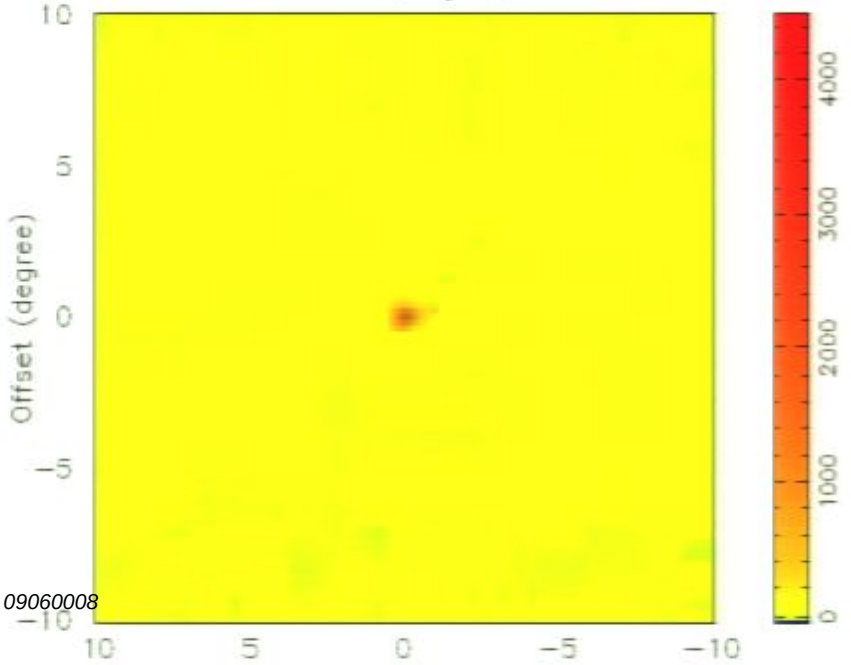

R7 band image
(1.0 – 2.0 keV)

Coma cluster 0.2-0.5 keV (ROSAT PSPC R2 band sky survey

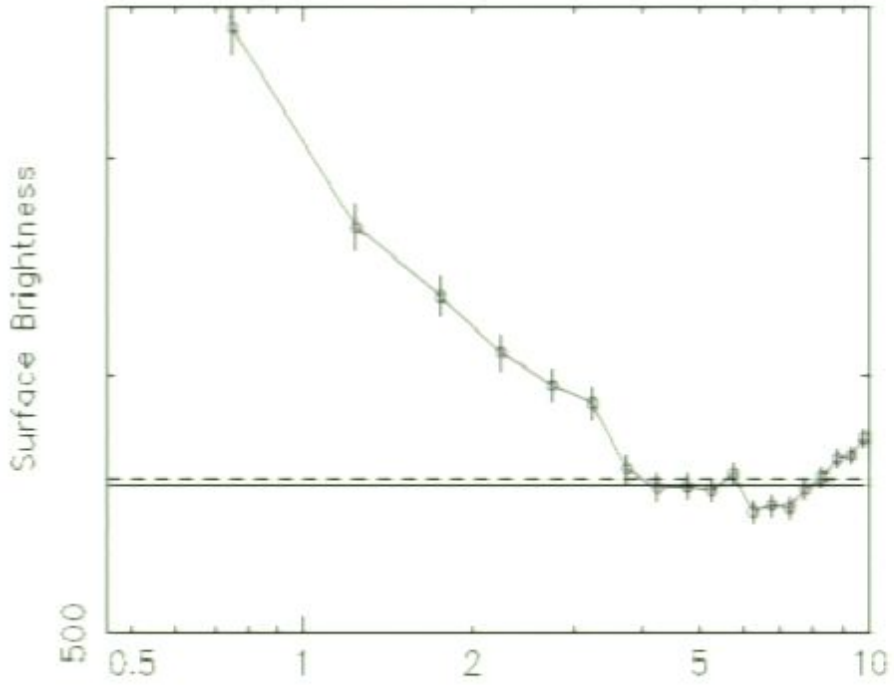

Coma cluster 1.0 – 2.0 keV ROSAT PSPC R7 band sky survey

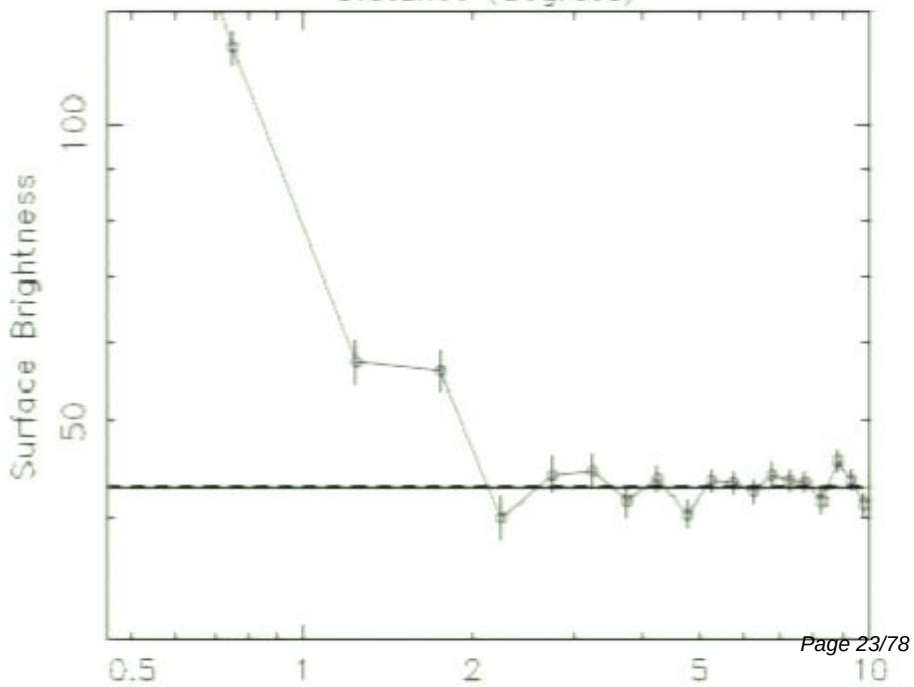

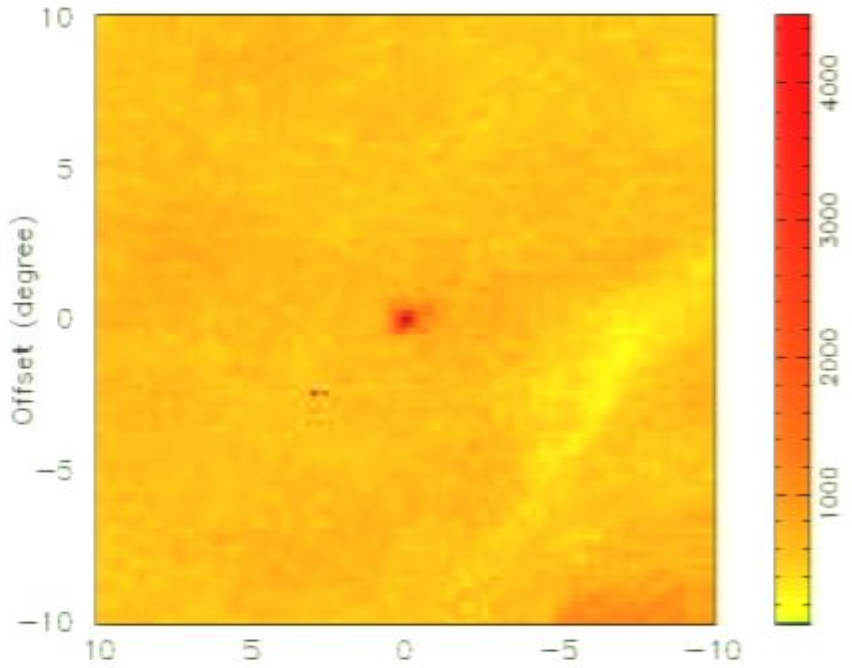

R2 band image
(0.2 – 0.5 keV)

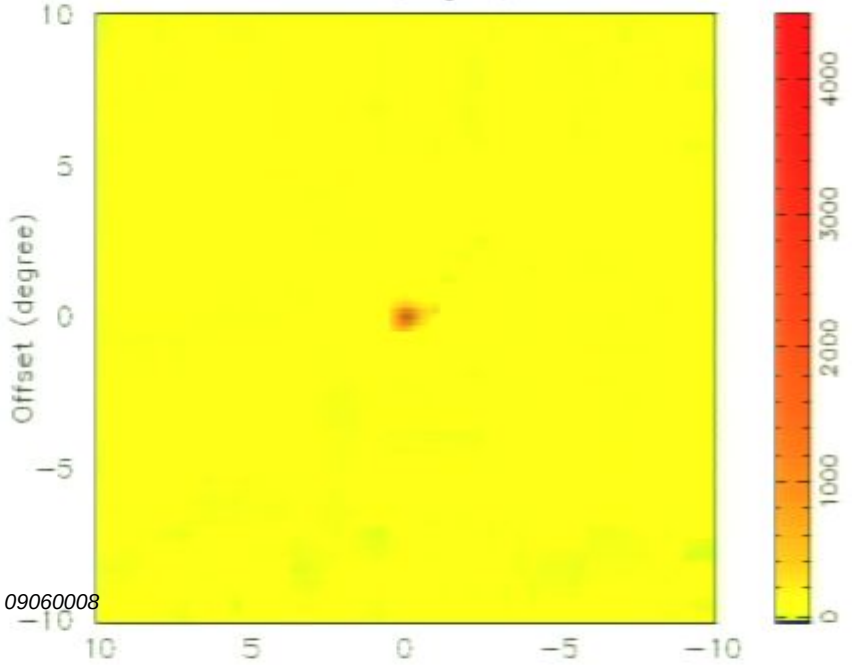

R7 band image
(1.0 – 2.0 keV)

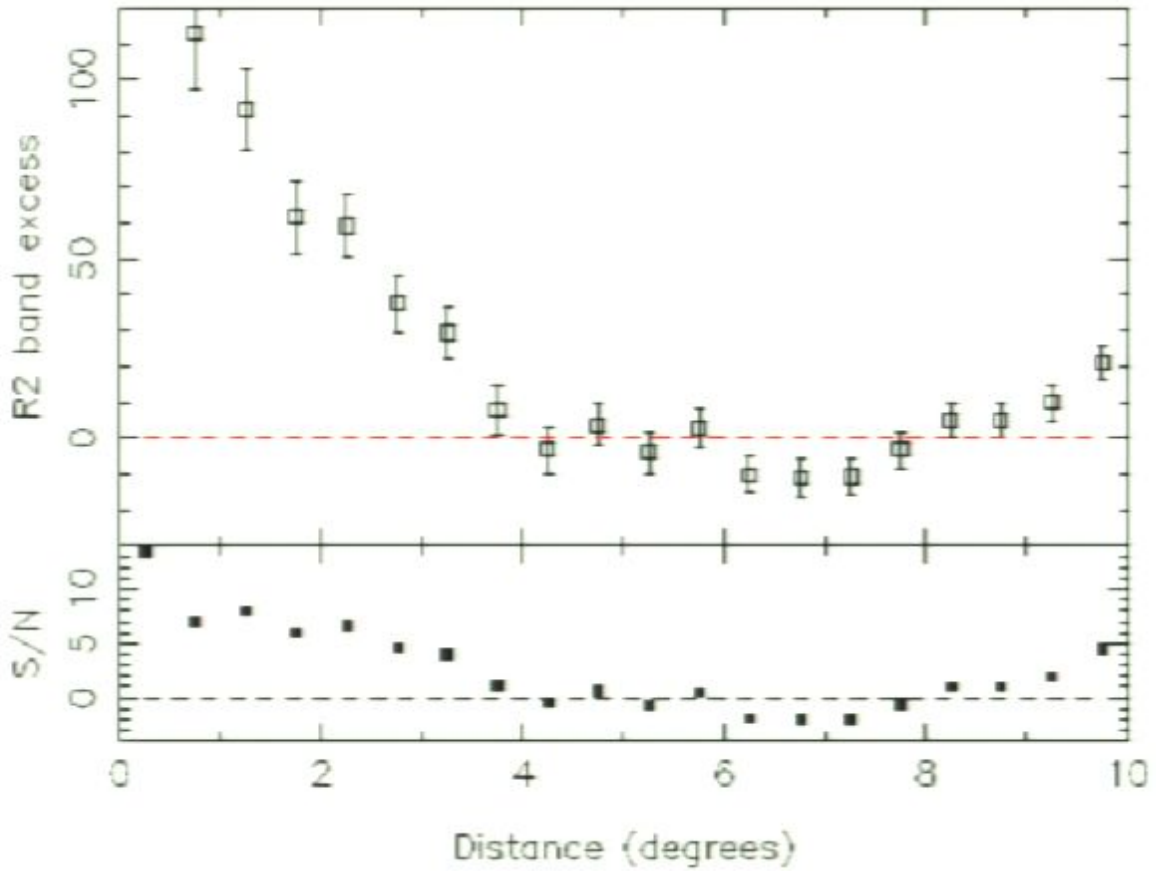
R2 band excess
100
50
0
S/N
0 5 10
0
2
4
6
8
10
Distance (degrees)

Same as previous slide but now all observations have been added. Again, there is no line at the expected redshift of Coma

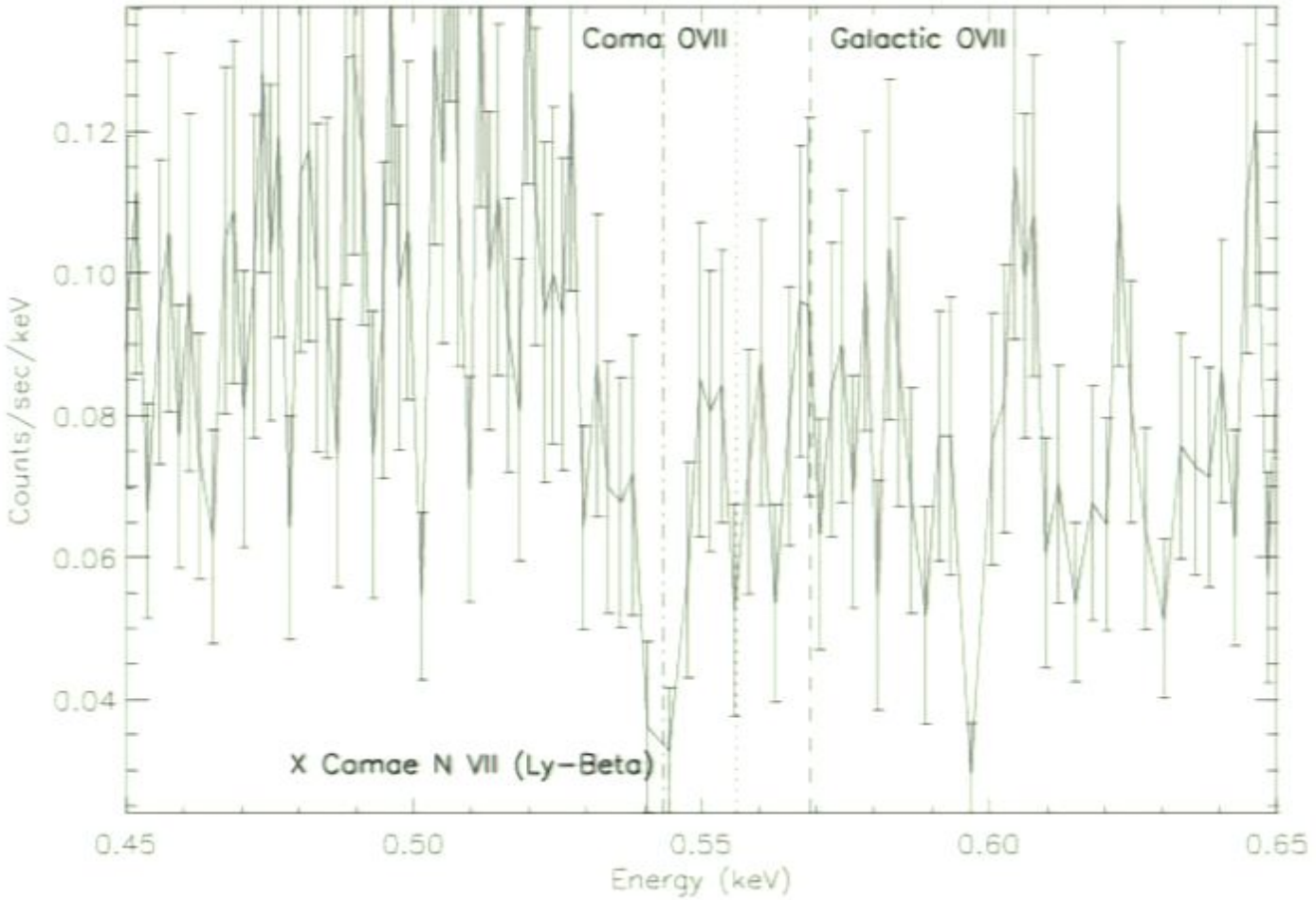

CMB Temperature smooth to 3 Decimal places

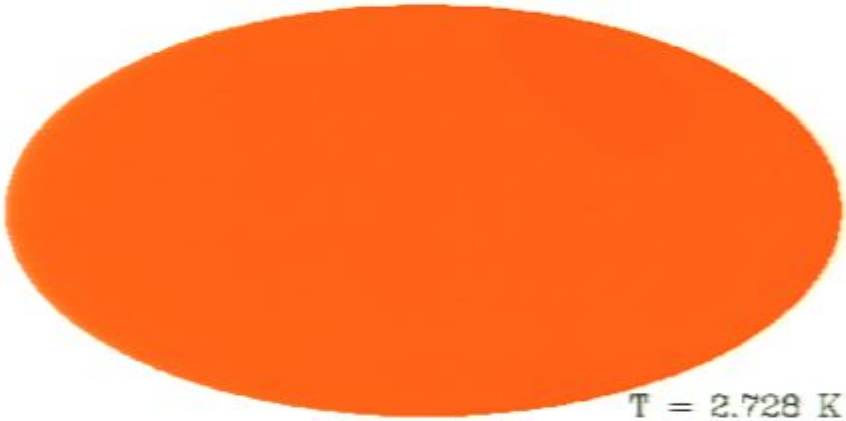

CMB "dipole" (at the 0.1% level)

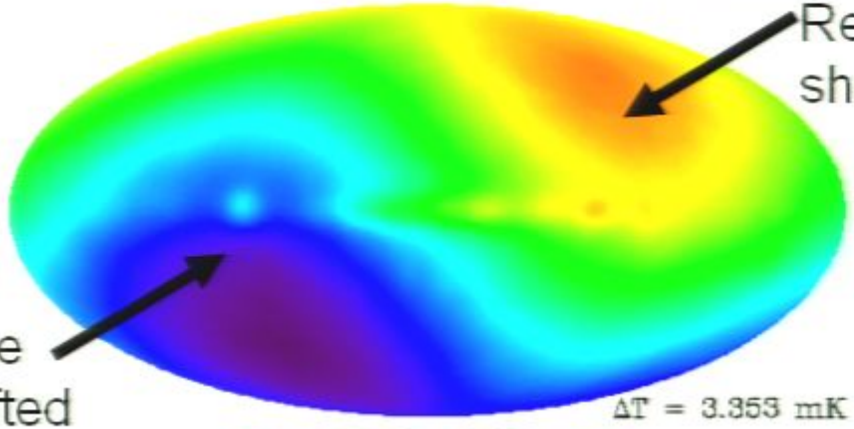

Interpret CMB dipole as red/blue shits due to our motion and remove to get "cosmic anisotropies"

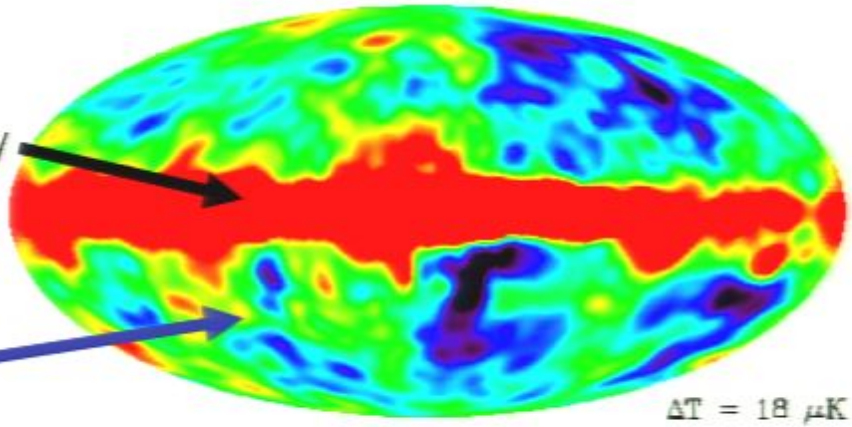

Comparing the sky maps of COBE (top) and WMAP year 1 (bottom)

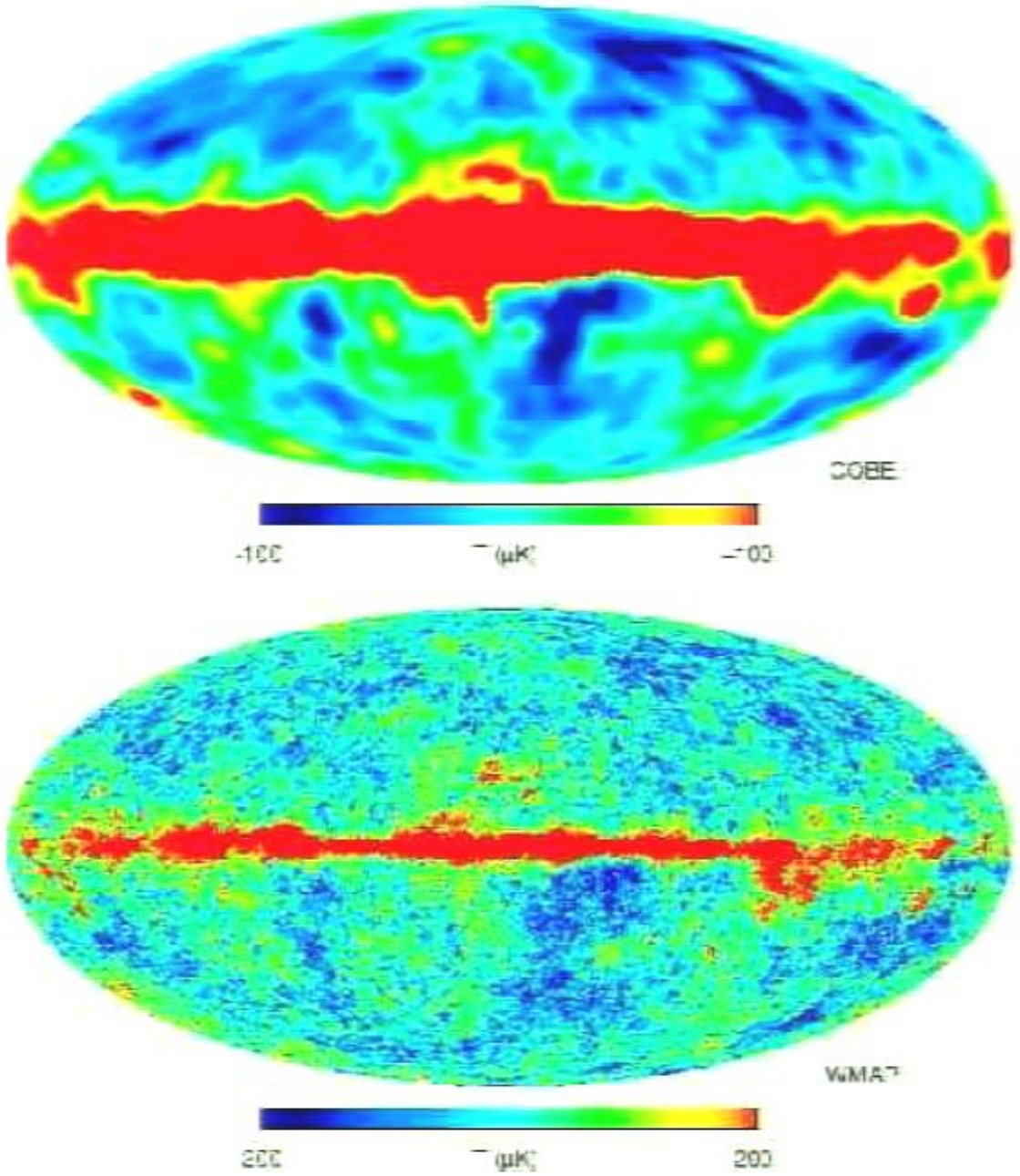

- WMAP surveys the sky in three cosmological filter passbands:

- Q band (41 GHz)
- V band (61 GHz)
- W band (94 GHz)

Comparing the sky maps of COBE (top) and WMAP year 1 (bottom)

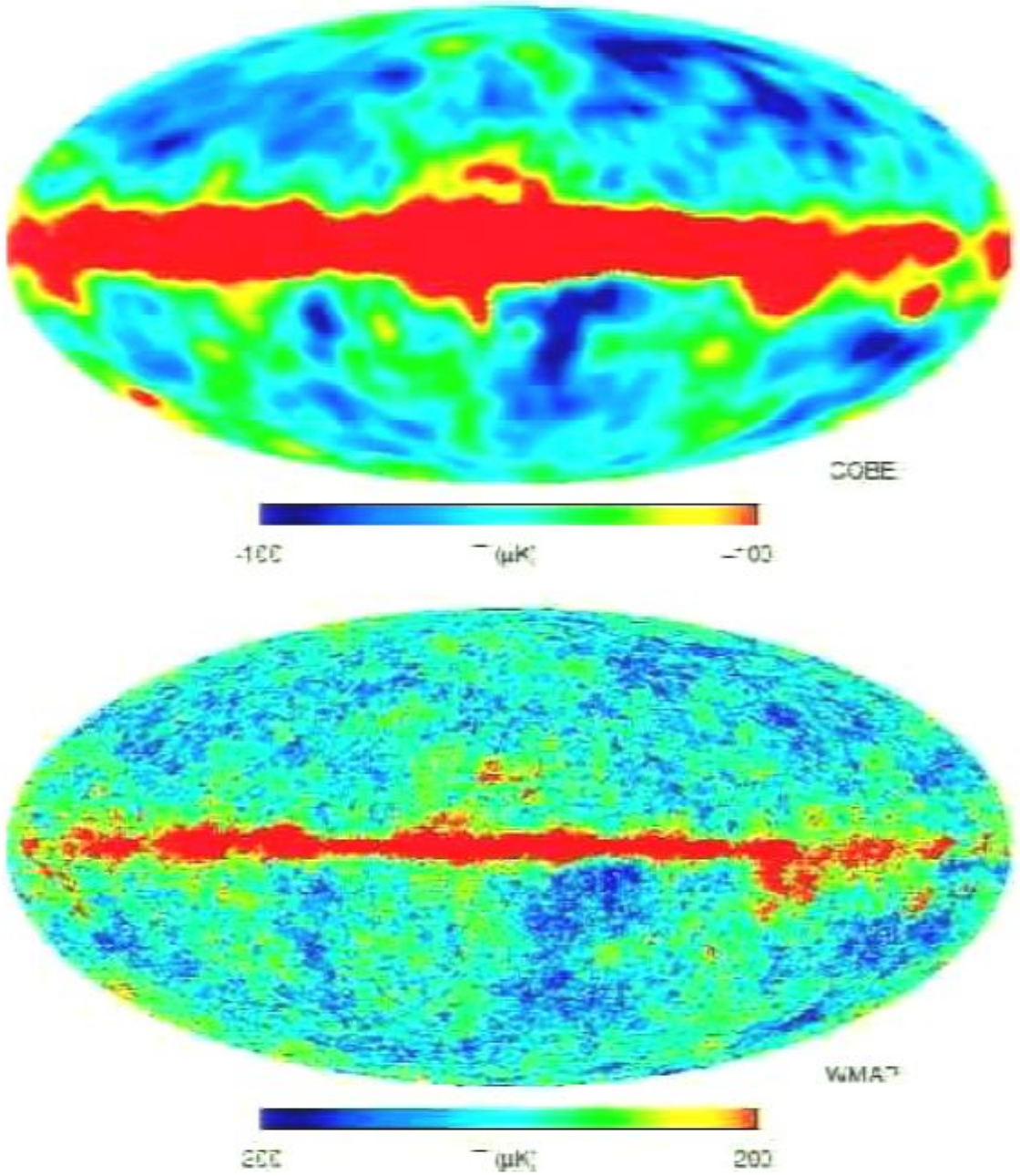

- WMAP surveys the sky in three cosmological filter passbands:

- Q band (41 GHz)
- V band (61 GHz)
- W band (94 GHz)

Simulated temperature difference maps

Simulation: $T_Q - T_V$

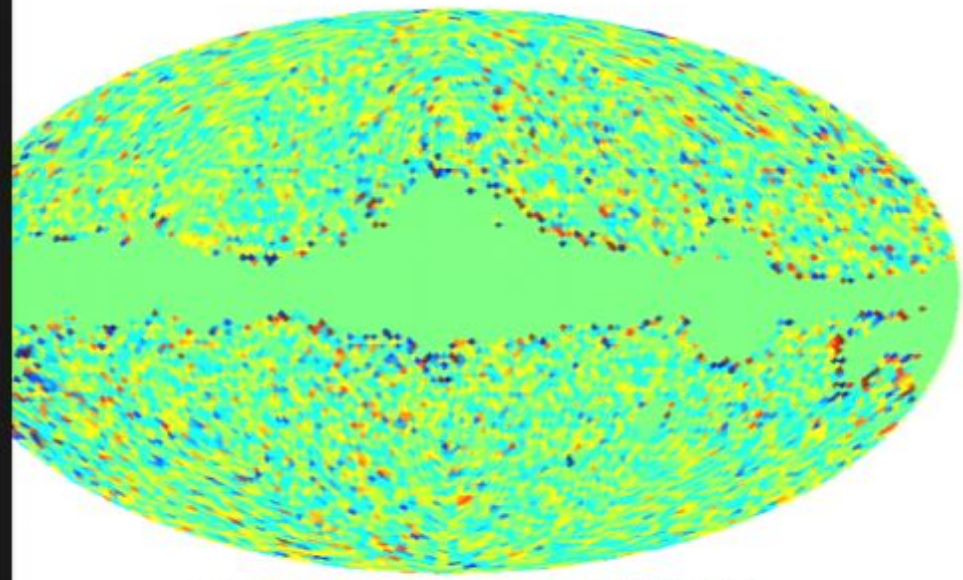

−0.020 0.020 (mK)

Simulation: $T_Q - T_W$

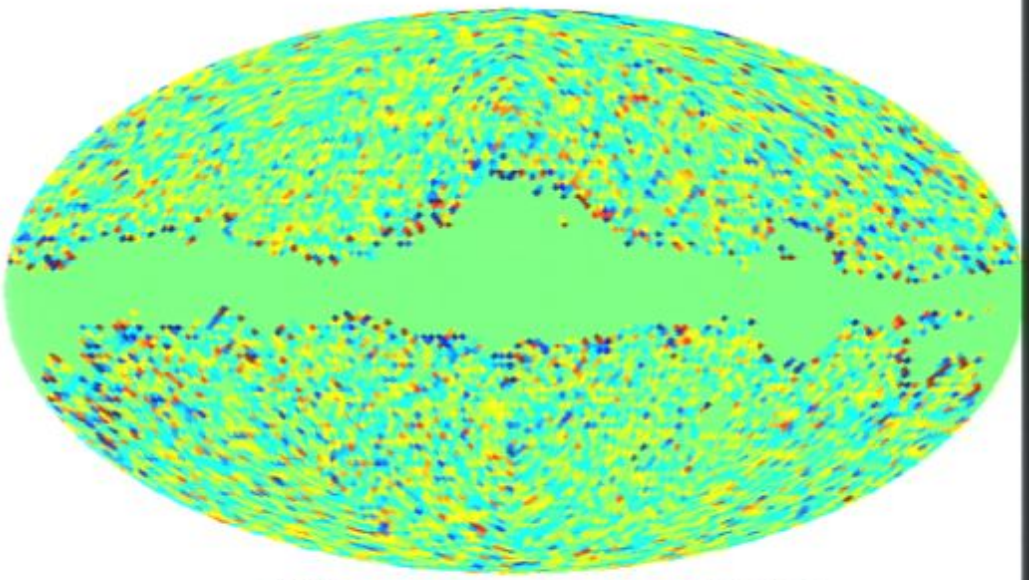

−0.020 0.020 (mK)

Simulation: $T_V - T_W$

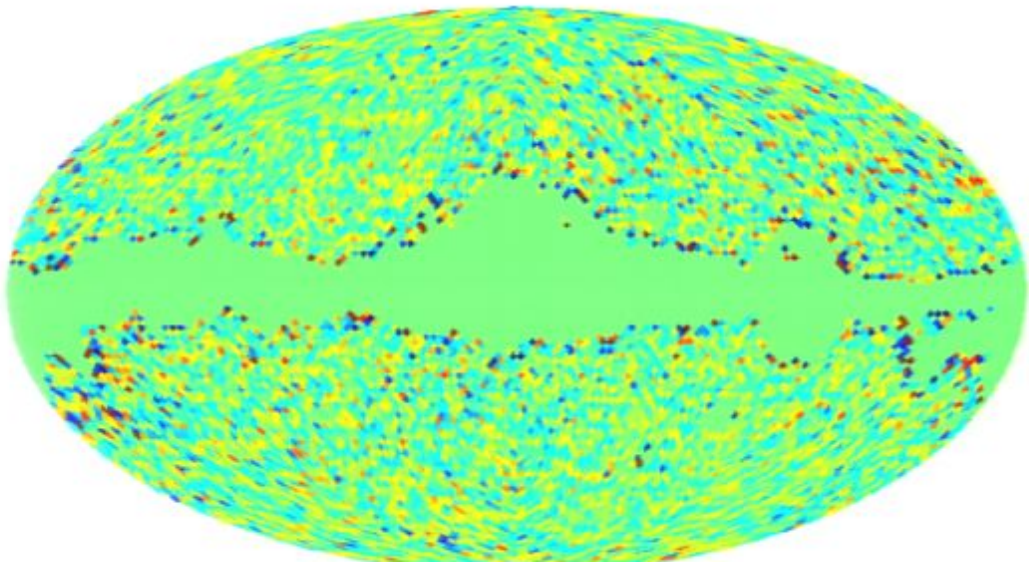

Actual temperature difference maps Q-V (left),Q-W (right),V-W (bottom)

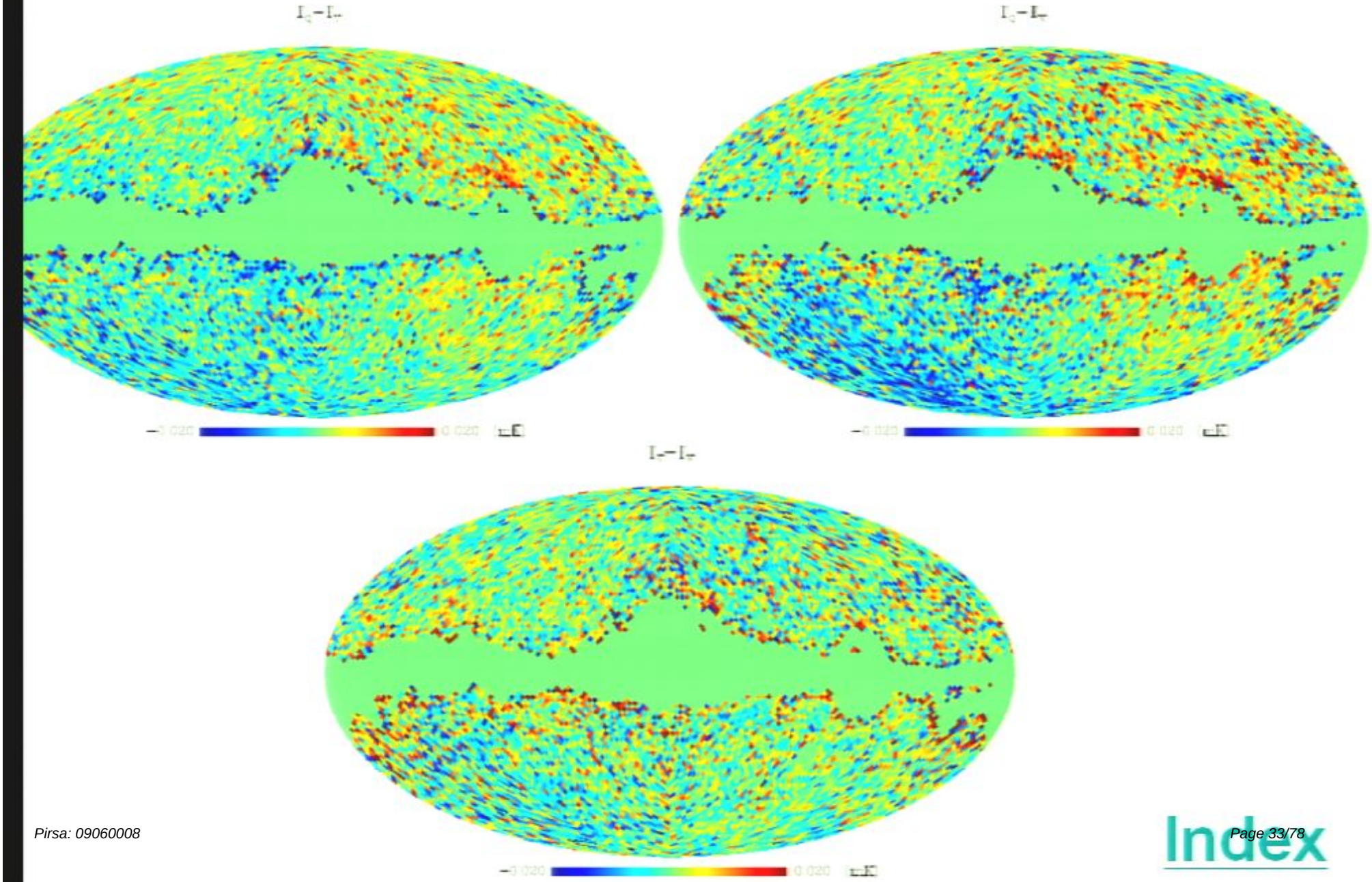

Simulated temperature difference maps

Simulation: $T_Q - T_V$

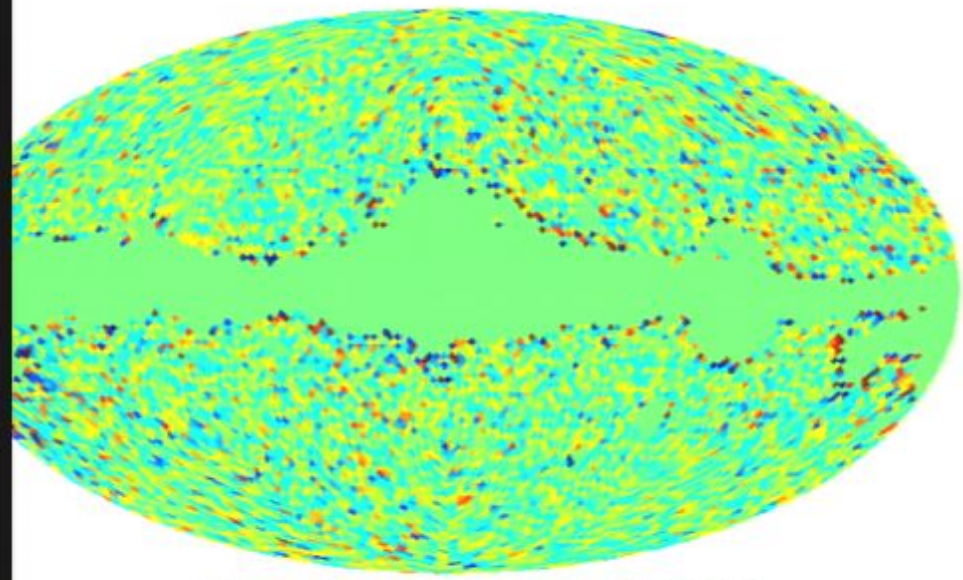

−0.020 0.020 (mK)

Simulation: $T_Q - T_W$

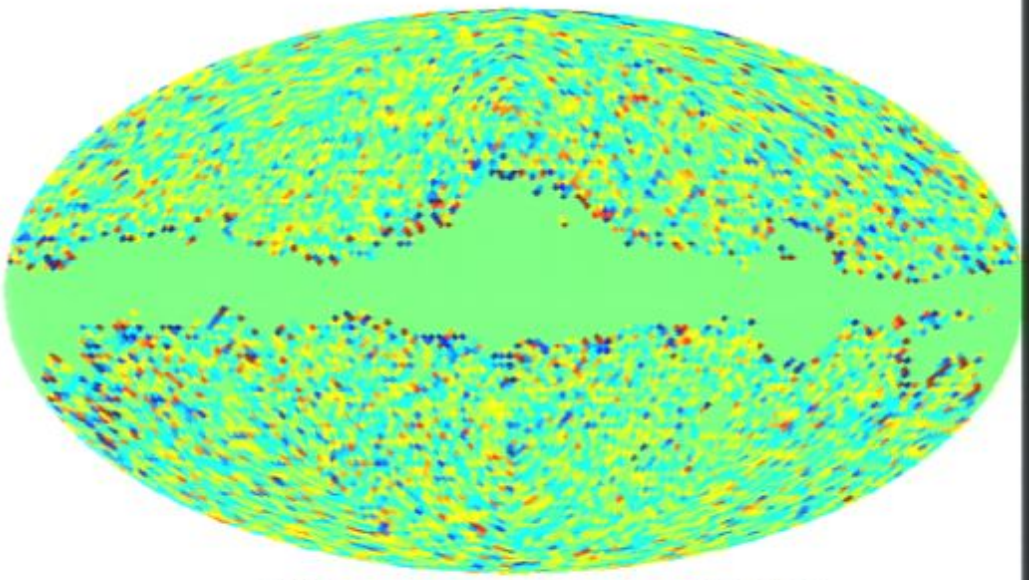

−0.020 0.020 (mK)

Simulation: $T_V - T_W$

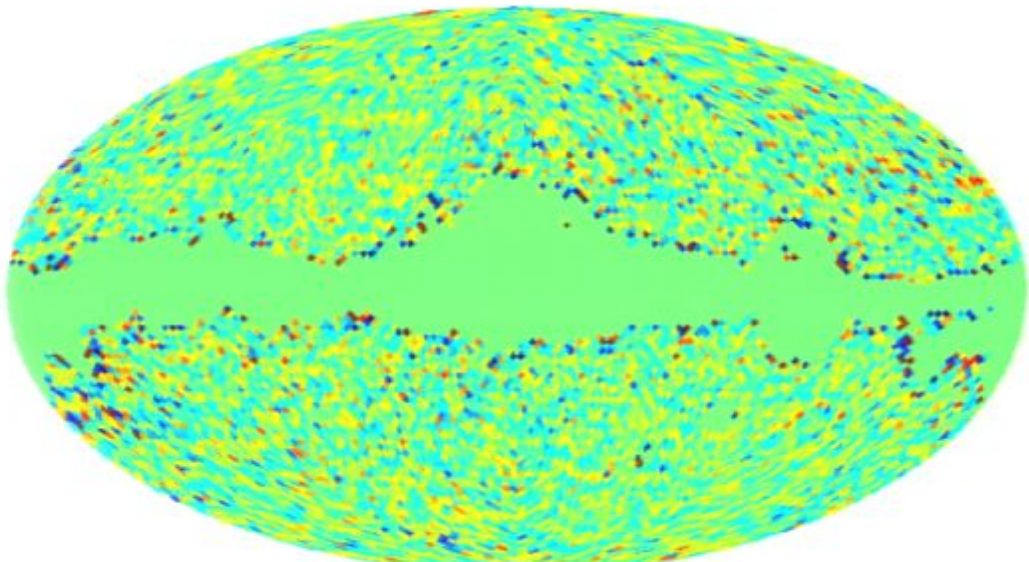

Actual temperature difference maps Q-V (left),Q-W (right),V-W (bottom)

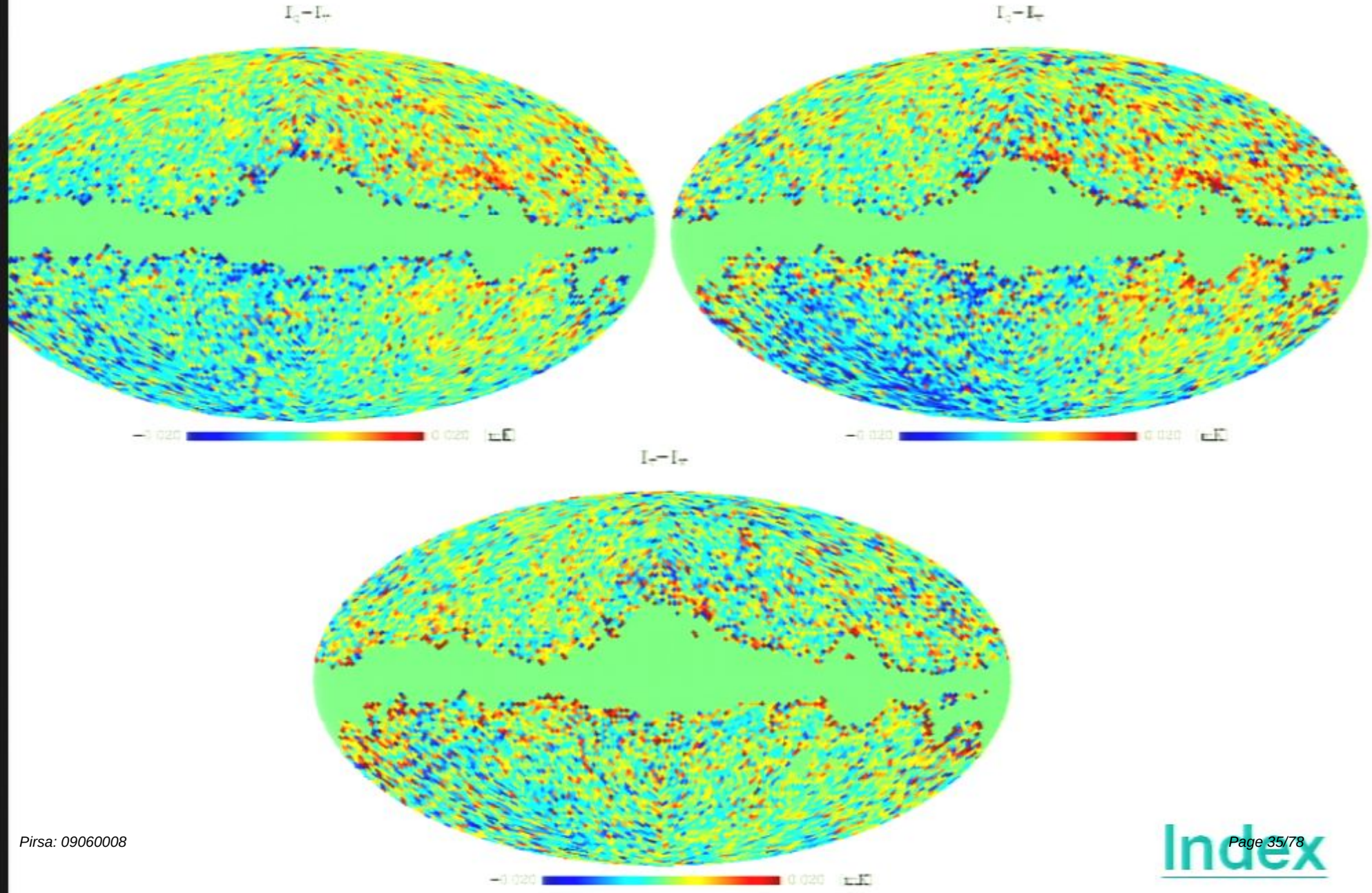

Simulated temperature difference maps

Simulation: $T_Q - T_V$

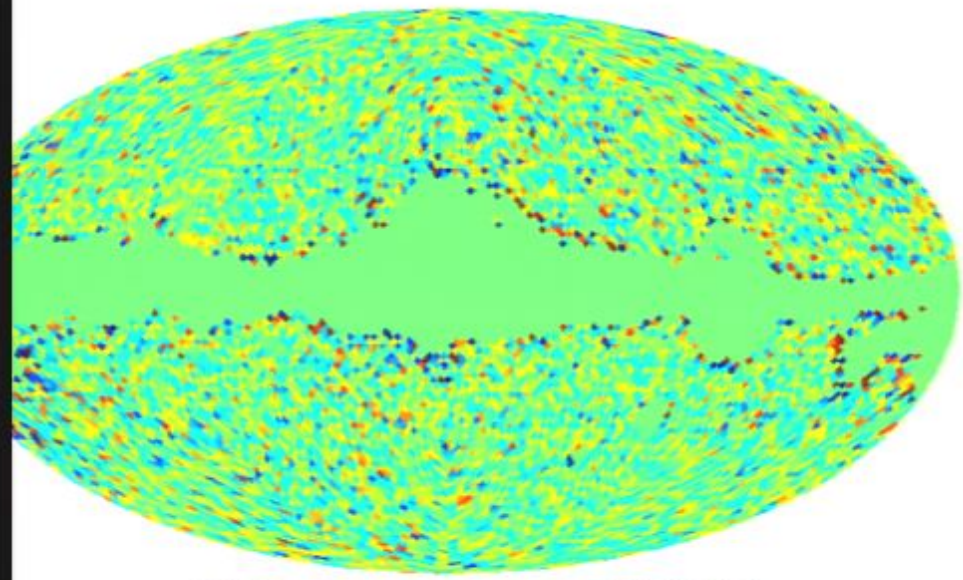

−0.020 0.020 (mK)

Simulation: $T_Q - T_W$

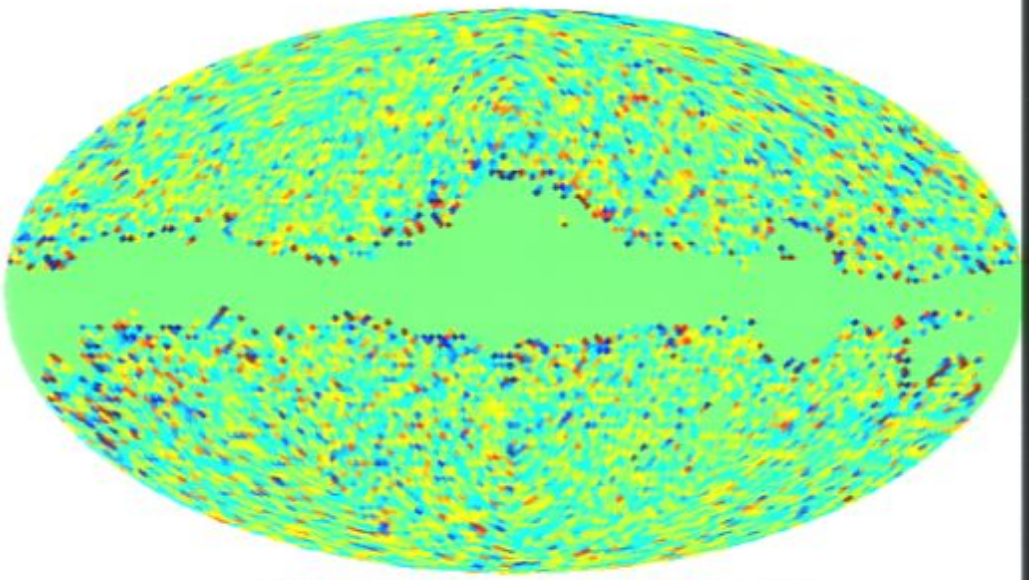

−0.020 0.020 (mK)

Simulation: $T_V - T_W$

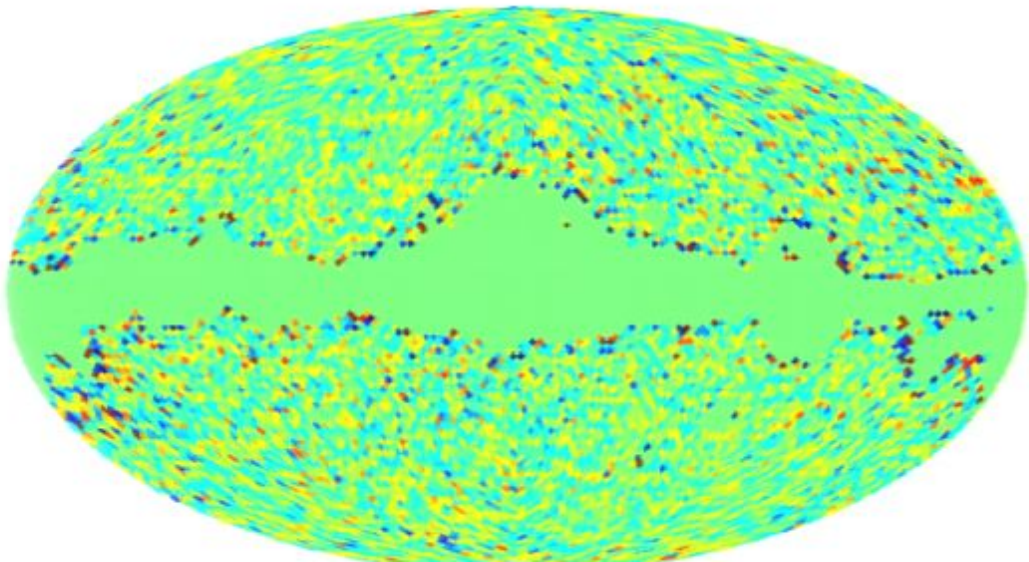

Actual temperature difference maps Q-V (left),Q-W (right),V-W (bottom)

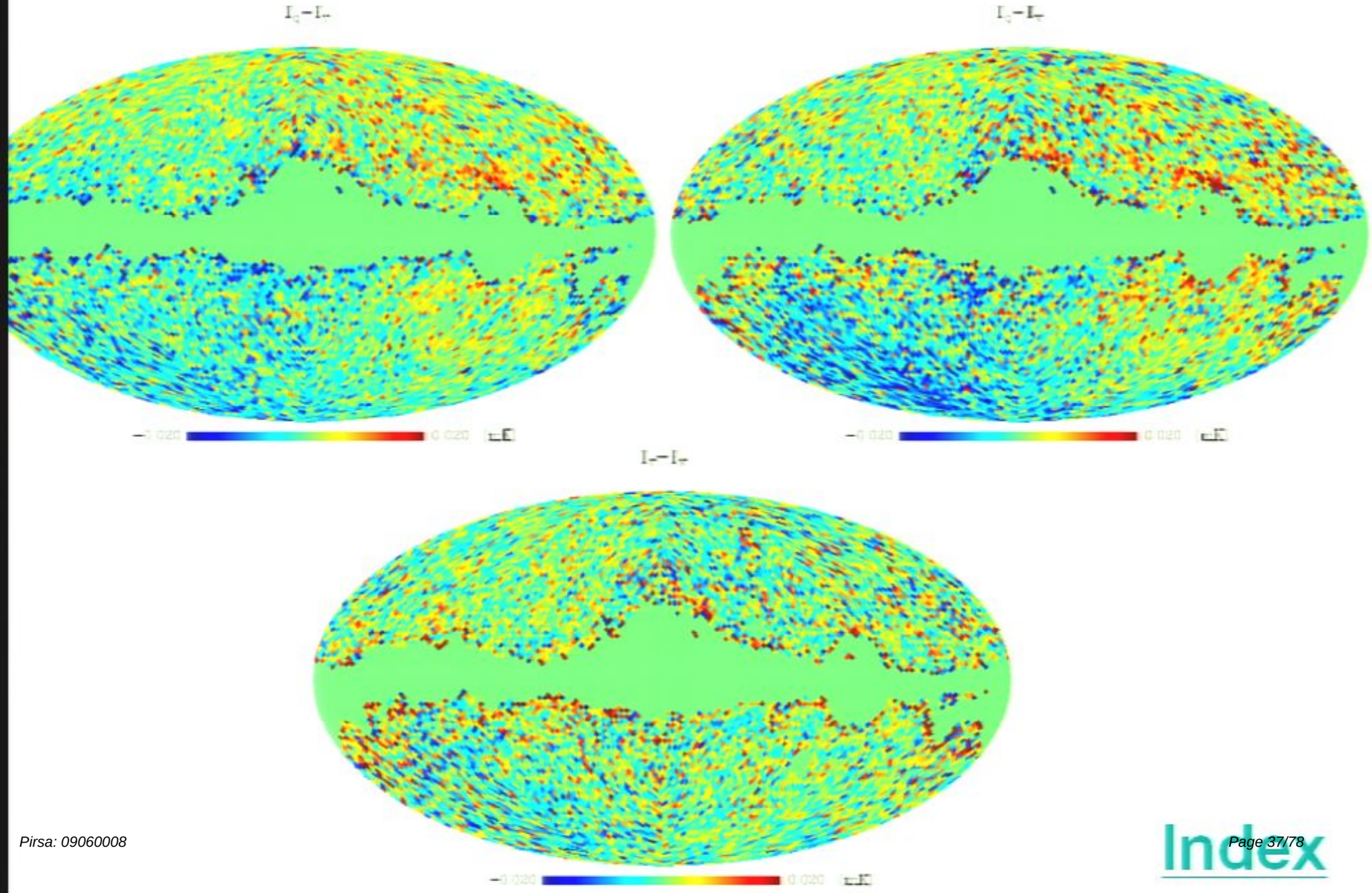

Simulated temperature difference maps

Simulation: $T_Q - T_V$

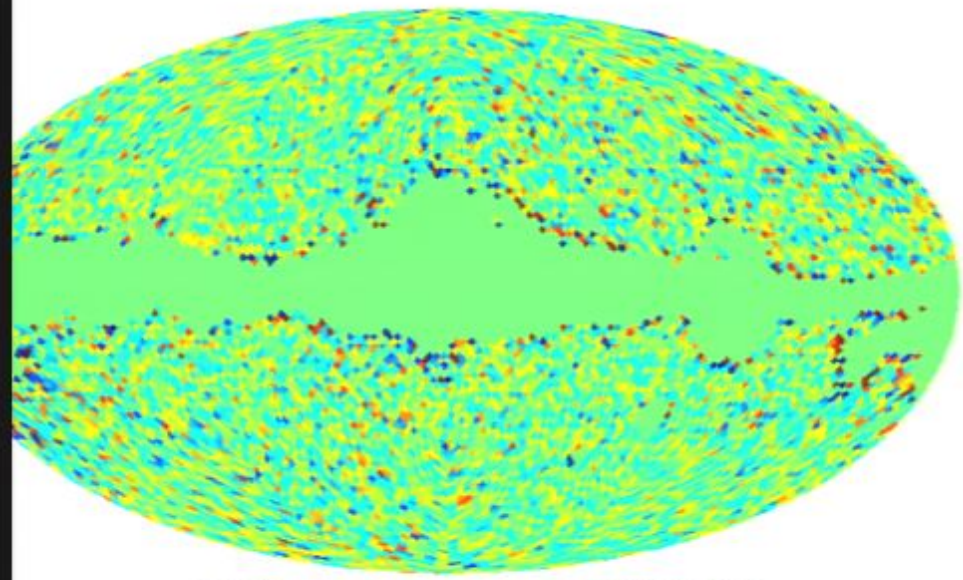

−0.020 0.020 (mK)

Simulation: $T_Q - T_W$

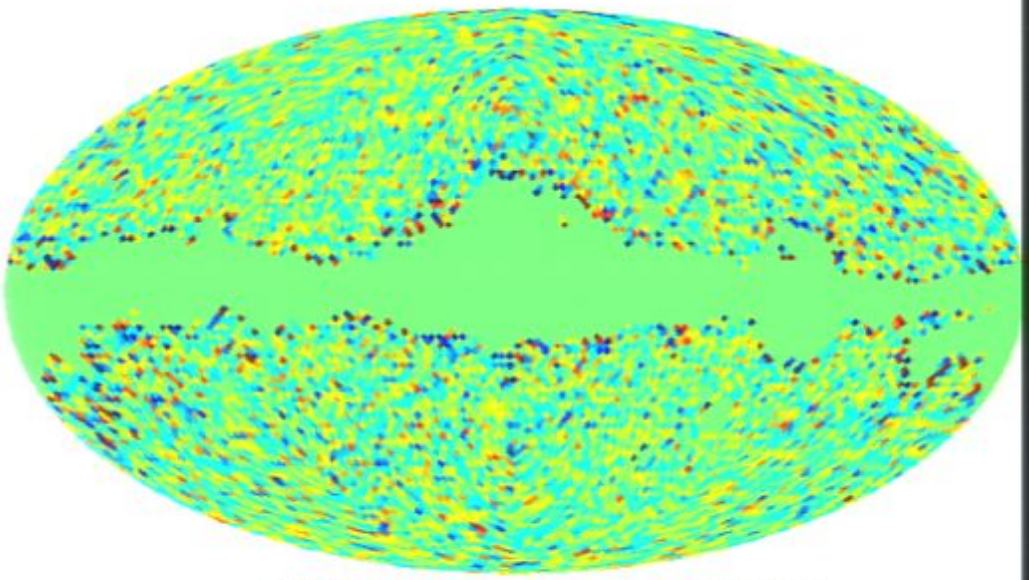

−0.020 0.020 (mK)

Simulation: $T_V - T_W$

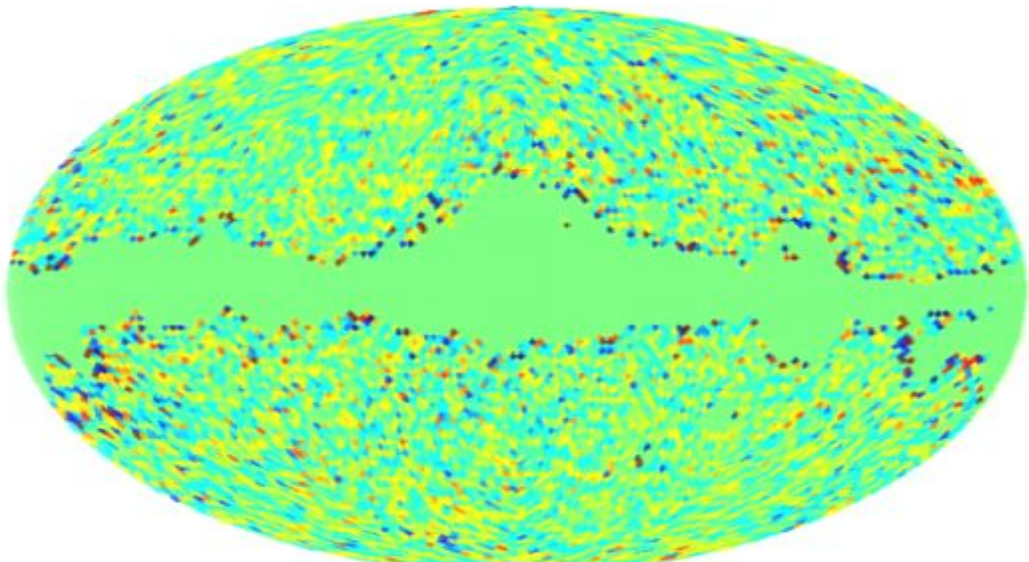

Actual temperature difference maps Q-V (left),Q-W (right),V-W (bottom)

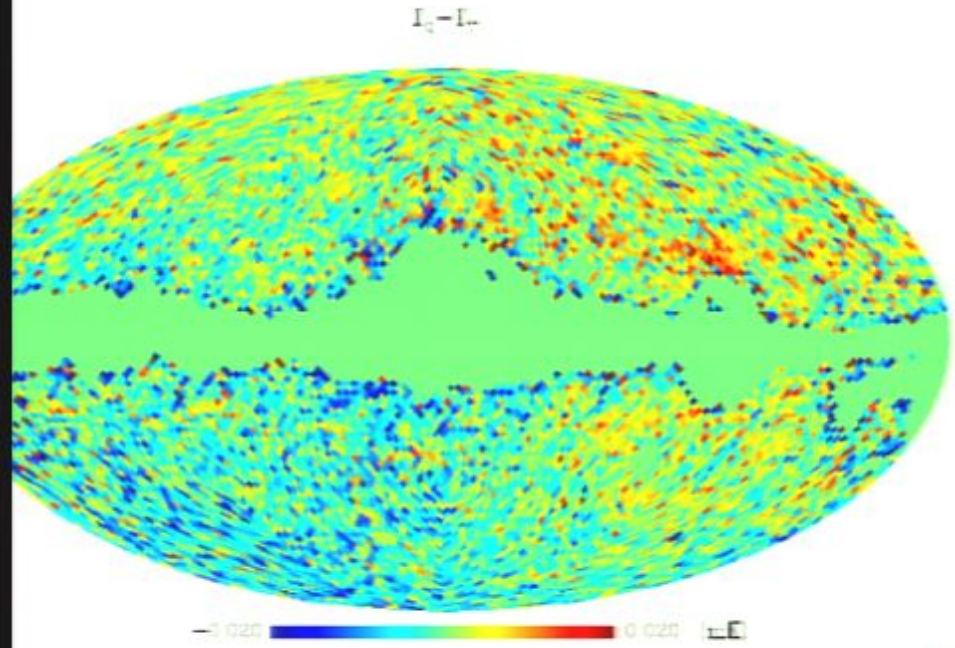

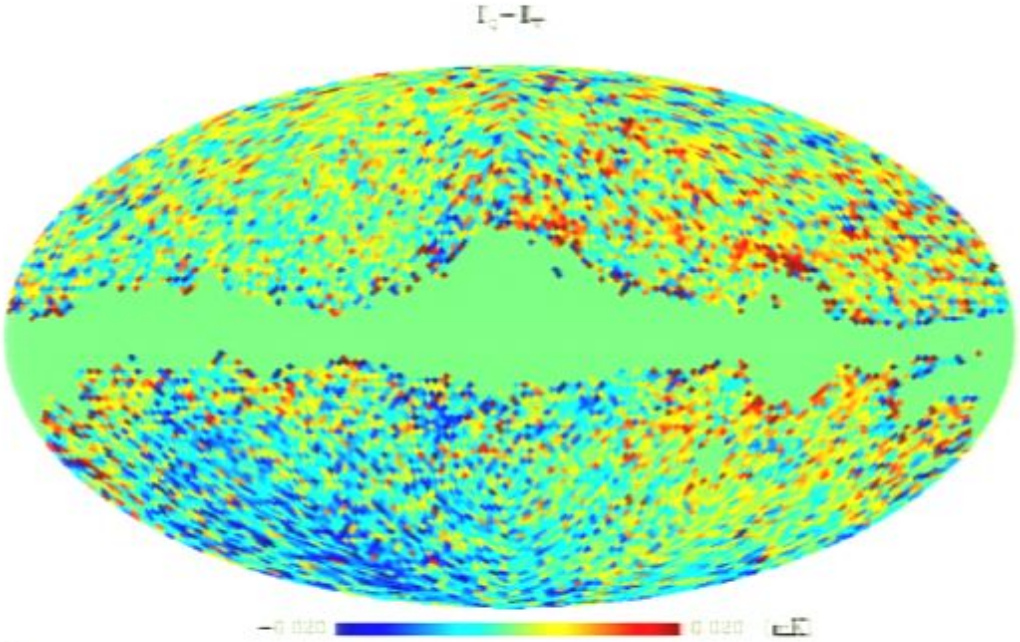

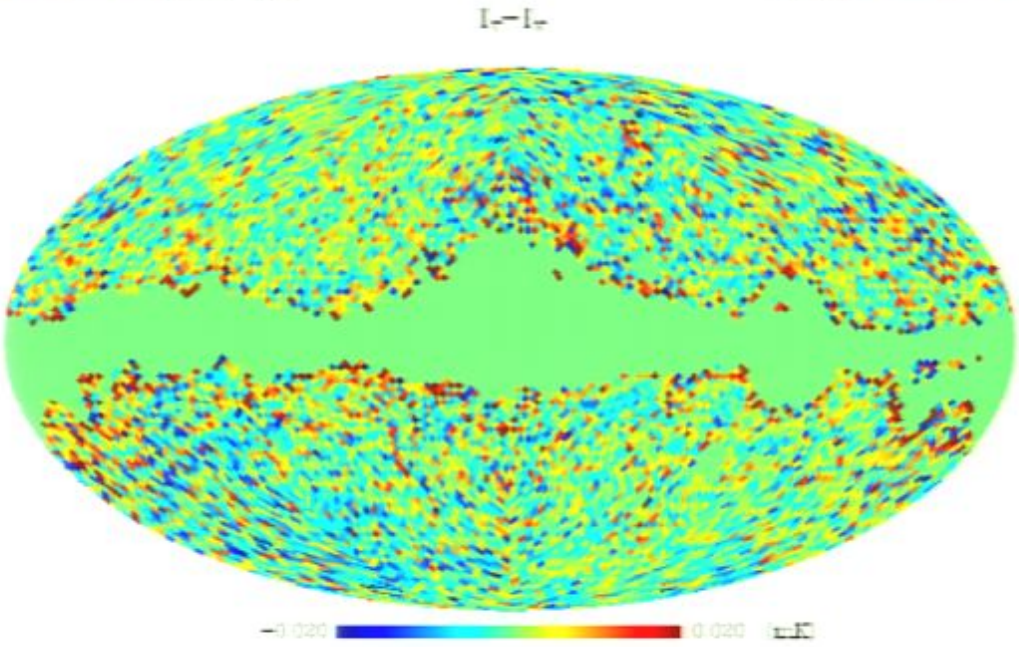

Simulated temperature difference maps

Simulation: $T_Q - T_V$

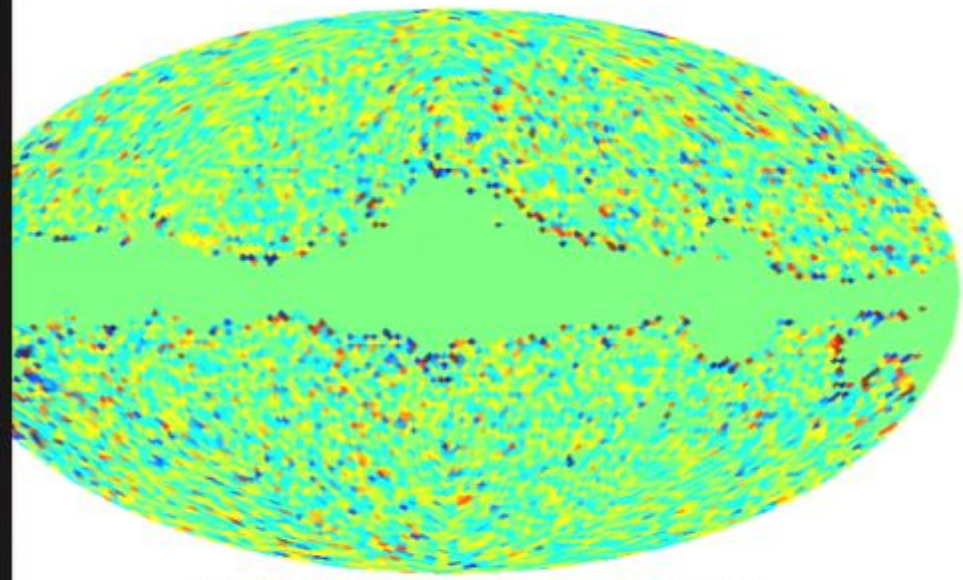

−0.020 0.020 (mK)

Simulation: $T_Q - T_W$

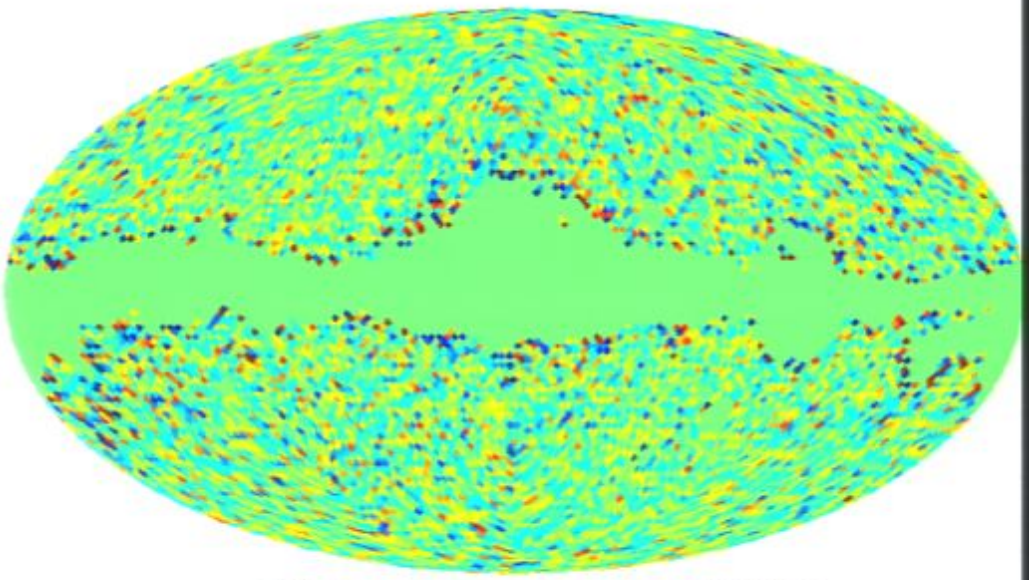

−0.020 0.020 (mK)

Simulation: $T_V - T_W$

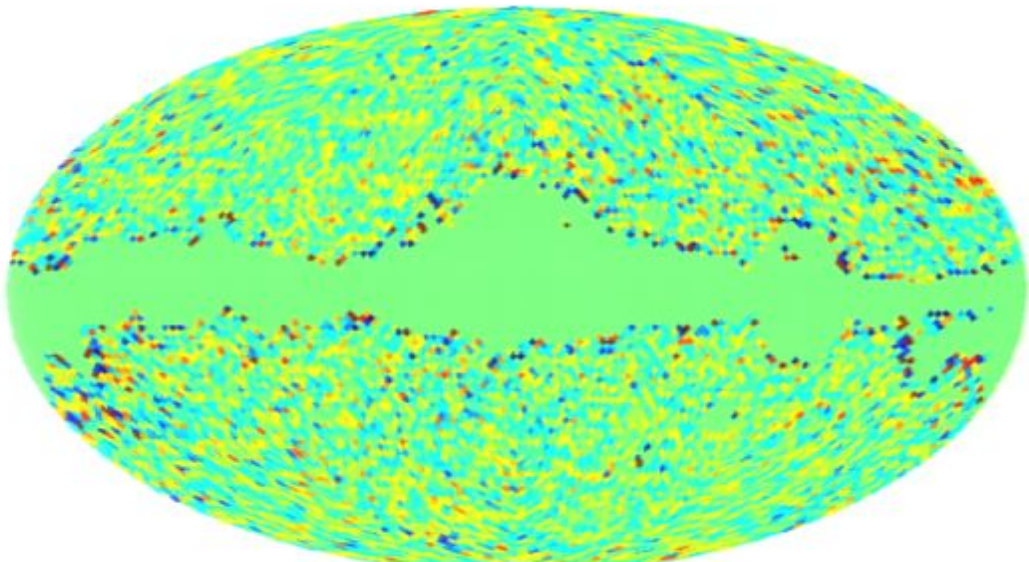

Actual temperature difference maps Q-V (left), Q-W (right), V-W (bottom)

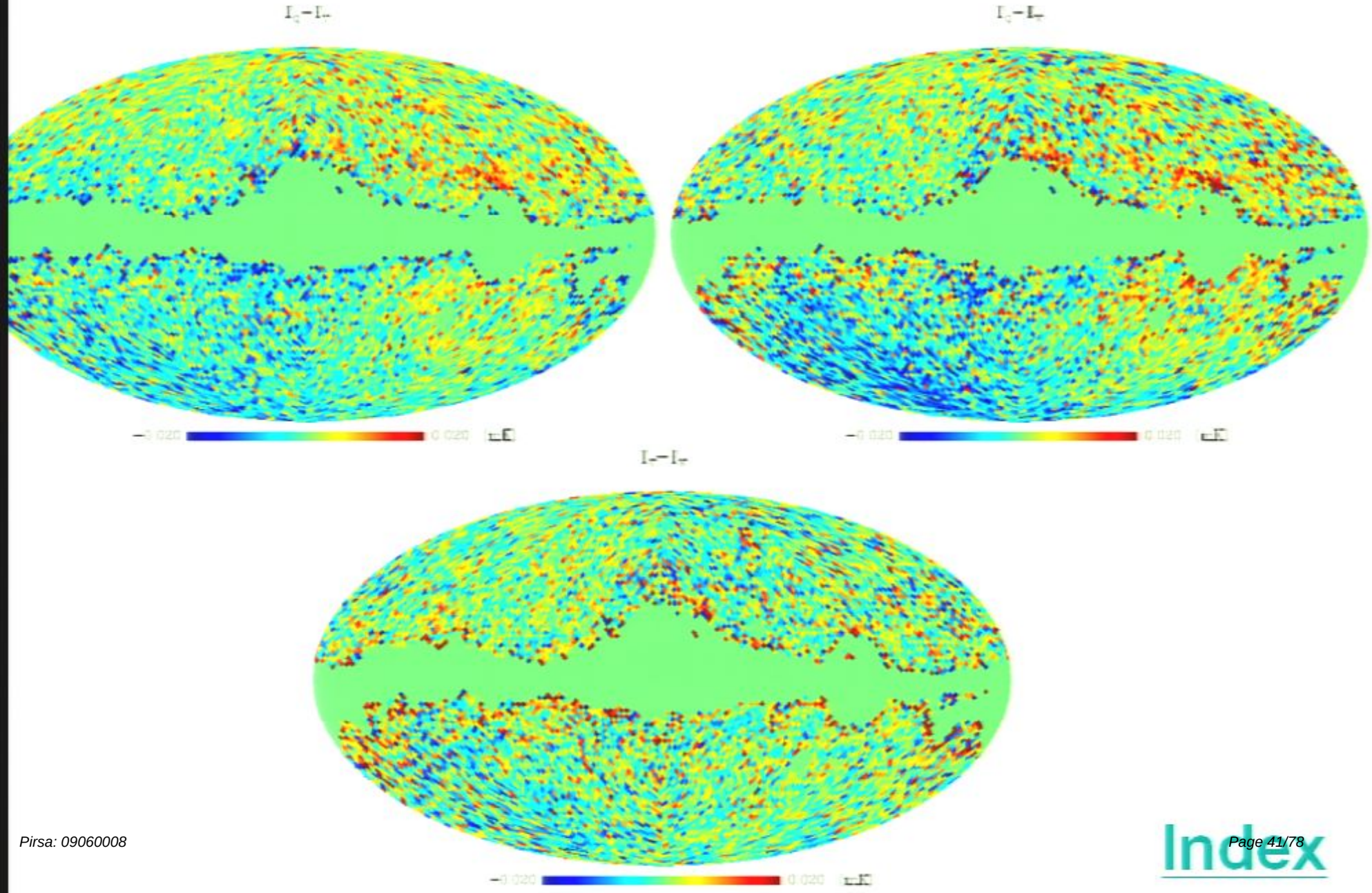

Simulated temperature difference maps

Simulation: $T_Q - T_V$

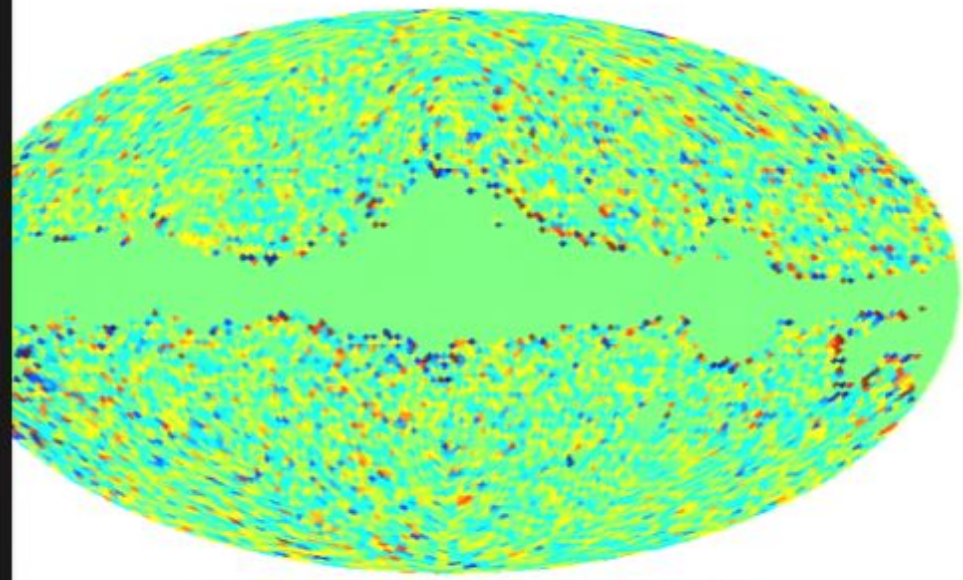

−0.020 0.020 (mK)

Simulation: $T_Q - T_W$

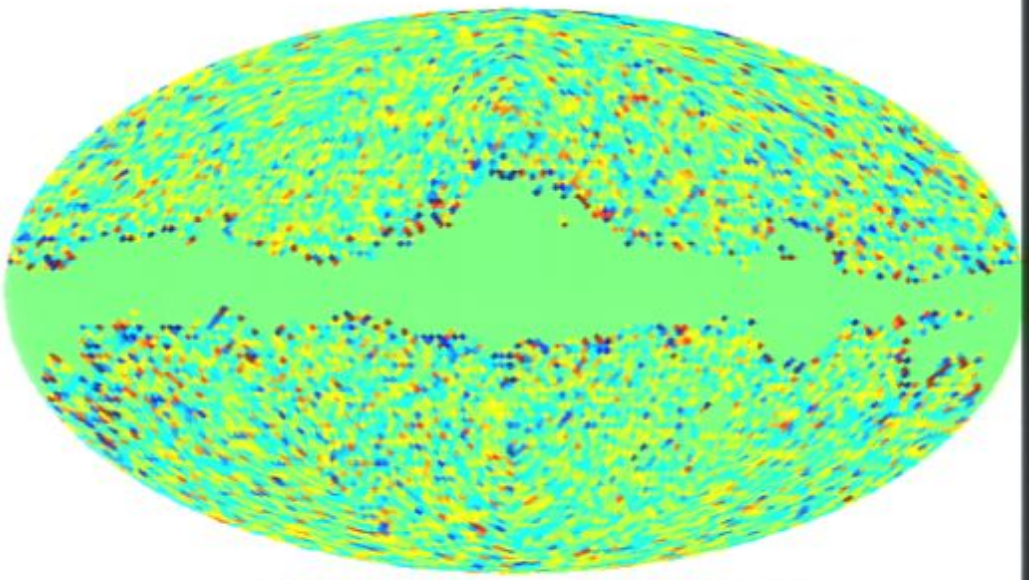

−0.020 0.020 (mK)

Simulation: $T_V - T_W$

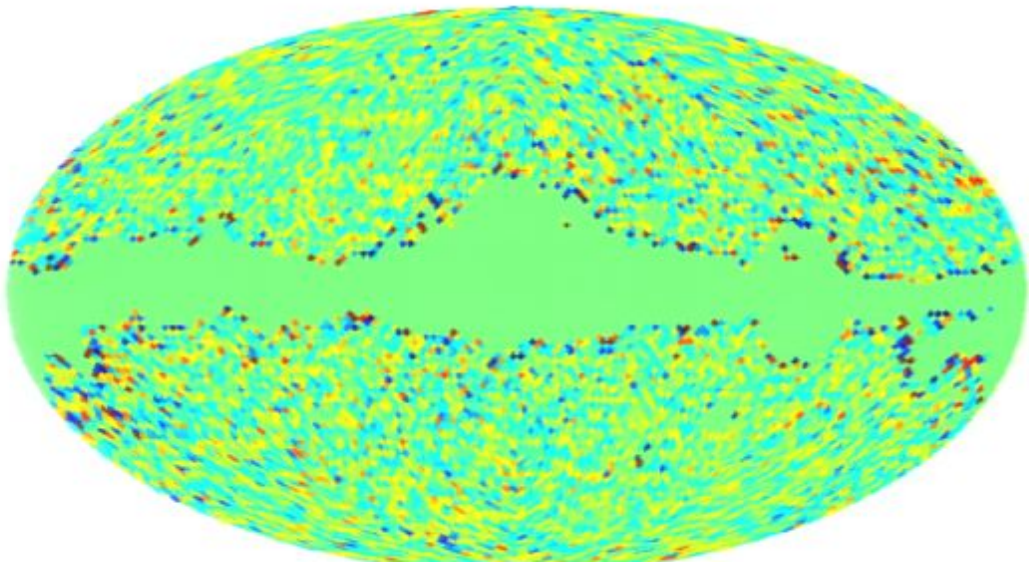

Actual temperature difference maps Q-V (left),Q-W (right),V-W (bottom)

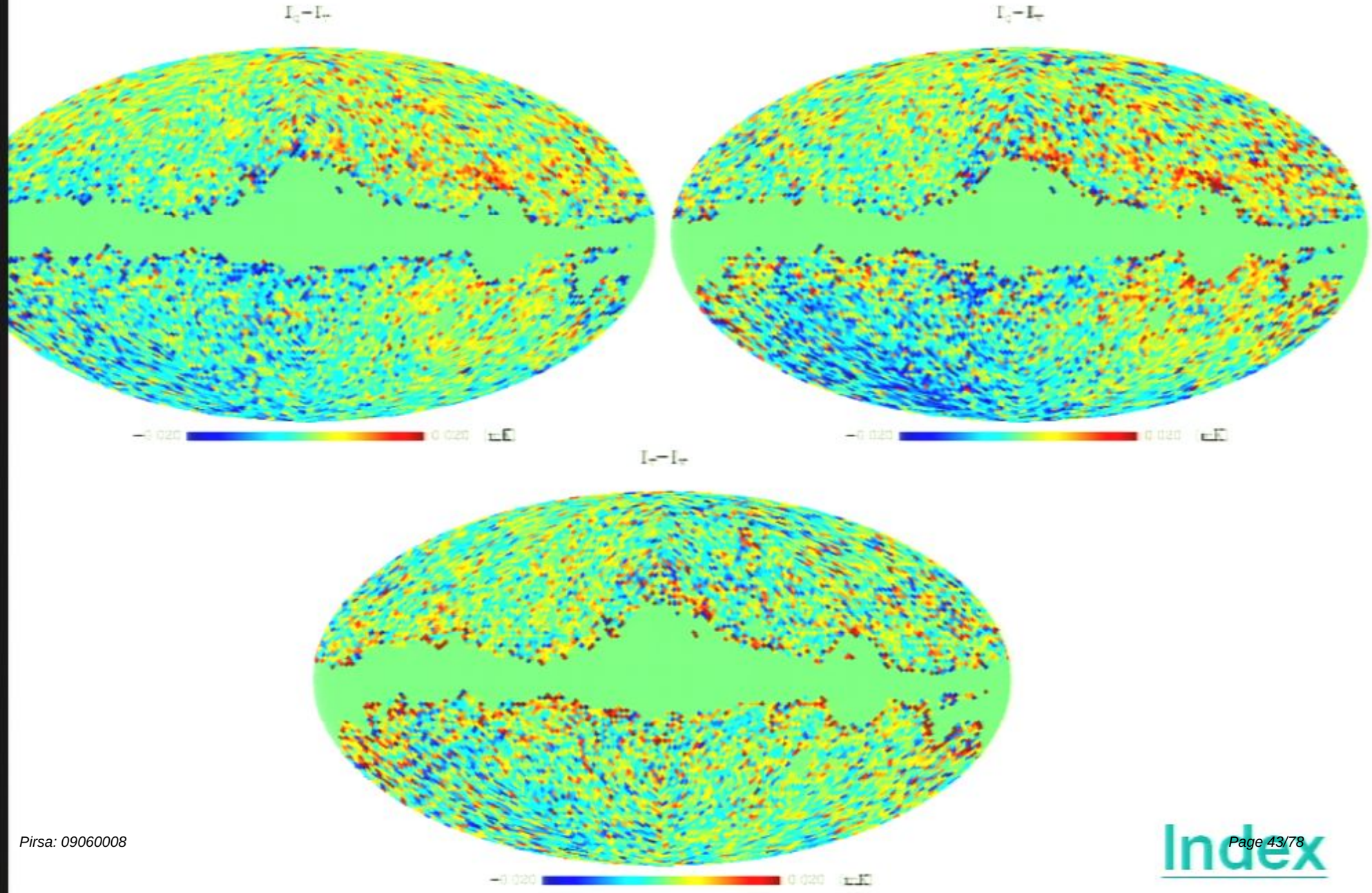

Simulated temperature difference maps

Simulation: $T_Q - T_V$

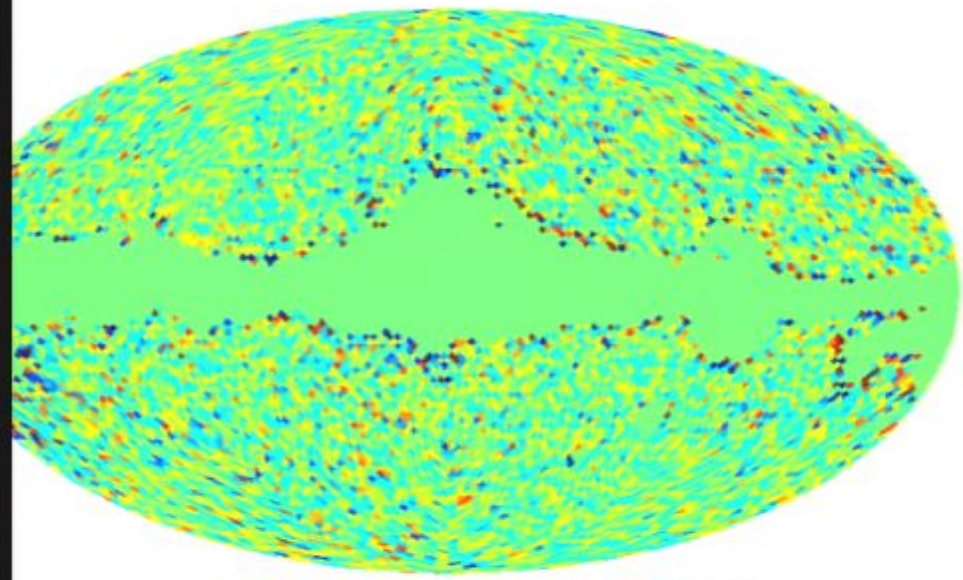

−0.020 0.020 (mK)

Simulation: $T_Q - T_W$

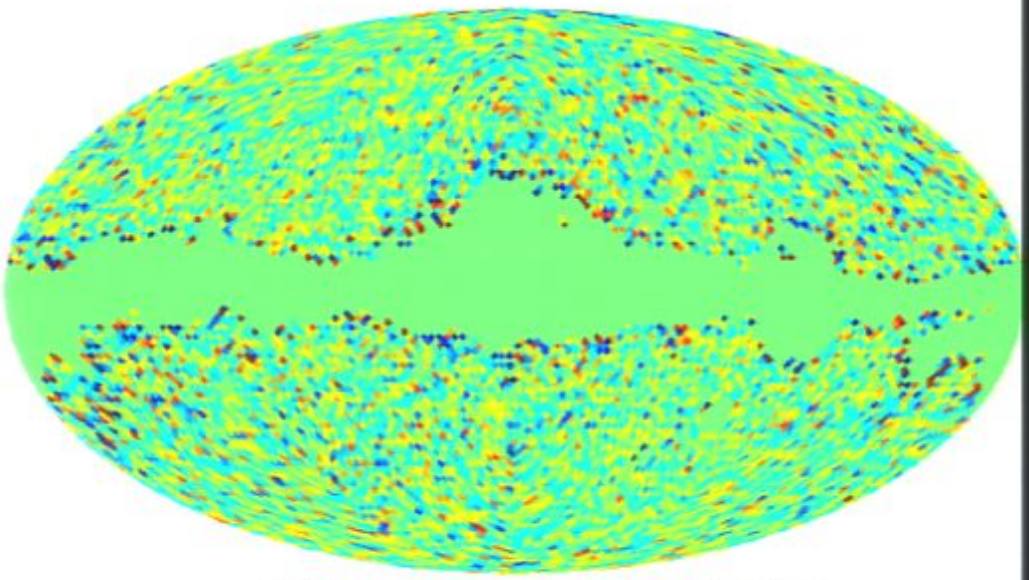

−0.020 0.020 (mK)

Simulation: $T_V - T_W$

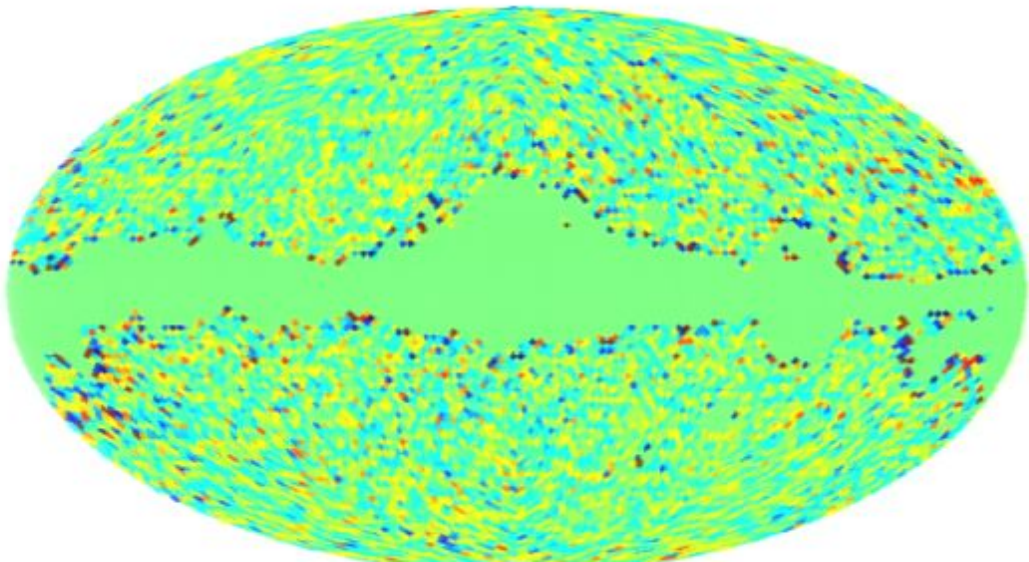

Actual temperature difference maps Q-V (left), Q-W (right), V-W (bottom)

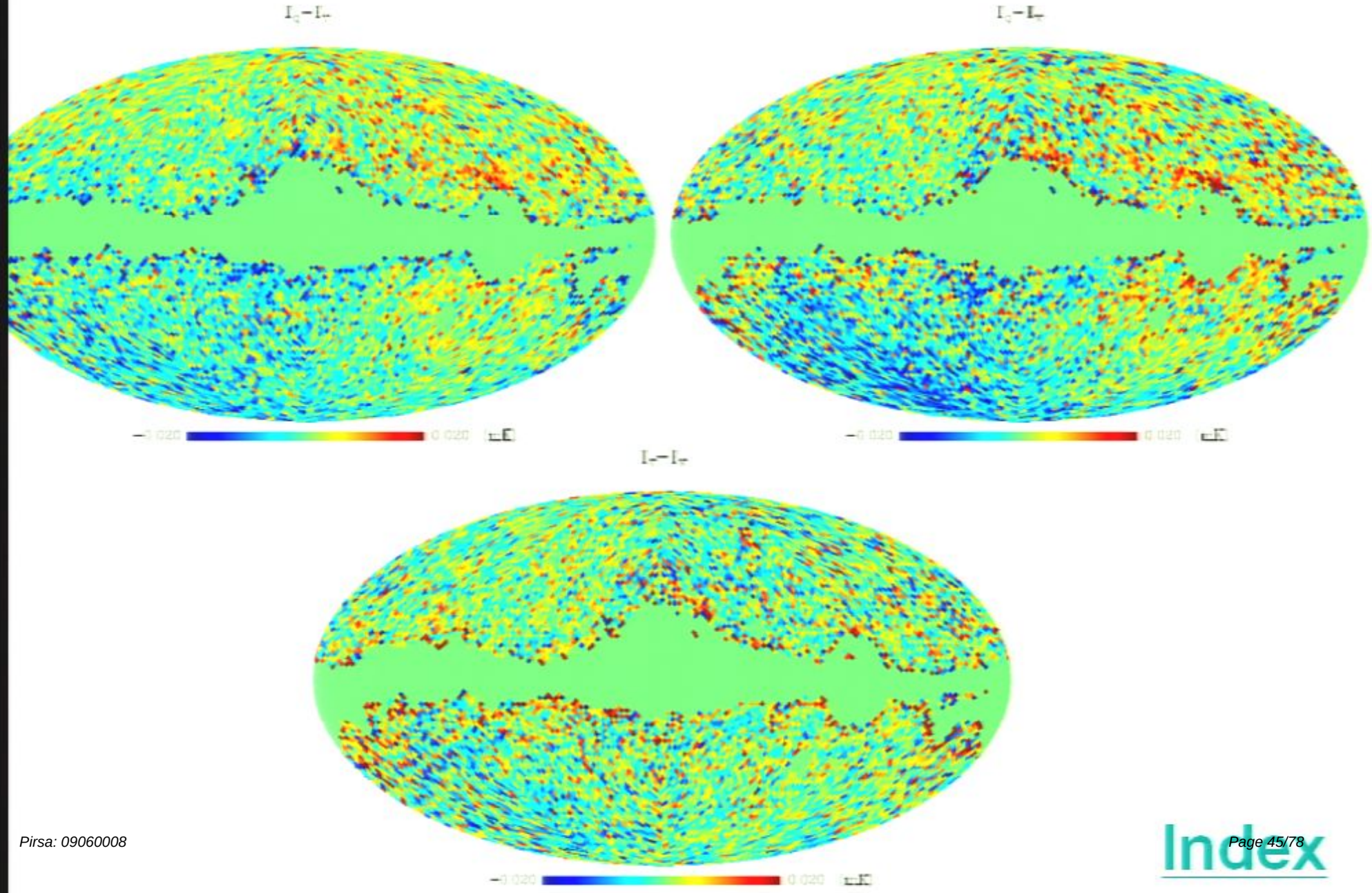

Dipole component of the Q-V and Q-W maps

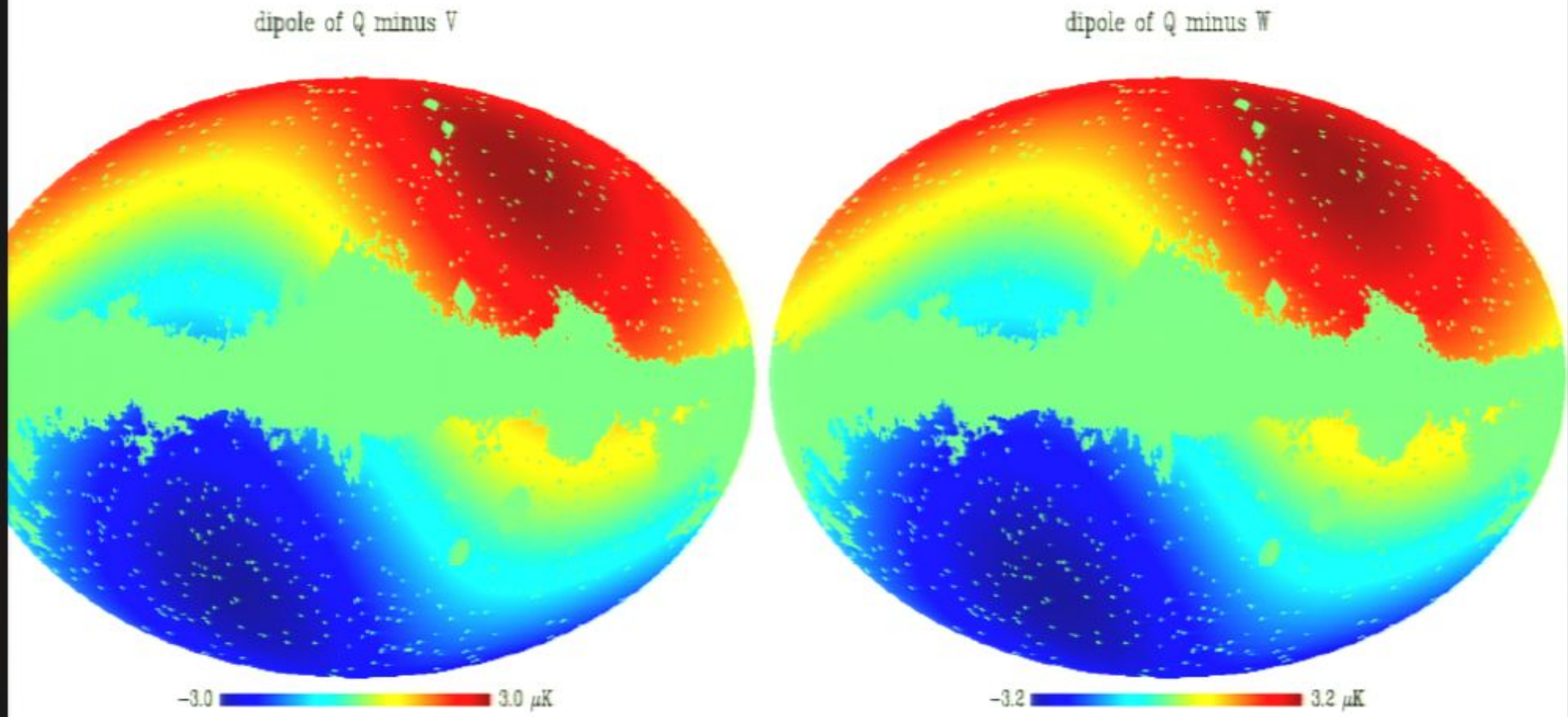

Quadrupole maps of Q-V (left),Q-W (right) & V-W (bottom)

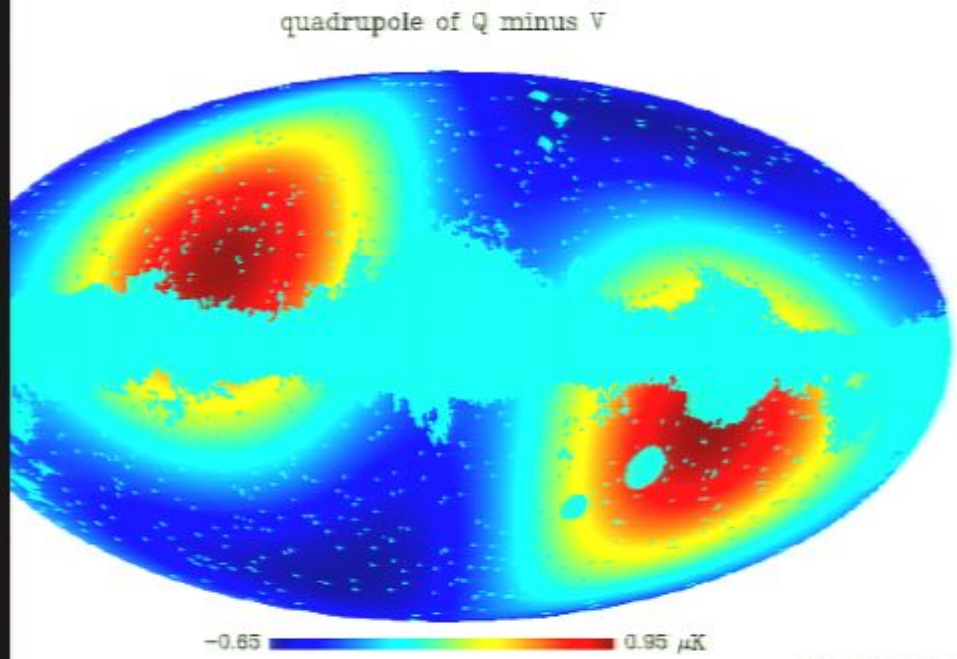

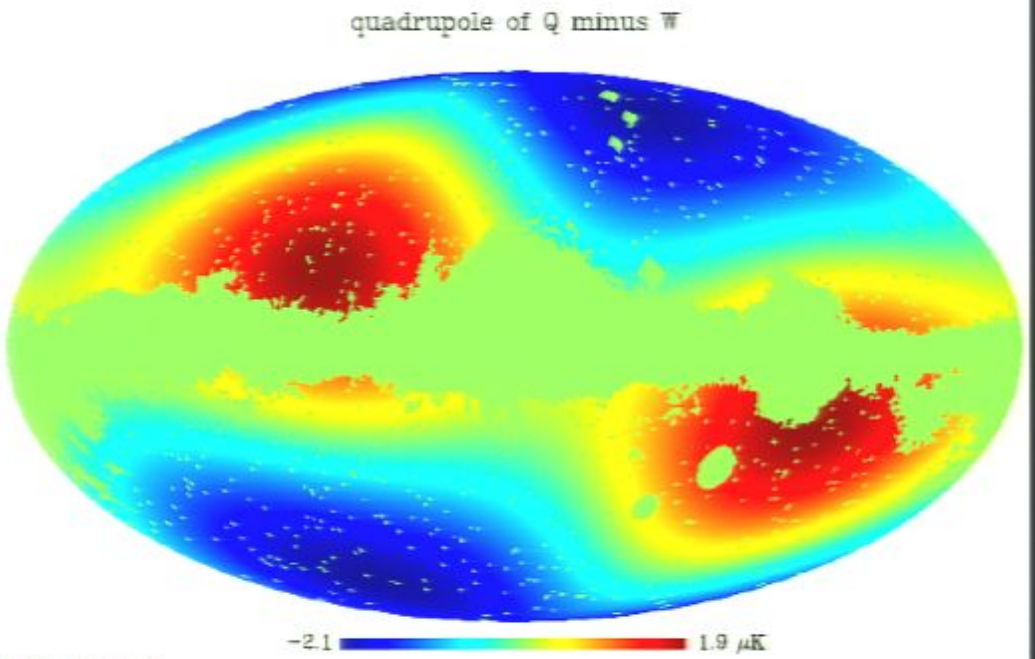

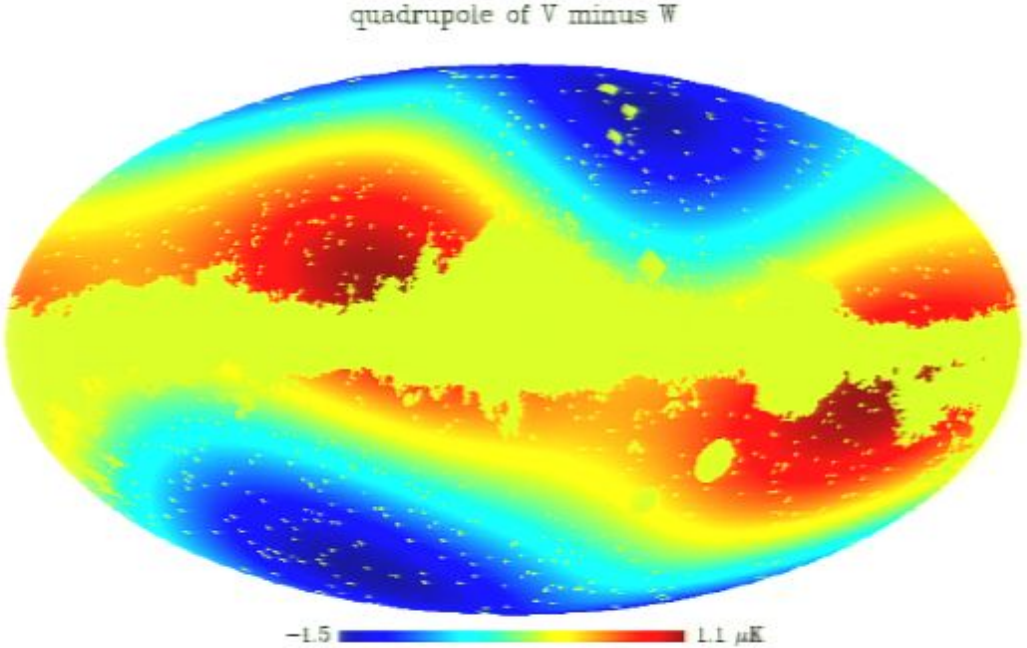

Dipole component of the Q-V and Q-W maps

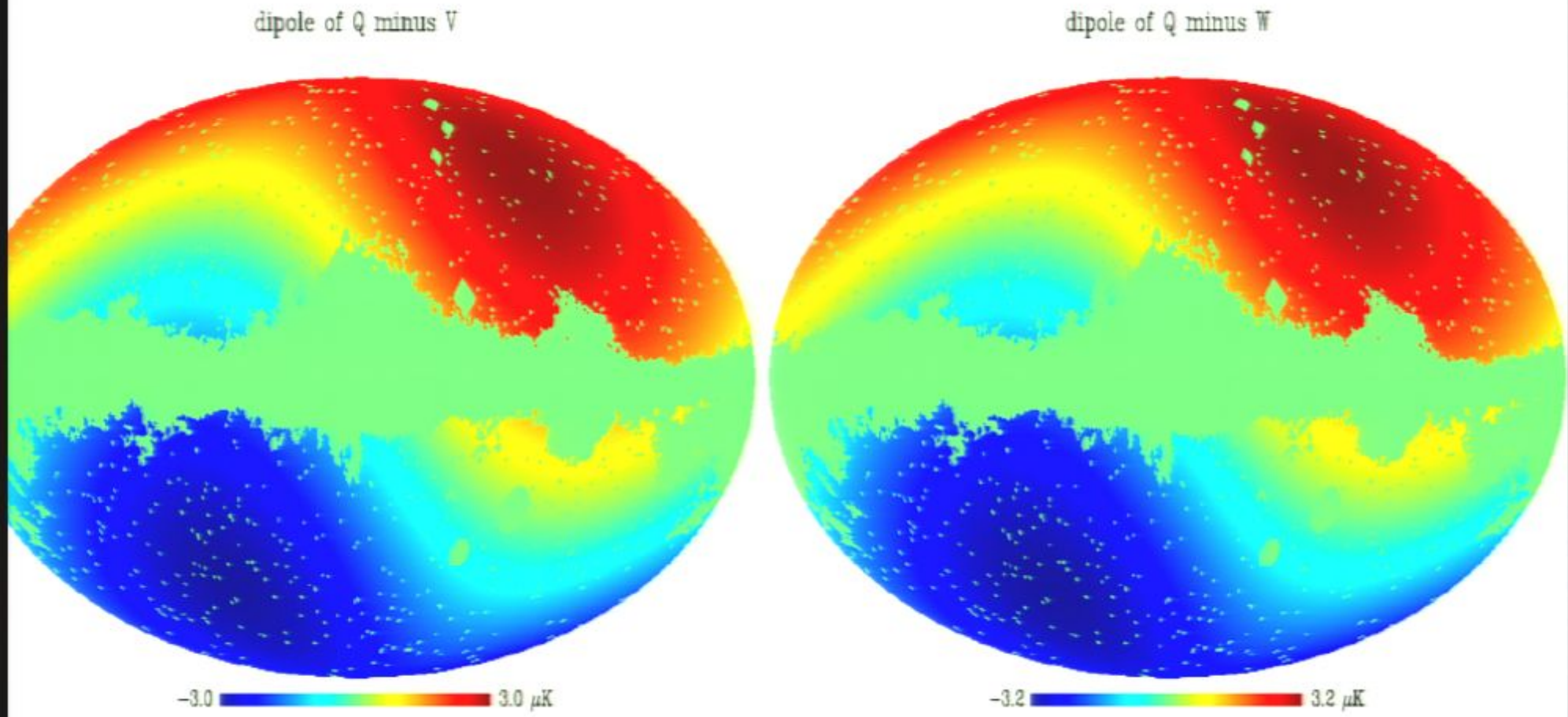

Quadrupole maps of Q-V (left),Q-W (right) & V-W (bottom)

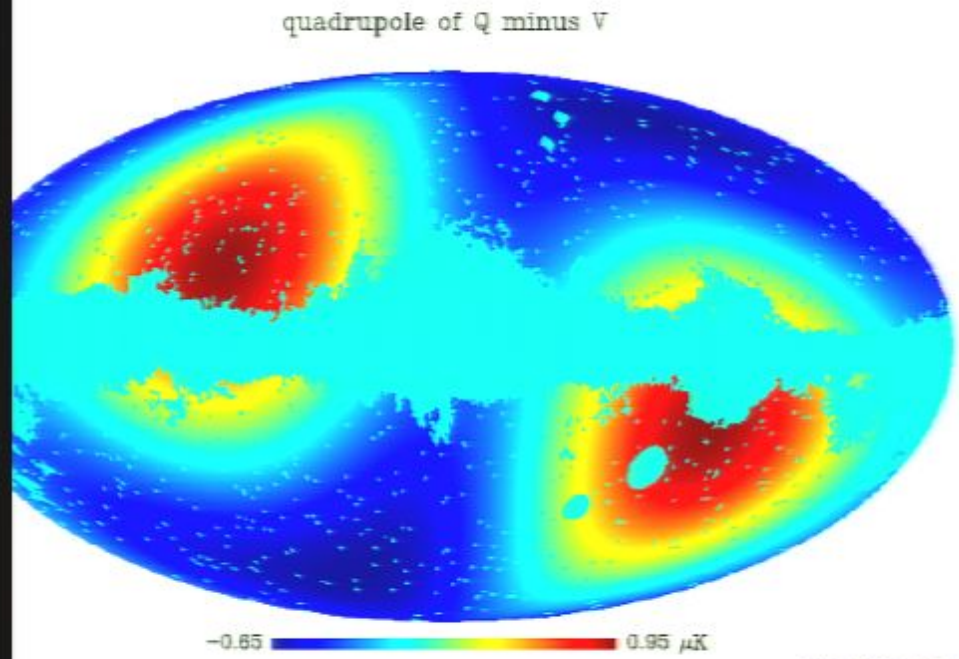

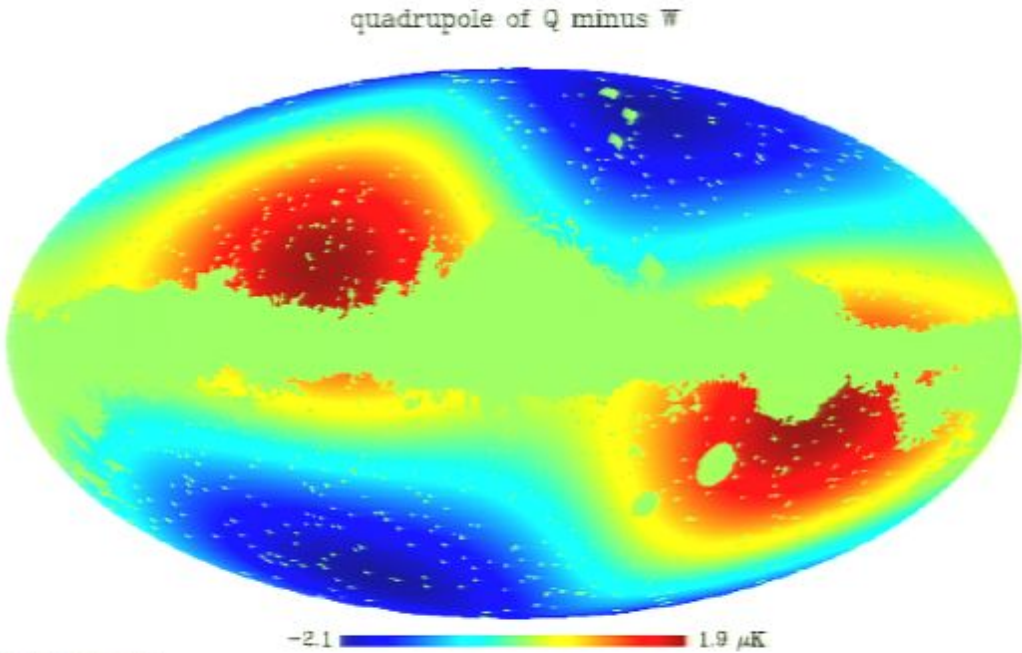

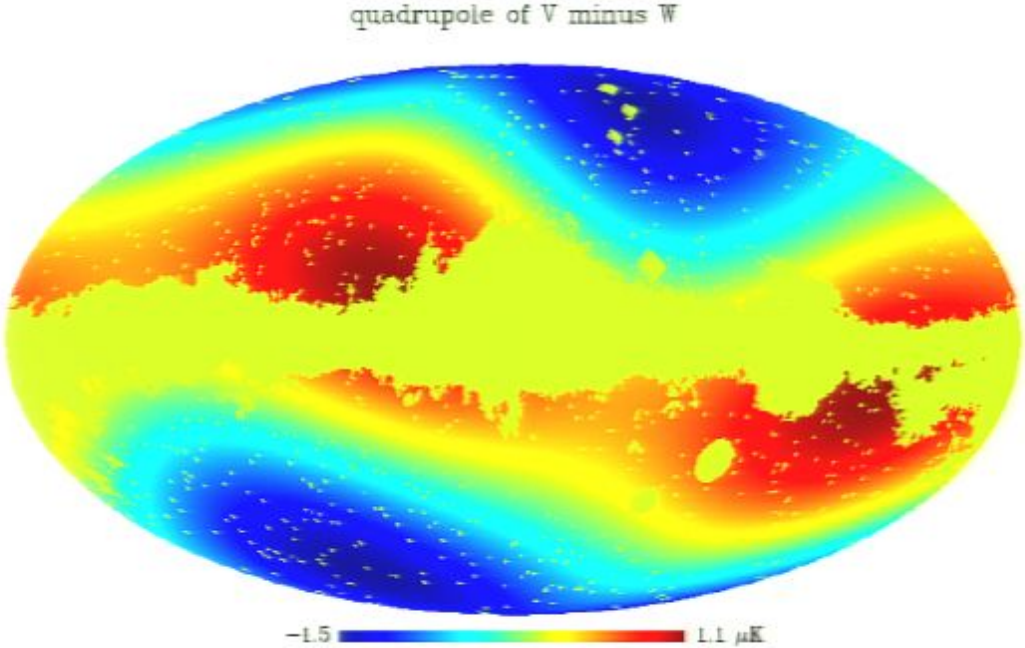

Quadrupole maps of Q-V (left),Q-W (right) & V-W (bottom)

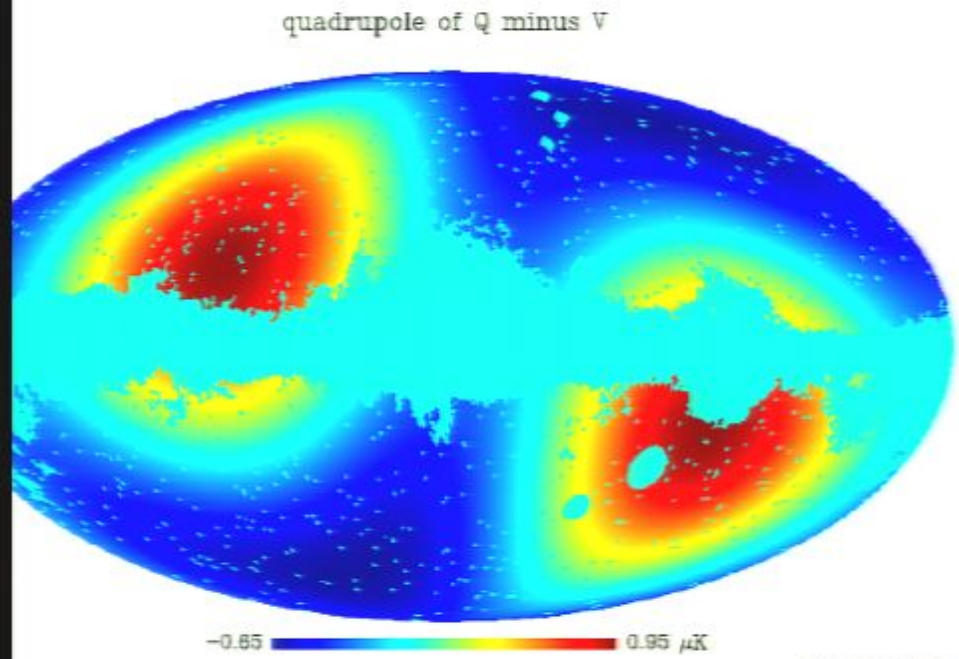

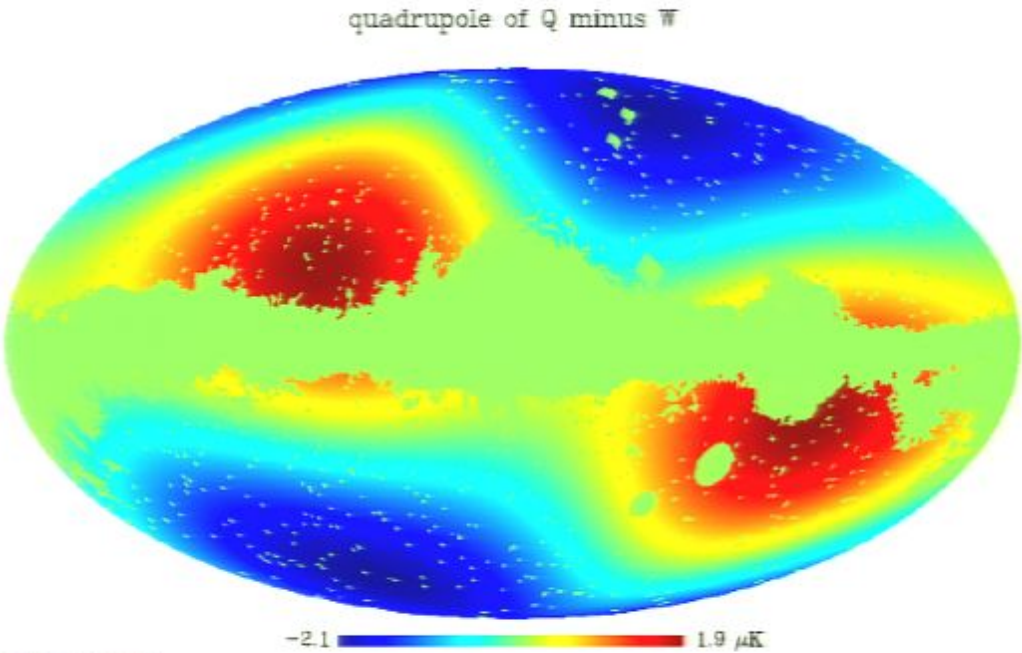

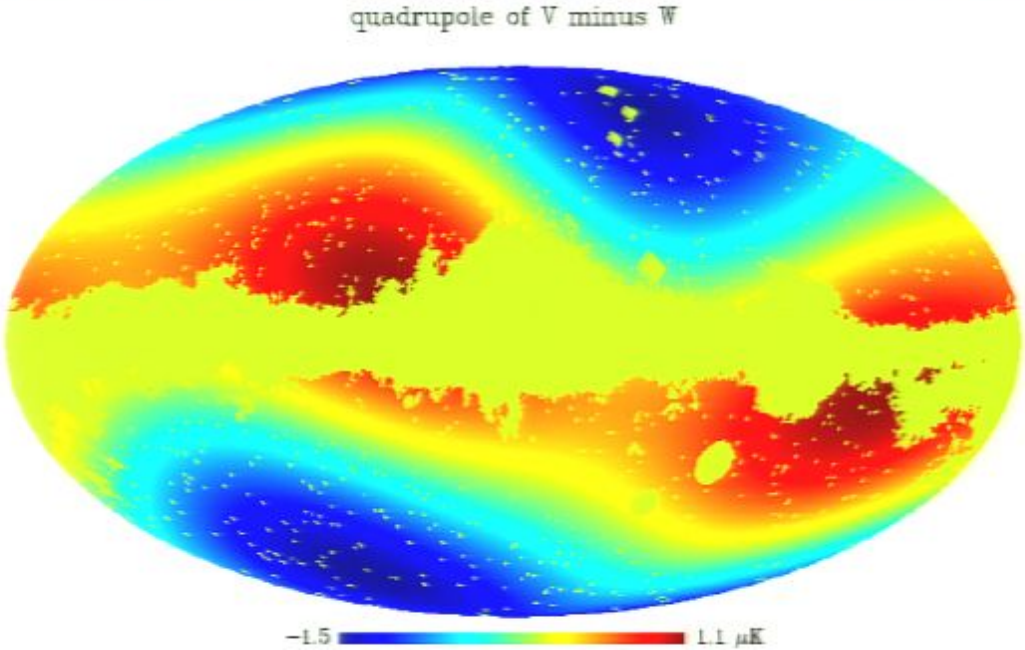

Low harmonic power spectra of the three temperature difference maps

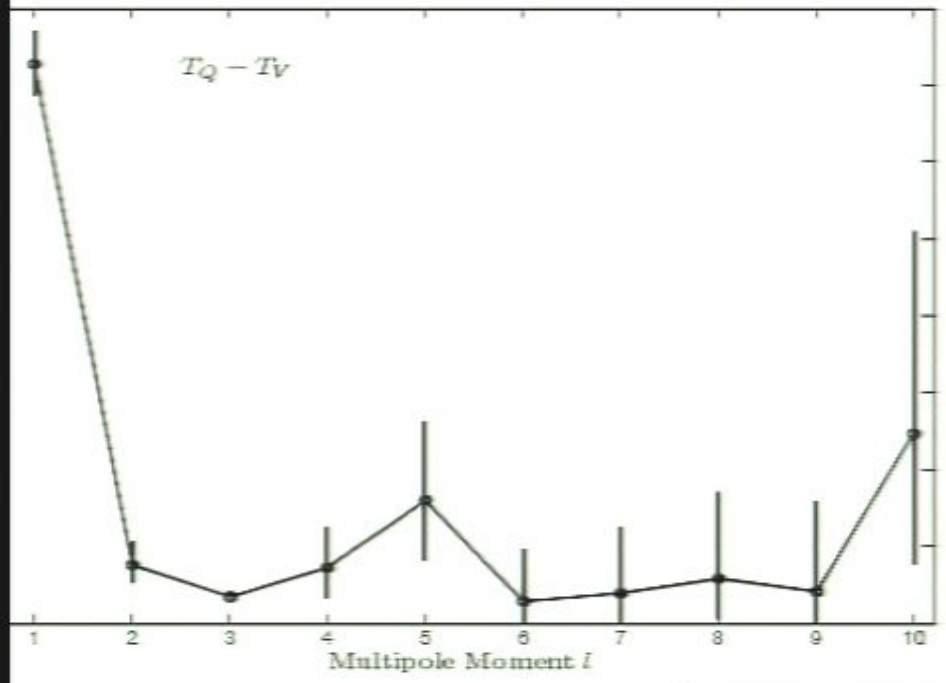

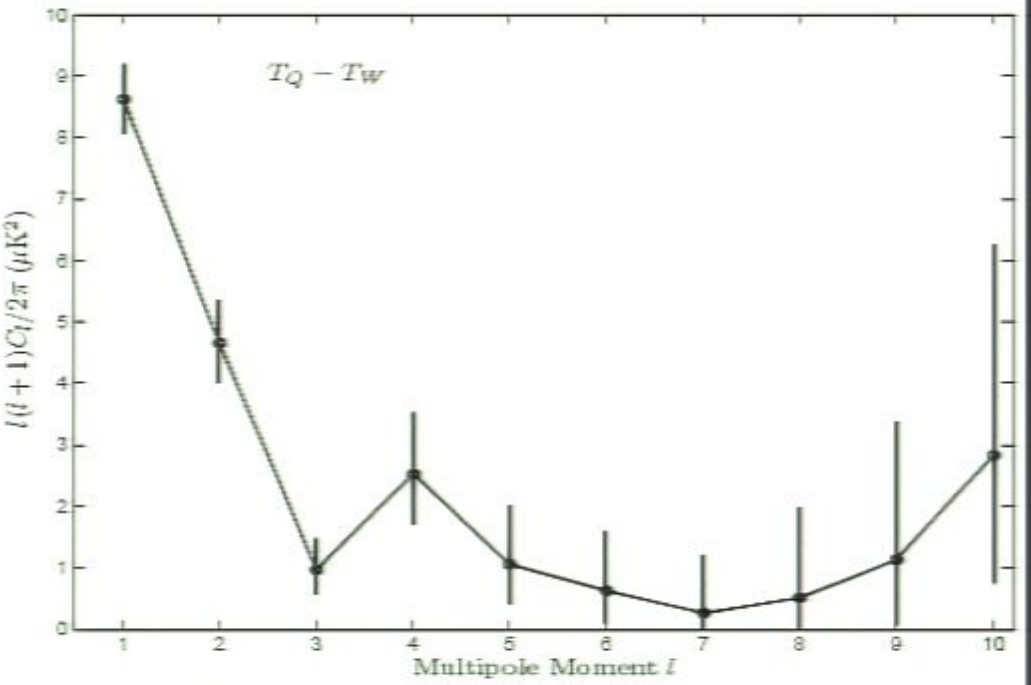

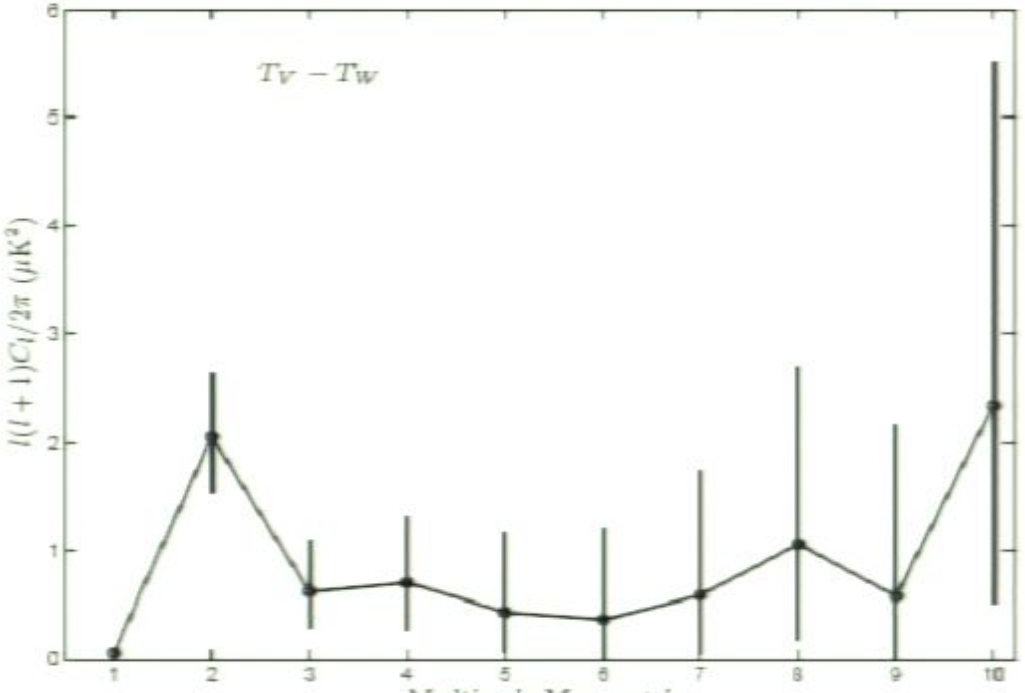

Notes:

Q-V top left
Q-W top right
V-W bottom

l=1 dipole
l=2 quadrupole

Actual temperature difference maps Q-V (left),Q-W (right),V-W (bottom)

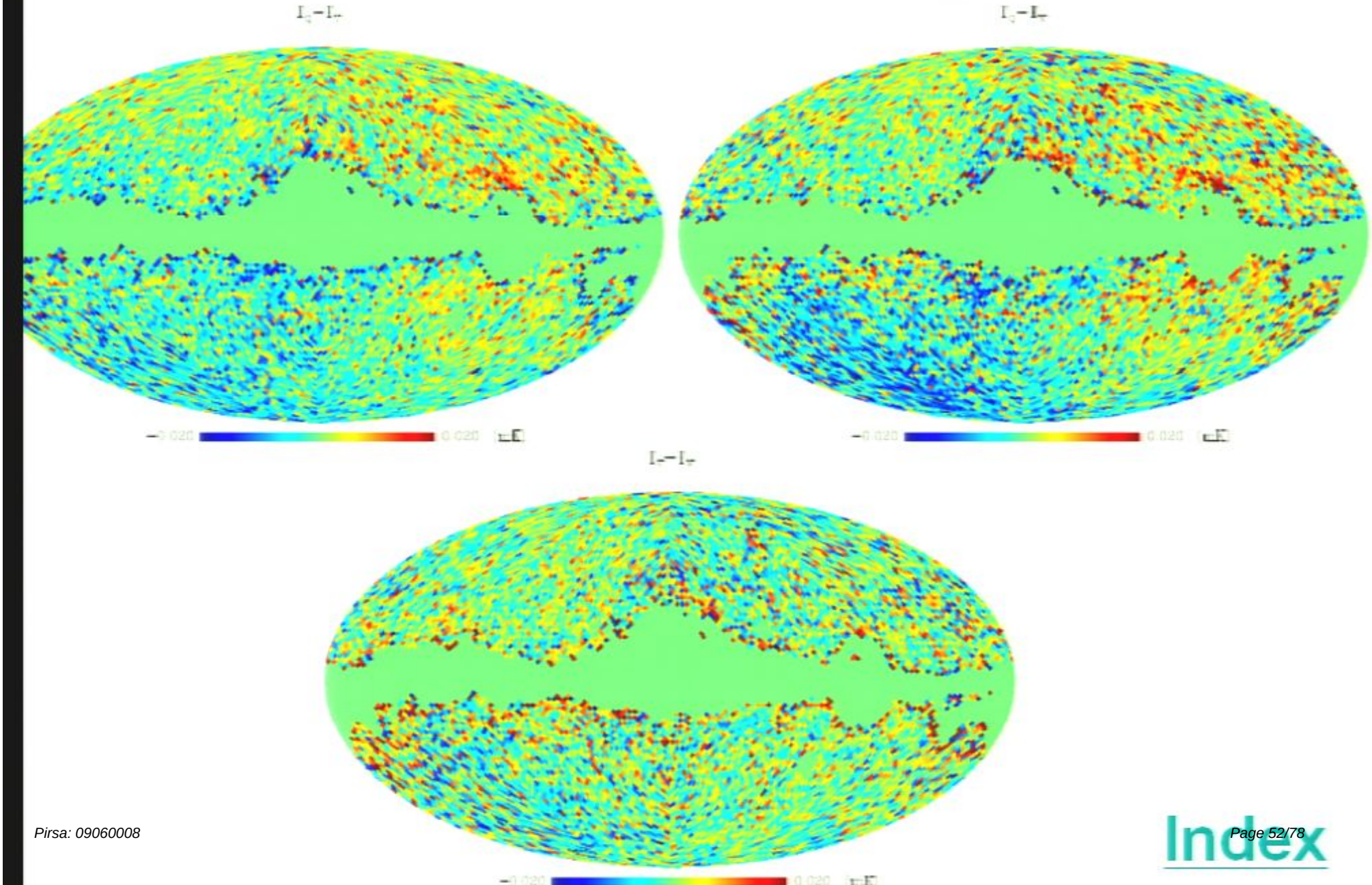

Quadrant sky distribution of Q-V temperature difference on 1-deg angular scale

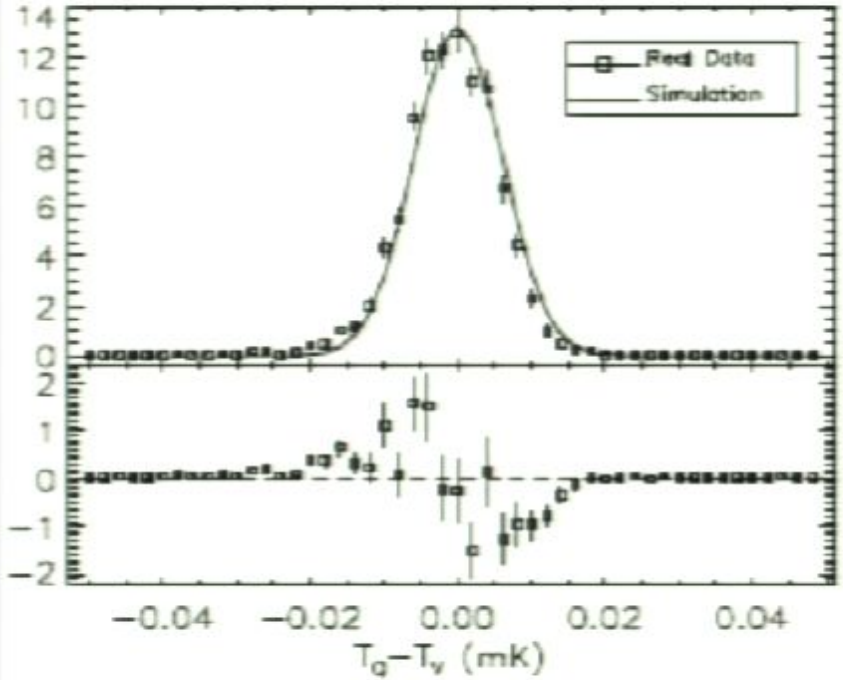

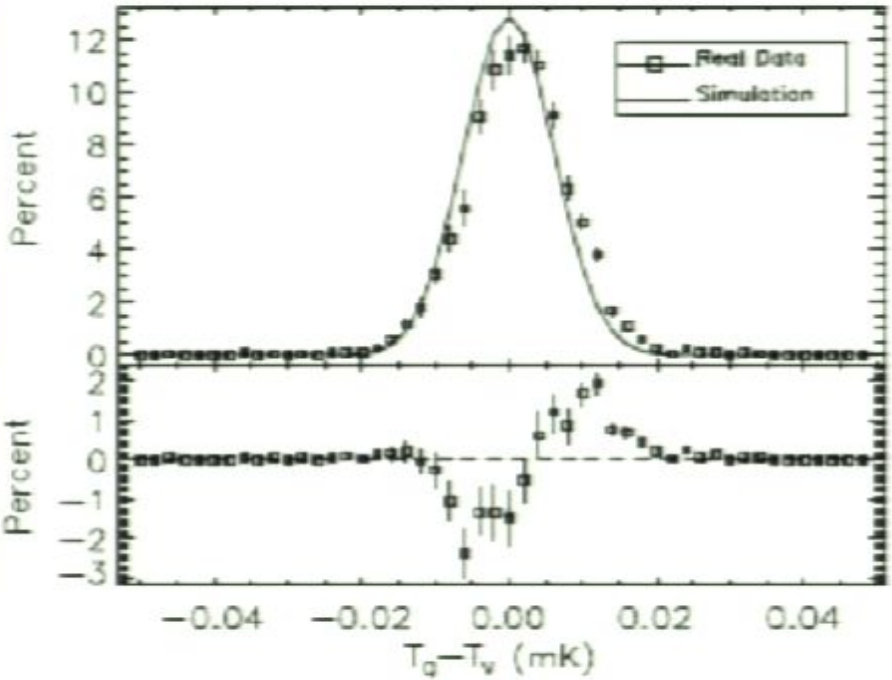

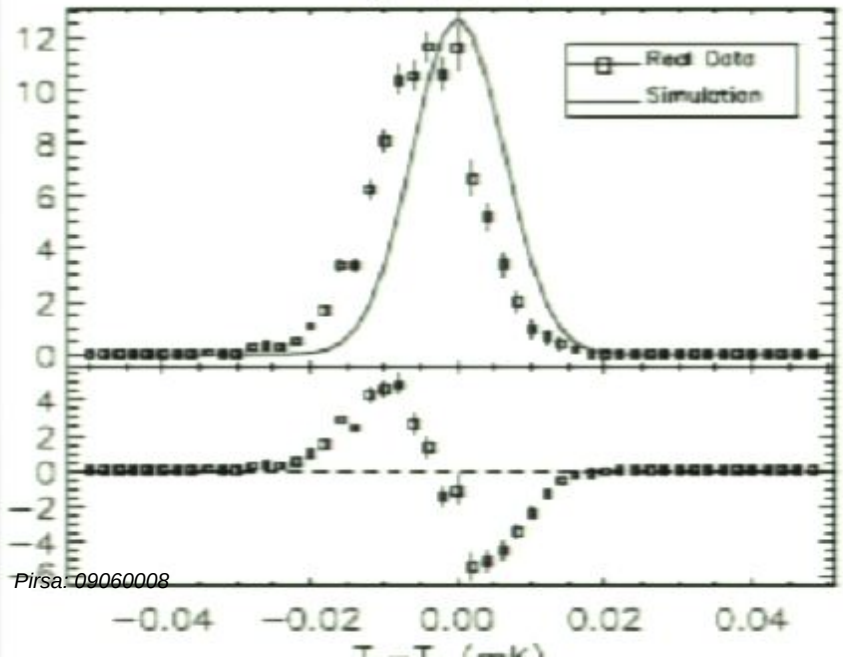

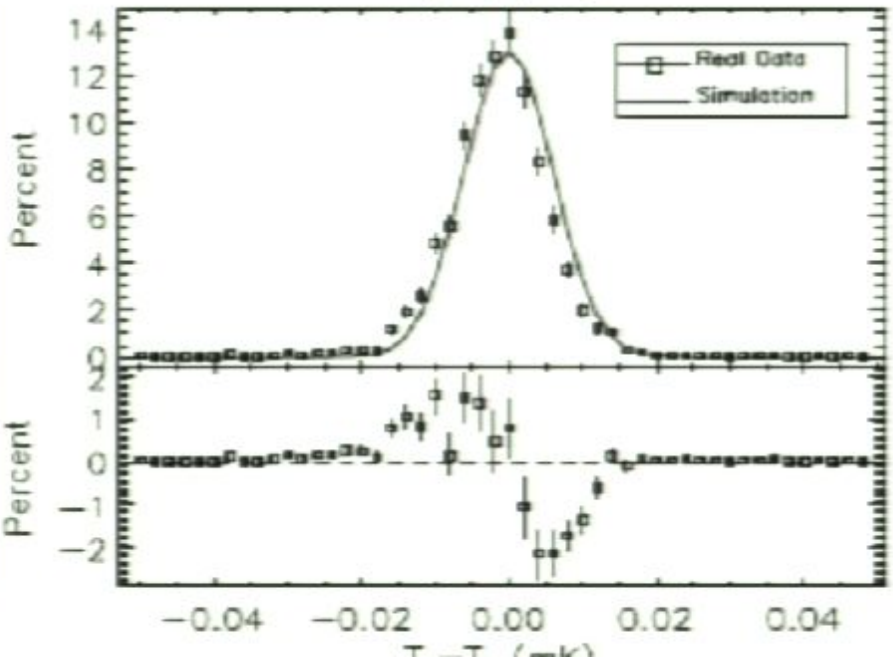

Actual temperature difference maps Q-V (left),Q-W (right),V-W (bottom)

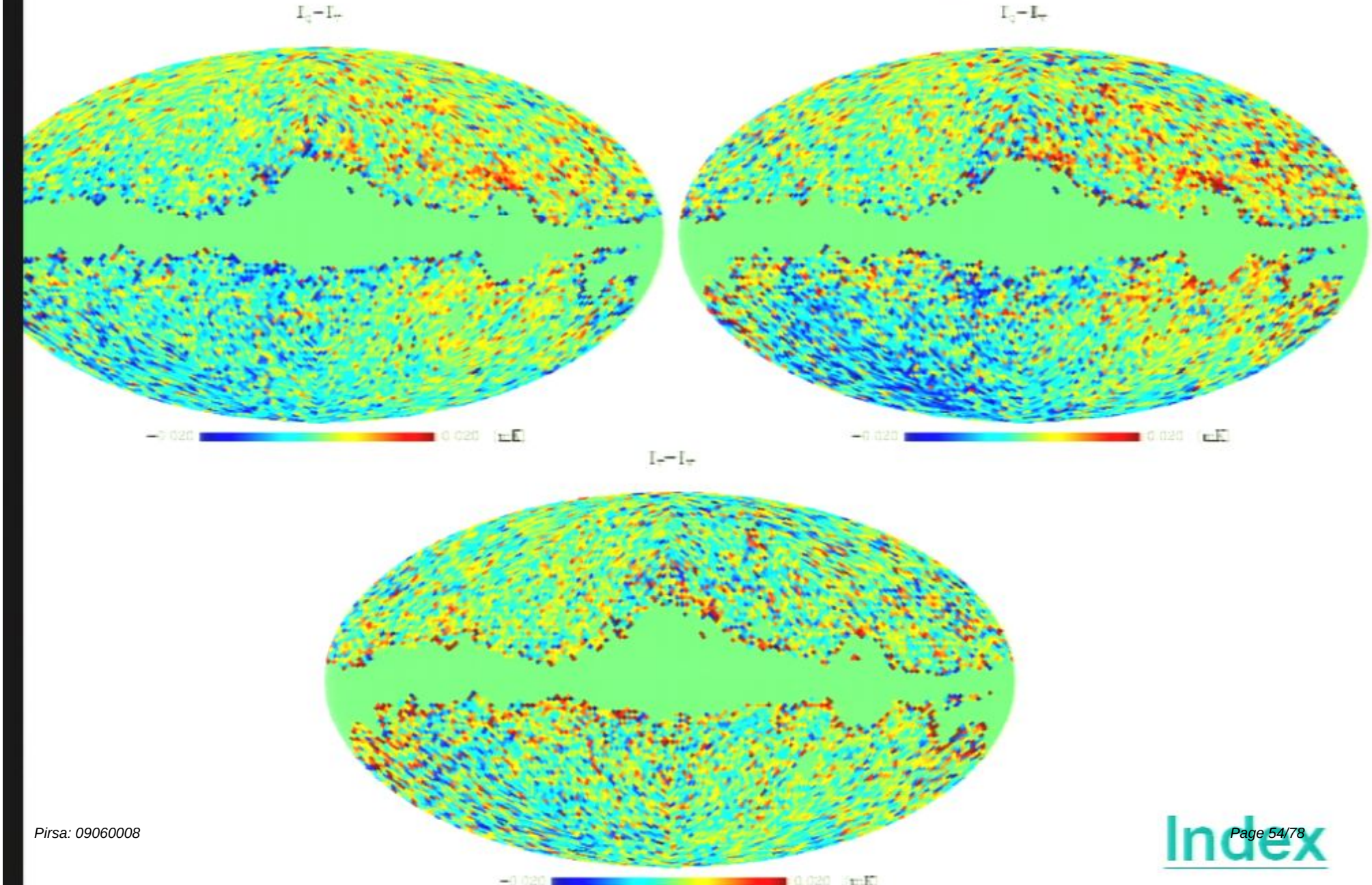

Quadrant sky distribution of Q-V temperature difference on 1-deg angular scale

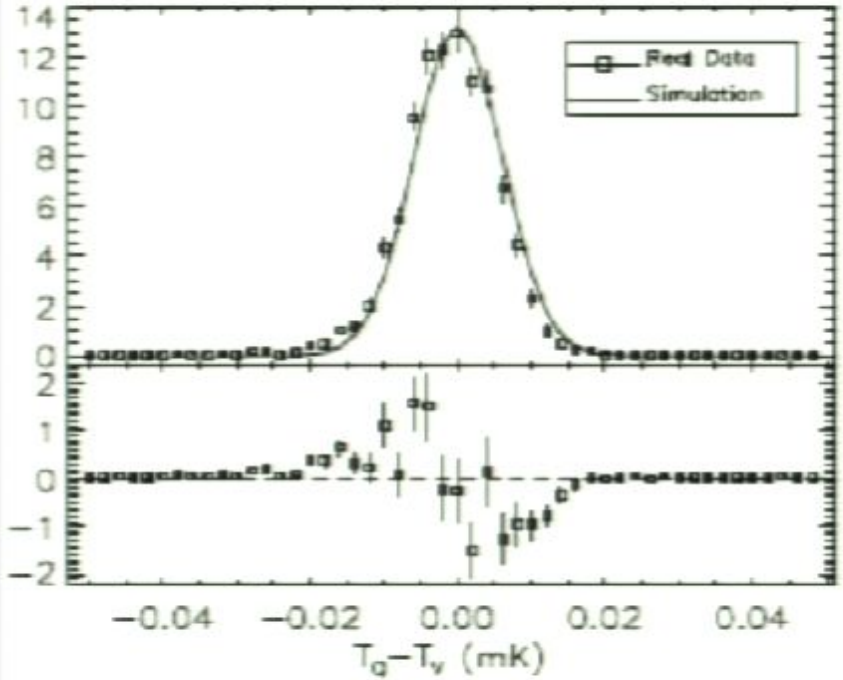

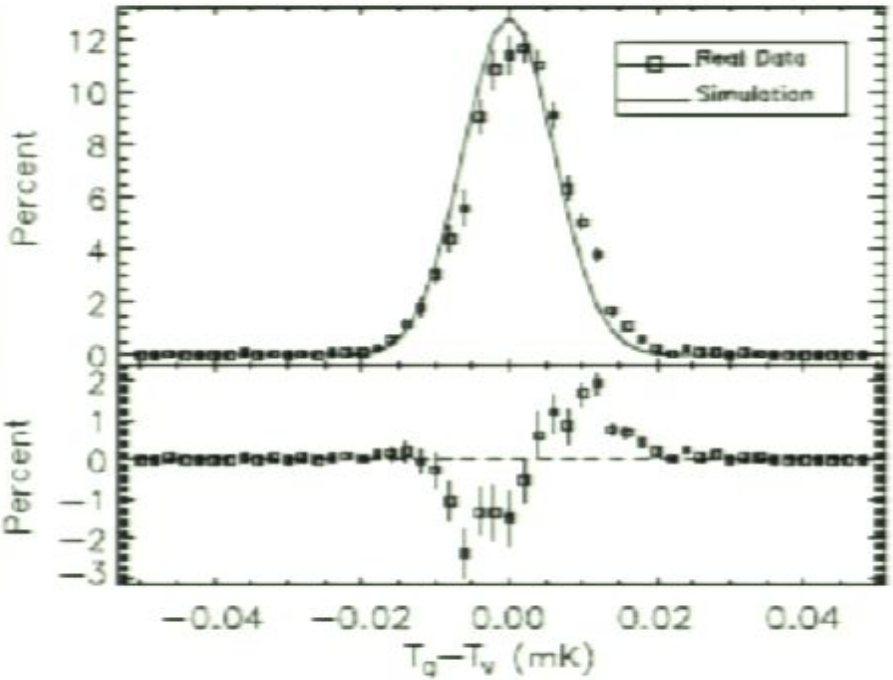

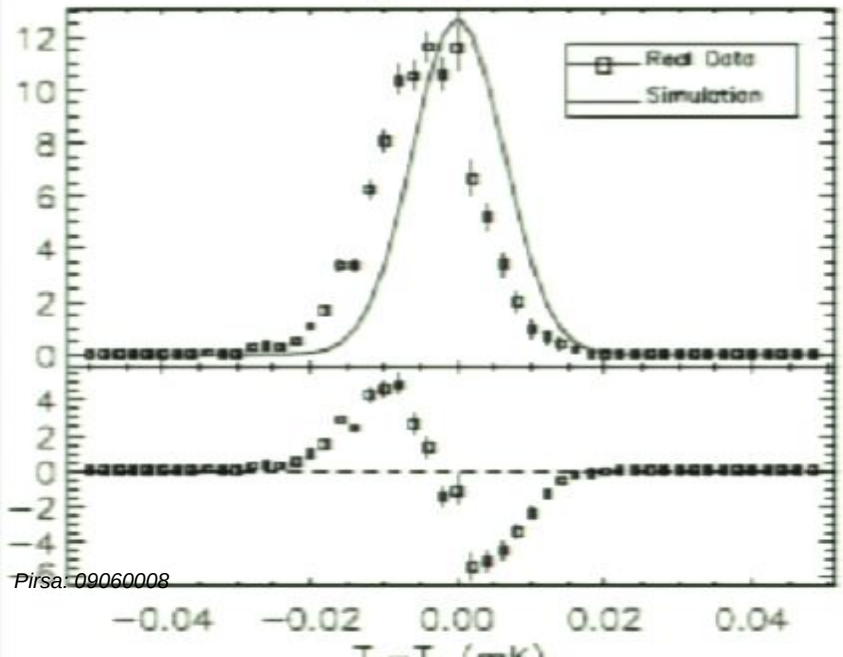

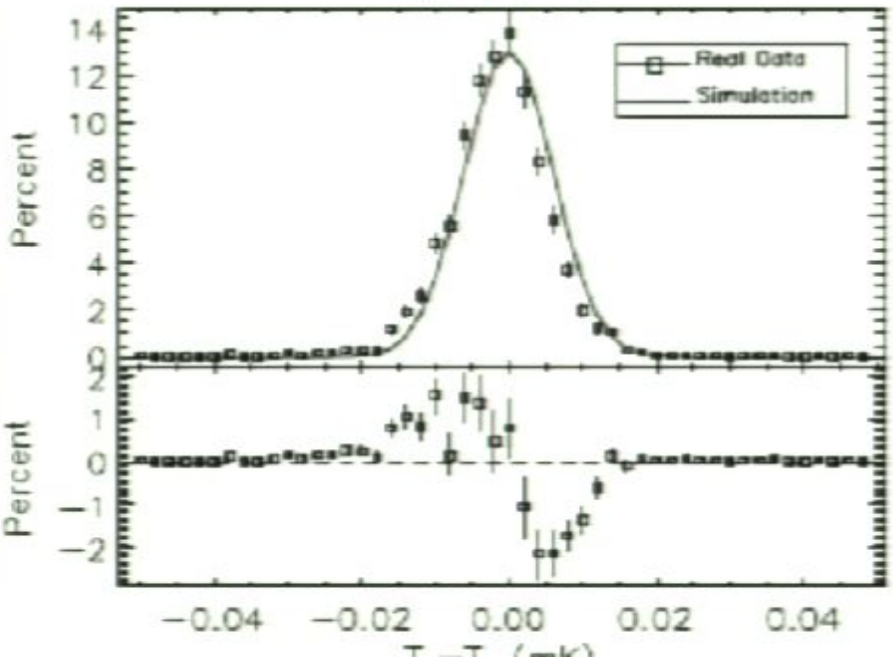

Distribution of 1-deg angular scale Q-V temperature: best gaussian parameters

Q - V		$\mu(\mu K)$	error (μK)	$\sigma(\mu K)$	error (μK)
Quadrant 1	WMAP5	1.17	0.13	6.85	0.10
	Simulation	0.0	0.0	6.11	0.10
	Difference Δ	1.17	0.13	3.10	0.30
Quadrant 2	WMAP5	-1.01	0.12	6.13	0.10
	Simulation	0.0	0.0	5.97	0.10
	Difference Δ	-1.01	0.12	1.39	0.59
Quadrant 3	WMAP5	-4.42	0.12	6.95	0.10
	Simulation	0.0	0.0	6.17	0.10
	Difference Δ	-4.42	0.12	3.20	0.30
Quadrant 4	WMAP5	-1.31	0.12	6.28	0.10
	Simulation	0.0	0.0	6.05	0.10
	Difference Δ	-1.31	0.12	1.68	0.52

Distribution of 1 deg angular scale Q-W temperature: best gaussian fits

Q - W		μ (μK)	error (μK)	σ (μK)	error (μK)
Quadrant 1	WMAP5	1.00	0.15	8.17	0.13
	Simulation	0.0	0.0	7.11	0.12
	Difference Δ	1.00	0.15	4.02	0.33
Quadrant 2	WMAP5	-0.43	0.14	6.66	0.12
	Simulation	0.0	0.0	6.92	0.12
	Difference Δ	-0.43	0.14	-1.88*	0.59
Quadrant 3	WMAP5	-4.83	0.16	8.39	0.15
	Simulation	0.0	0.0	7.14	0.12
	Difference Δ	-4.83	0.16	4.41	0.35
Quadrant 4	WMAP5	-0.90	0.14	7.34	0.11
	Simulation	0.0	0.0	7.04	0.11
	Difference Δ	-0.90	0.14	2.08	0.53

Quadrant sky distribution of Q-W temperatures on 1-deg angular scale

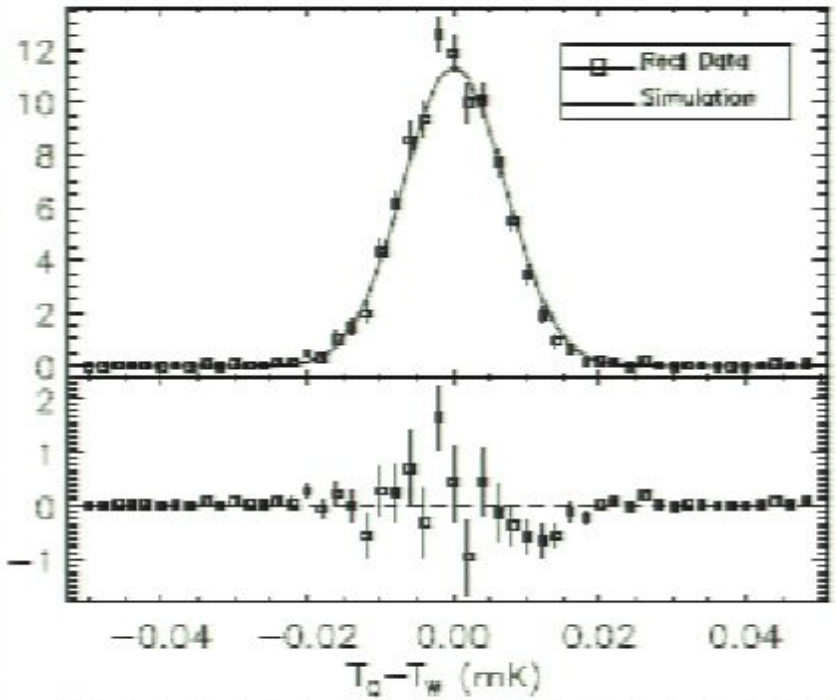

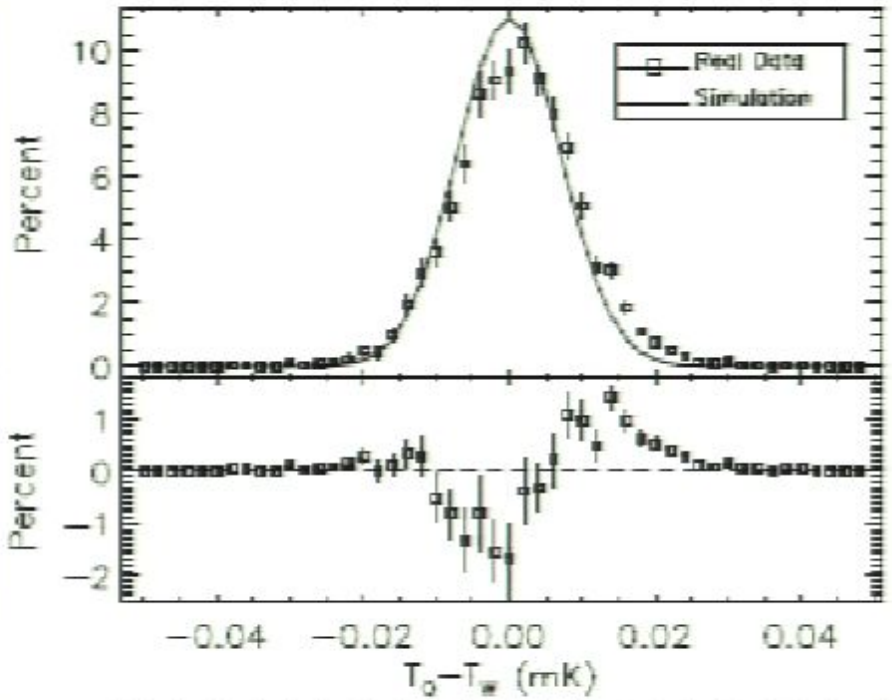

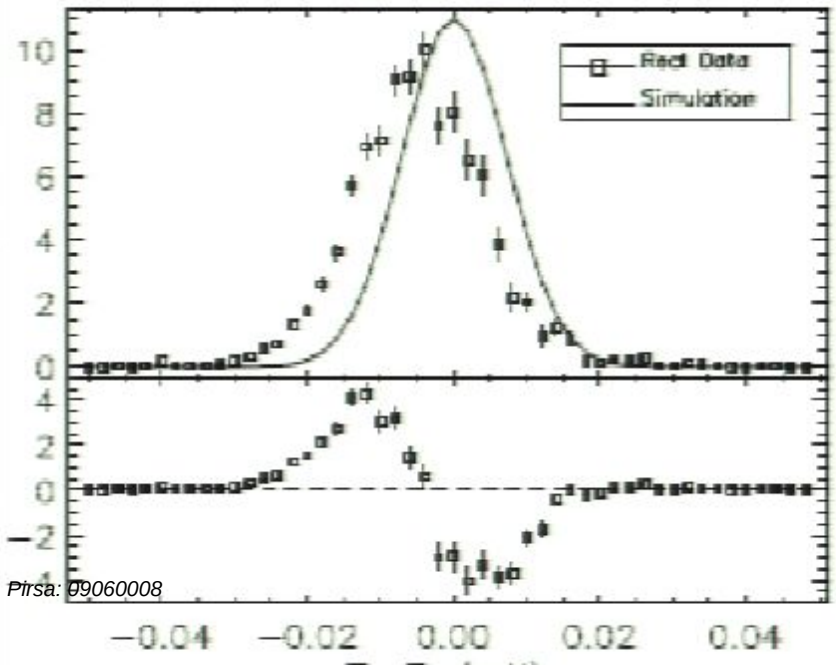

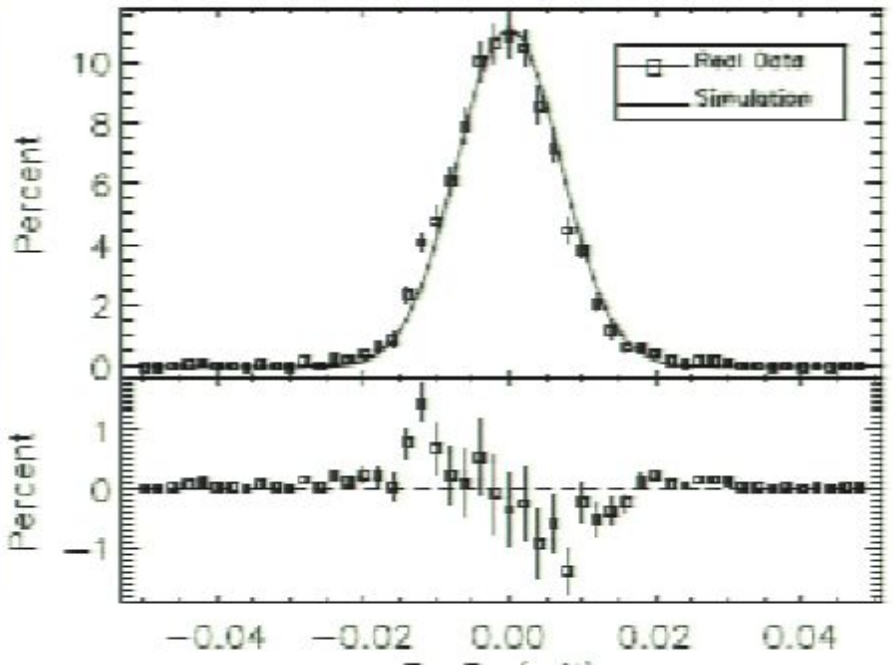

Distribution of 1 deg angular scale Q-W temperature: best gaussian fits

Q - W		μ (μK)	error (μK)	σ (μK)	error (μK)
Quadrant 1	WMAP5	1.00	0.15	8.17	0.13
	Simulation	0.0	0.0	7.11	0.12
	Difference Δ	1.00	0.15	4.02	0.33
Quadrant 2	WMAP5	-0.43	0.14	6.66	0.12
	Simulation	0.0	0.0	6.92	0.12
	Difference Δ	-0.43	0.14	-1.88*	0.59
Quadrant 3	WMAP5	-4.83	0.16	8.39	0.15
	Simulation	0.0	0.0	7.14	0.12
	Difference Δ	-4.83	0.16	4.41	0.35
Quadrant 4	WMAP5	-0.90	0.14	7.34	0.11
	Simulation	0.0	0.0	7.04	0.11
	Difference Δ	-0.90	0.14	2.08	0.53

Quadrant sky distribution of Q-W temperatures on 1-deg angular scale

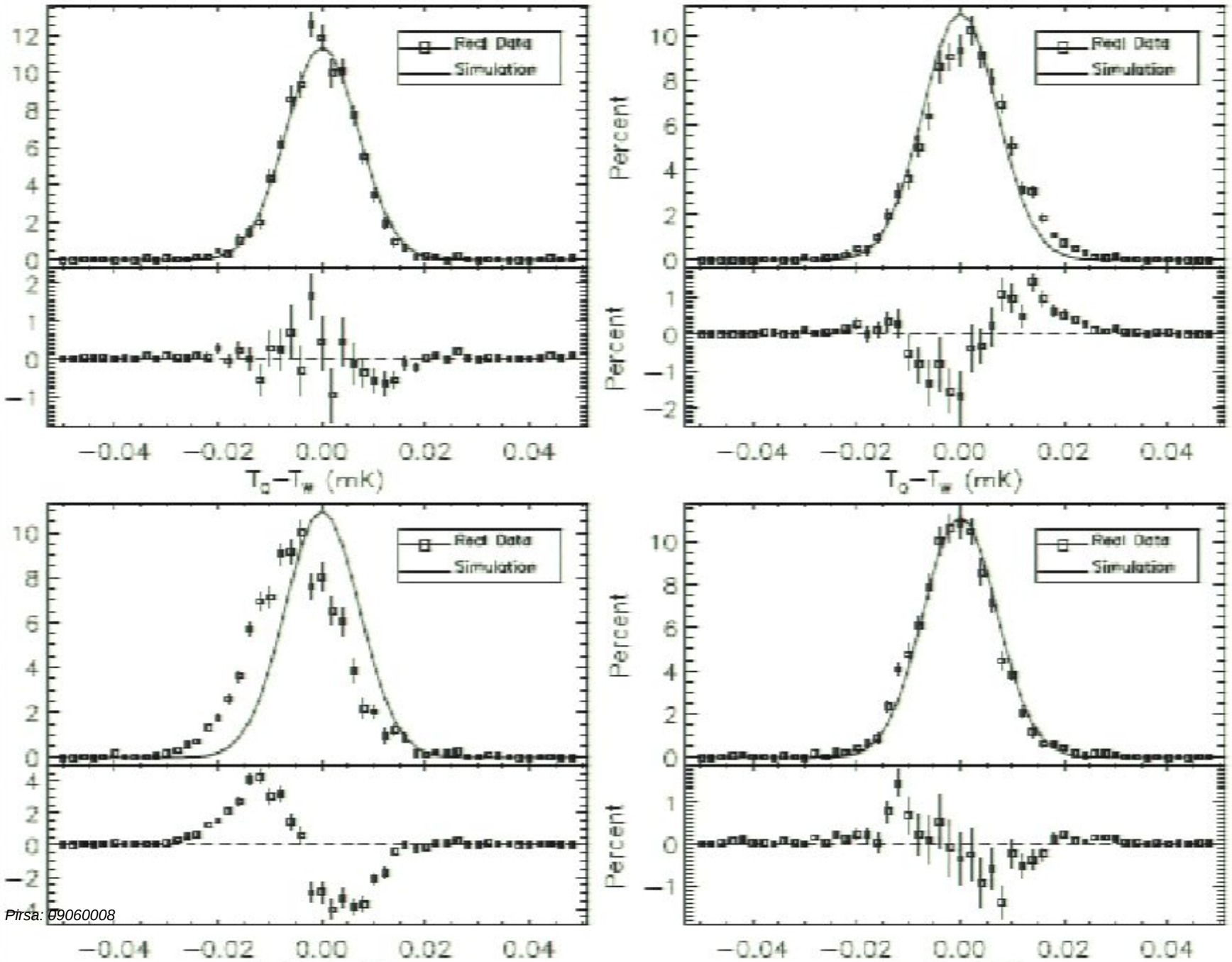

Distribution of 1 deg angular scale Q-W temperature: best gaussian fits

Q - W		μ (μK)	error (μK)	σ (μK)	error (μK)
Quadrant 1	WMAP5	1.00	0.15	8.17	0.13
	Simulation	0.0	0.0	7.11	0.12
	Difference Δ	1.00	0.15	4.02	0.33
Quadrant 2	WMAP5	-0.43	0.14	6.66	0.12
	Simulation	0.0	0.0	6.92	0.12
	Difference Δ	-0.43	0.14	-1.88*	0.59
Quadrant 3	WMAP5	-4.83	0.16	8.39	0.15
	Simulation	0.0	0.0	7.14	0.12
	Difference Δ	-4.83	0.16	4.41	0.35
Quadrant 4	WMAP5	-0.90	0.14	7.34	0.11
	Simulation	0.0	0.0	7.04	0.11
	Difference Δ	-0.90	0.14	2.08	0.53

Quadrant sky distribution of V-W temperatures on 1-deg angular scale

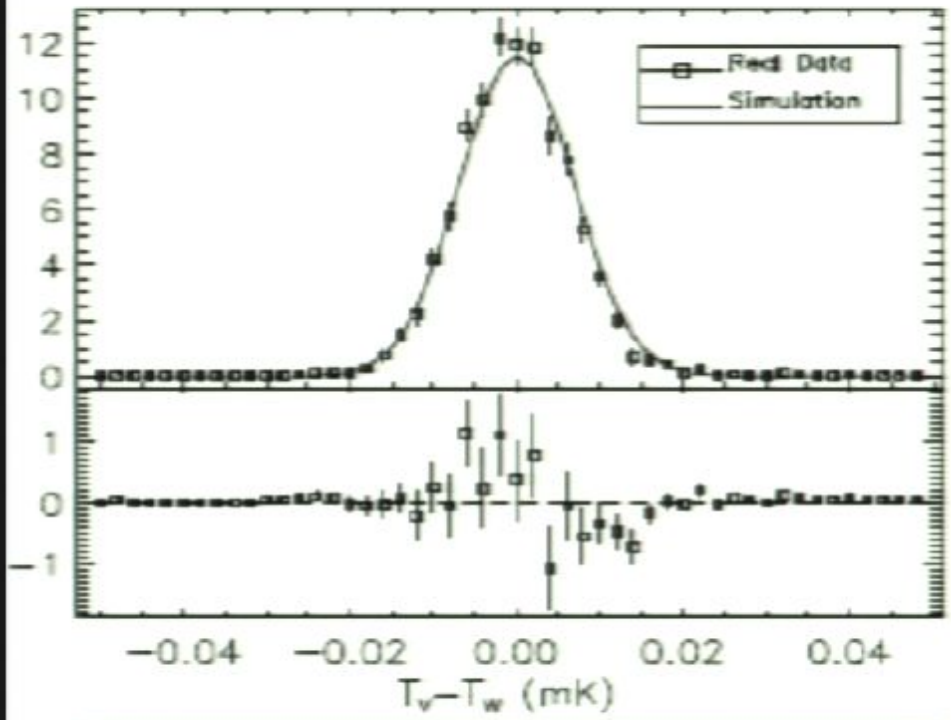

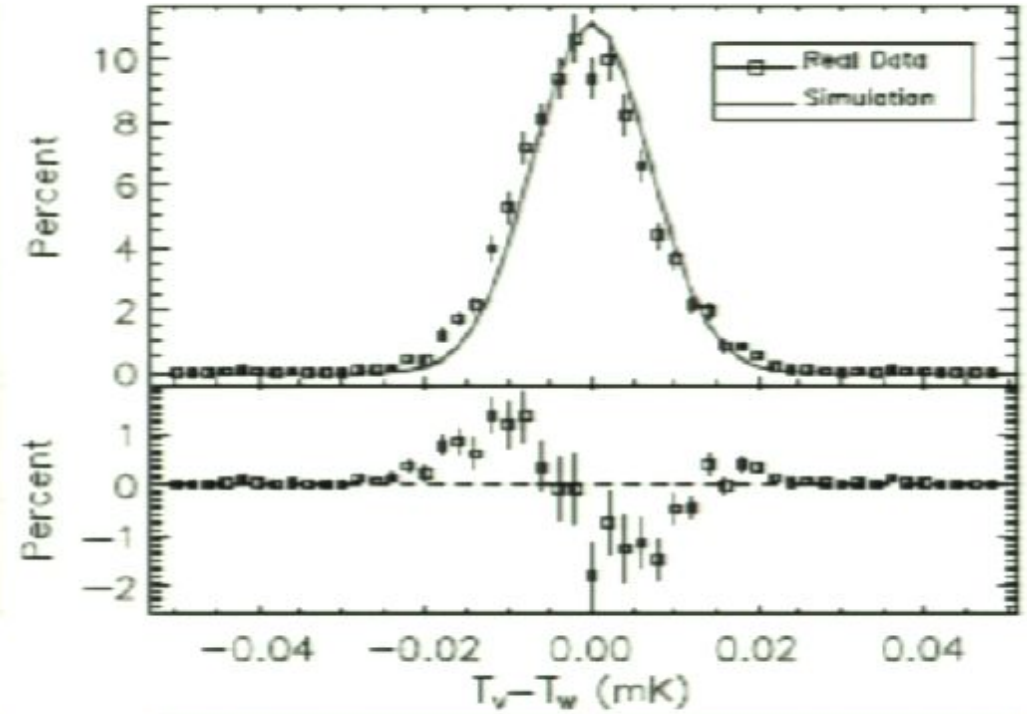

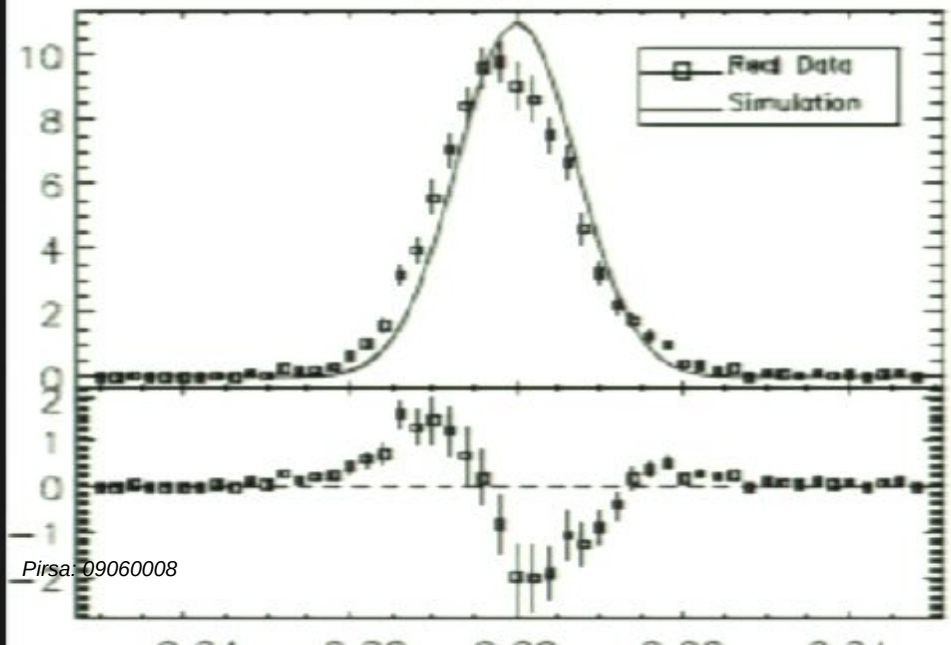

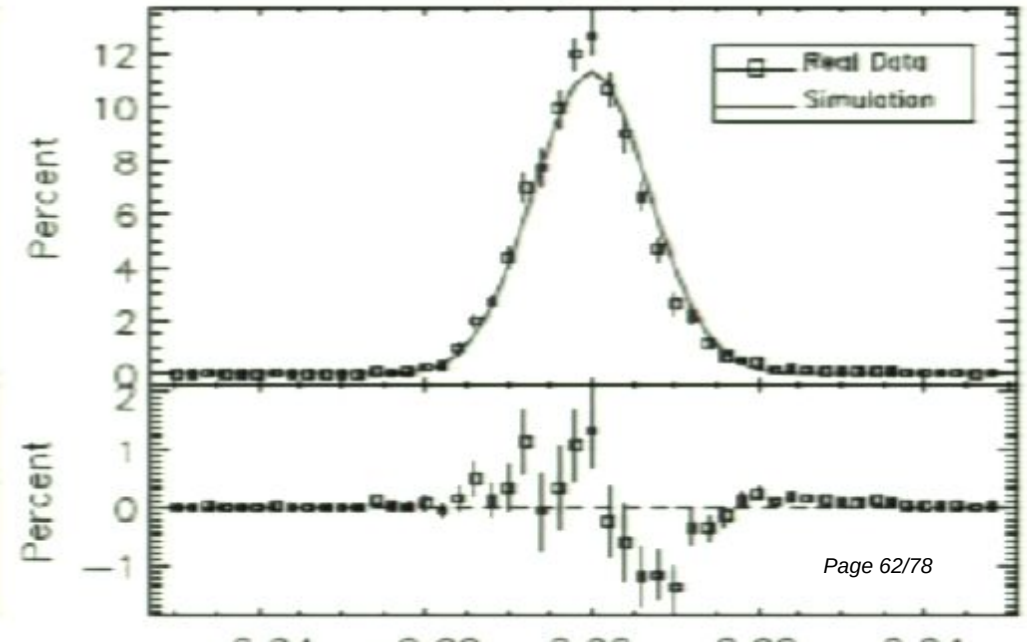

Distribution of 1 deg angular scale V-W temperature: best gaussian fits

V - W		$\mu(\mu K)$	error (μK)	$\sigma(\mu K)$	error (μK)
Quadrant 1	WMAP5	-1.11	0.15	7.90	0.13
	Simulation	0.0	0.0	7.04	0.12
	Difference Δ	-1.11	0.15	3.58	0.36
Quadrant 2	WMAP5	-0.40	0.14	6.53	0.11
	Simulation	0.0	0.0	6.83	0.12
	Difference Δ	-0.40	0.14	-2.00*	0.53
Quadrant 3	WMAP5	-1.23	0.16	8.25	0.13
	Simulation	0.0	0.0	7.09	0.12
	Difference Δ	-1.23	0.16	4.22	0.33
Quadrant 4	WMAP5	-0.73	0.14	6.79	0.11
	Simulation	0.0	0.0	6.94	0.11
	Difference Δ	-0.73	0.14	-1.44*	0.74

Quadrupole maps of Q-V (left),Q-W (right) & V-W (bottom)

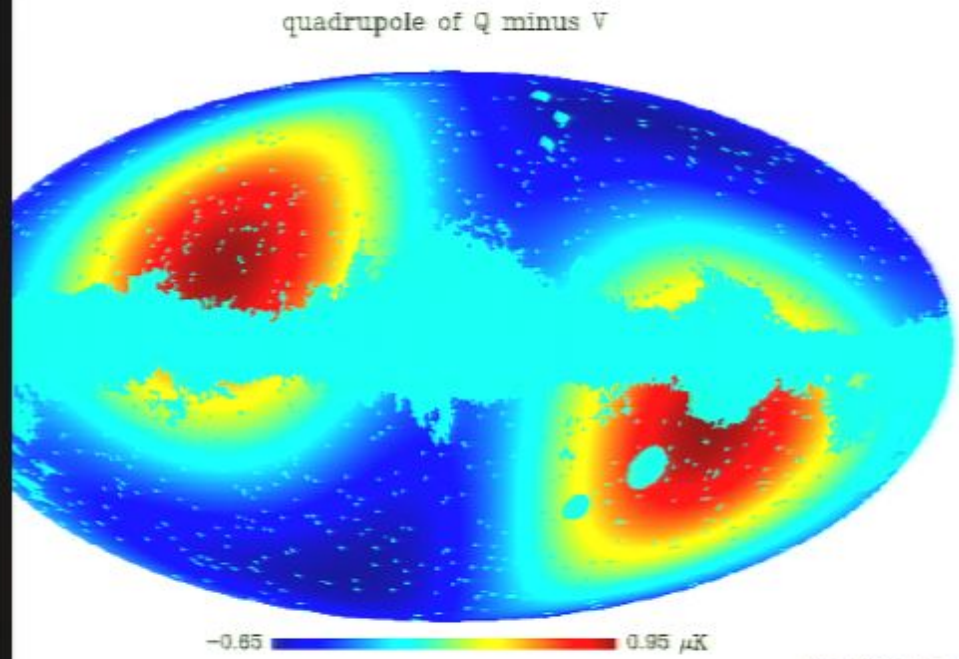

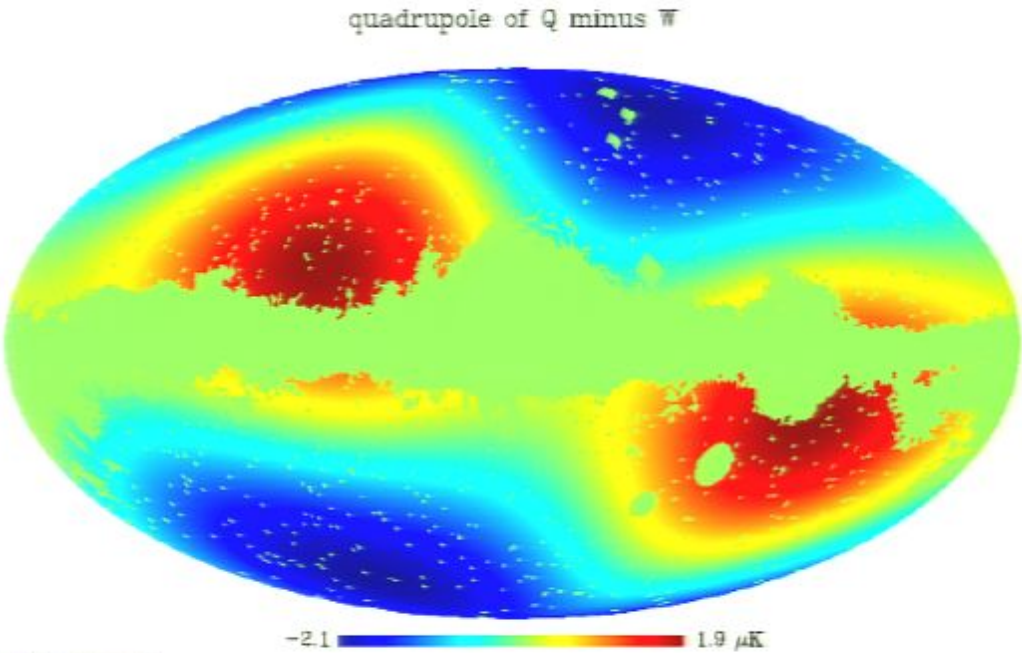

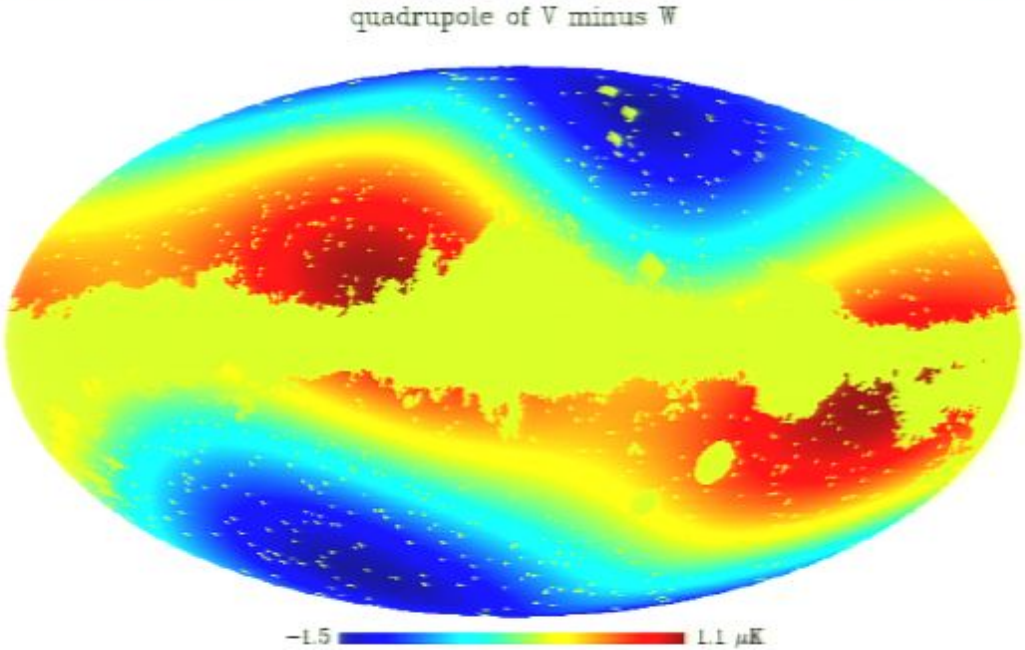

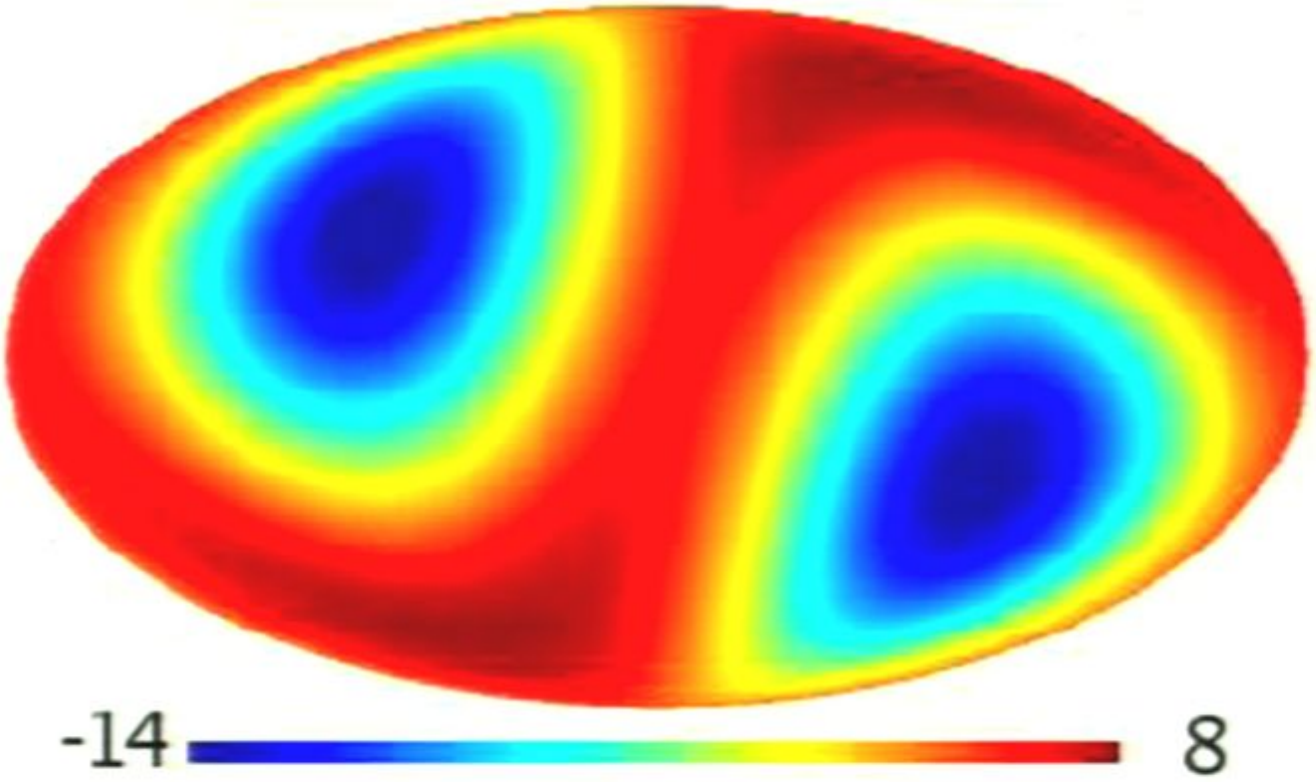

Dust emission model of Diego et al 2009

Quadrupole maps of Q-V (left),Q-W (right) & V-W (bottom)

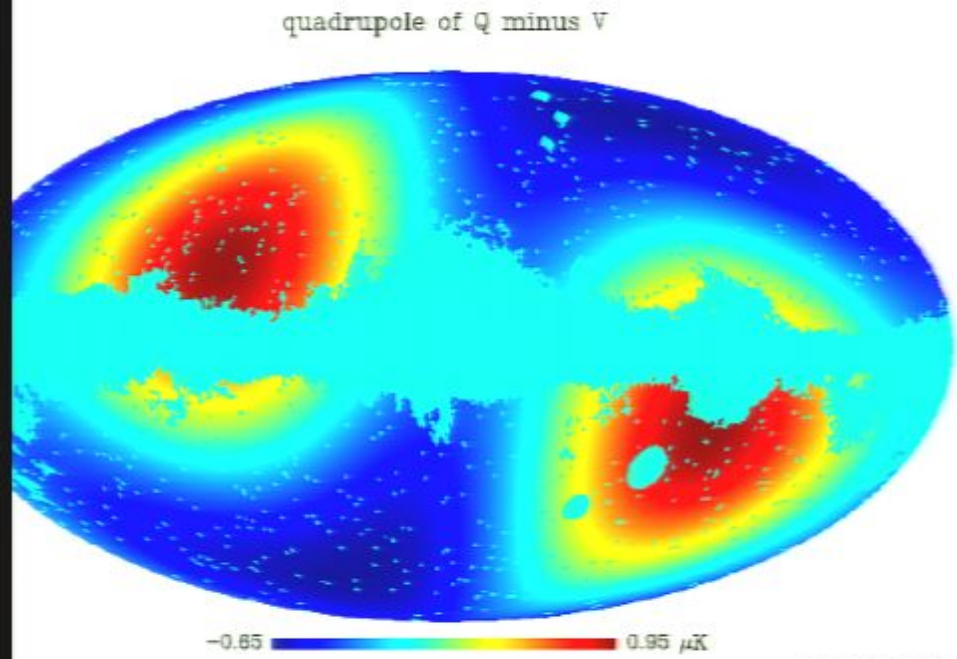

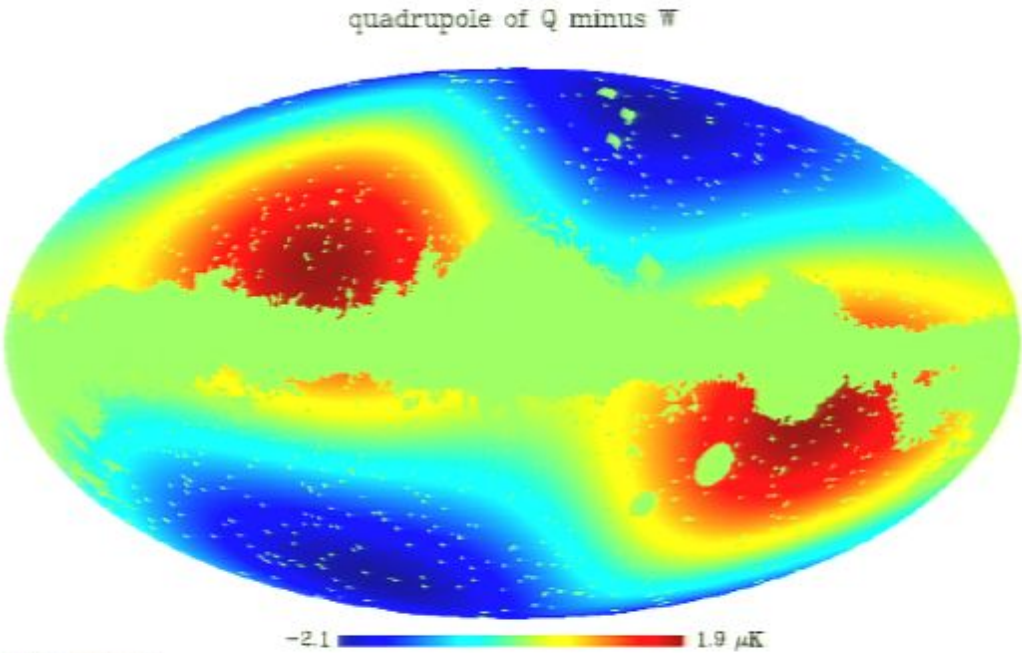

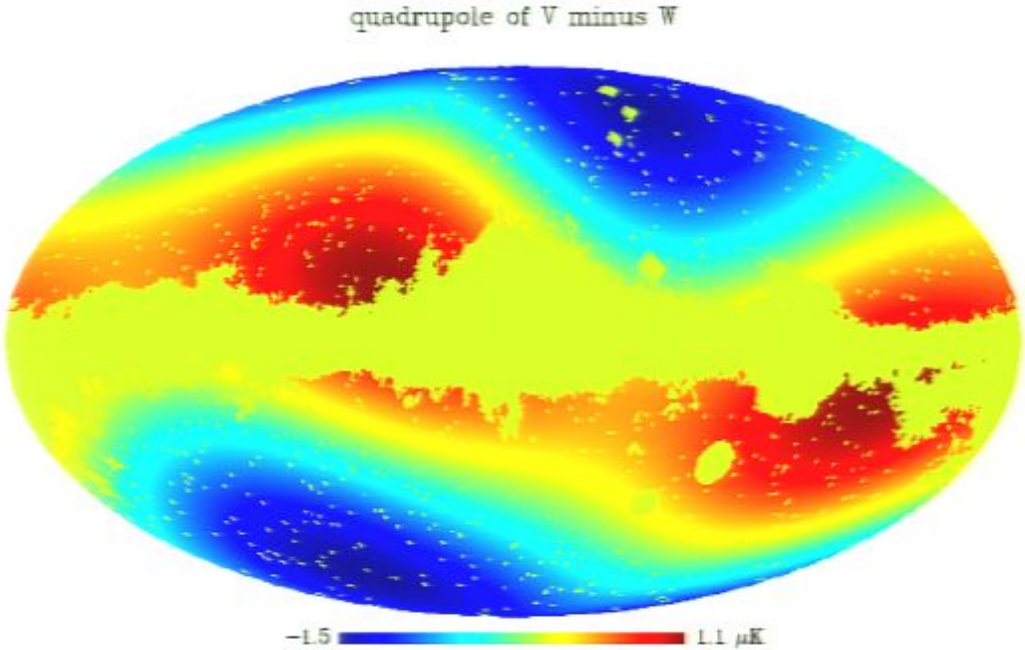

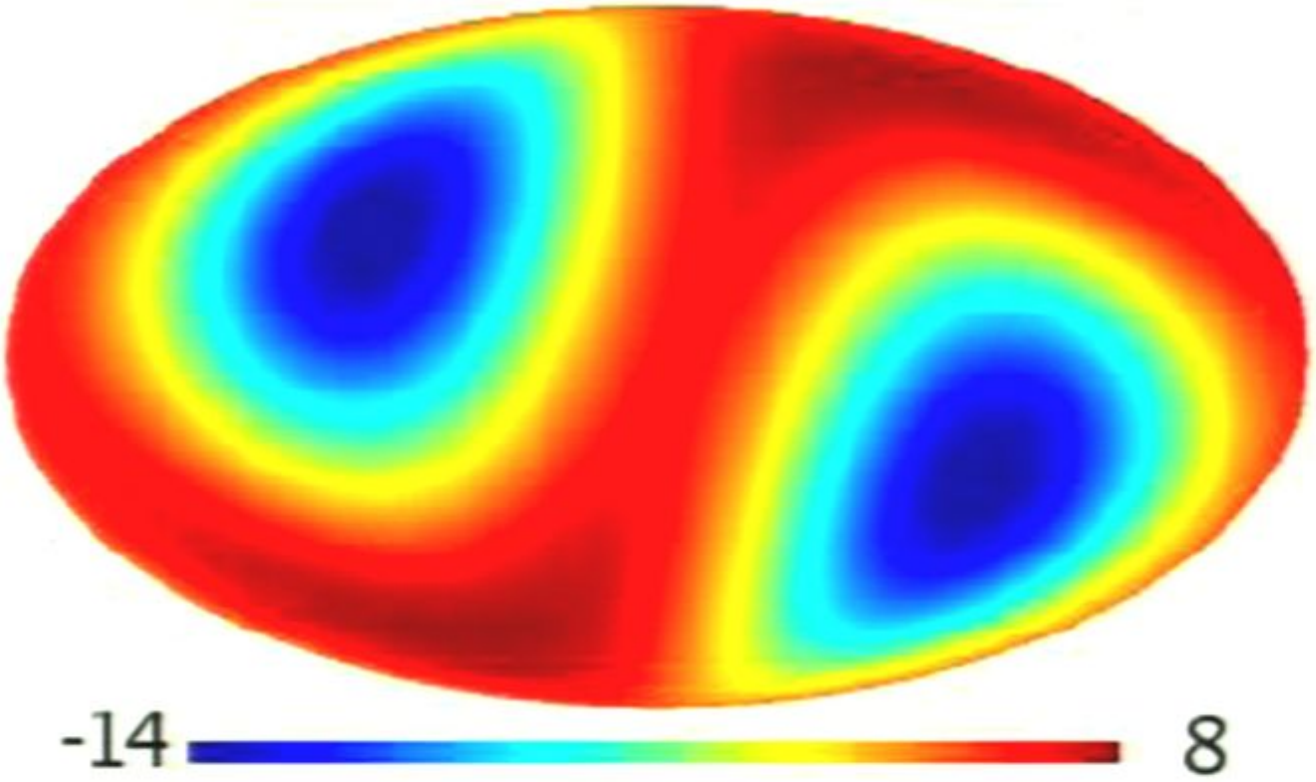

Dust emission model of Diego et al 2009

Quadrupole maps of Q-V (left),Q-W (right) & V-W (bottom)

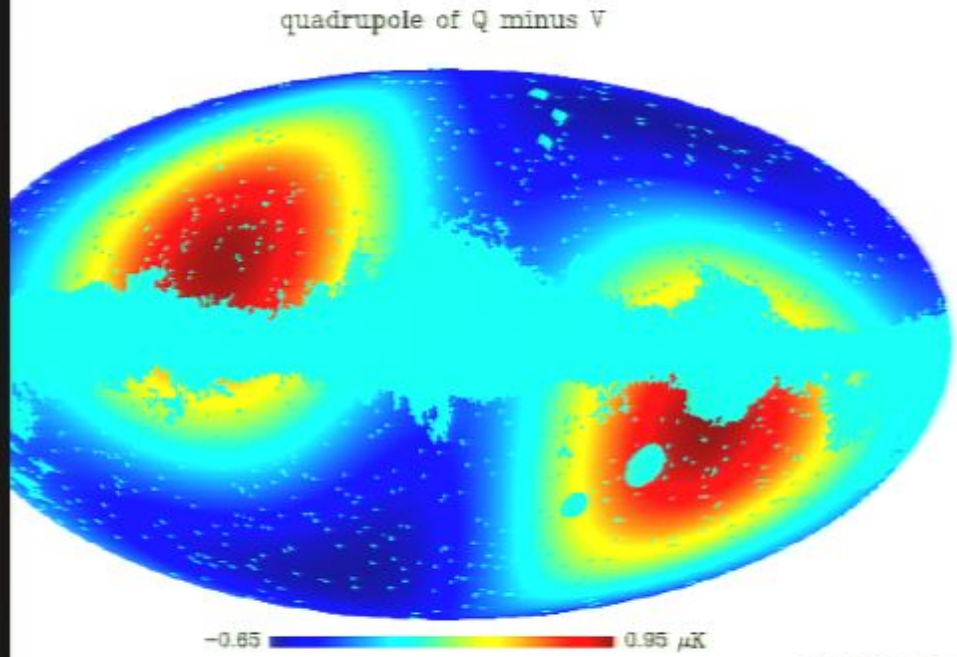

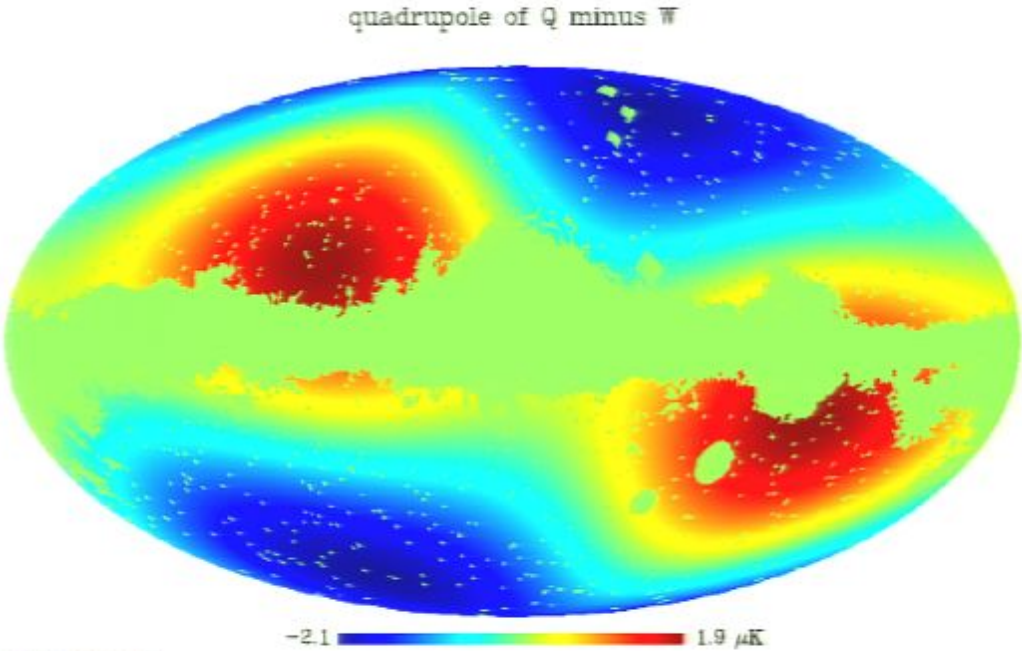

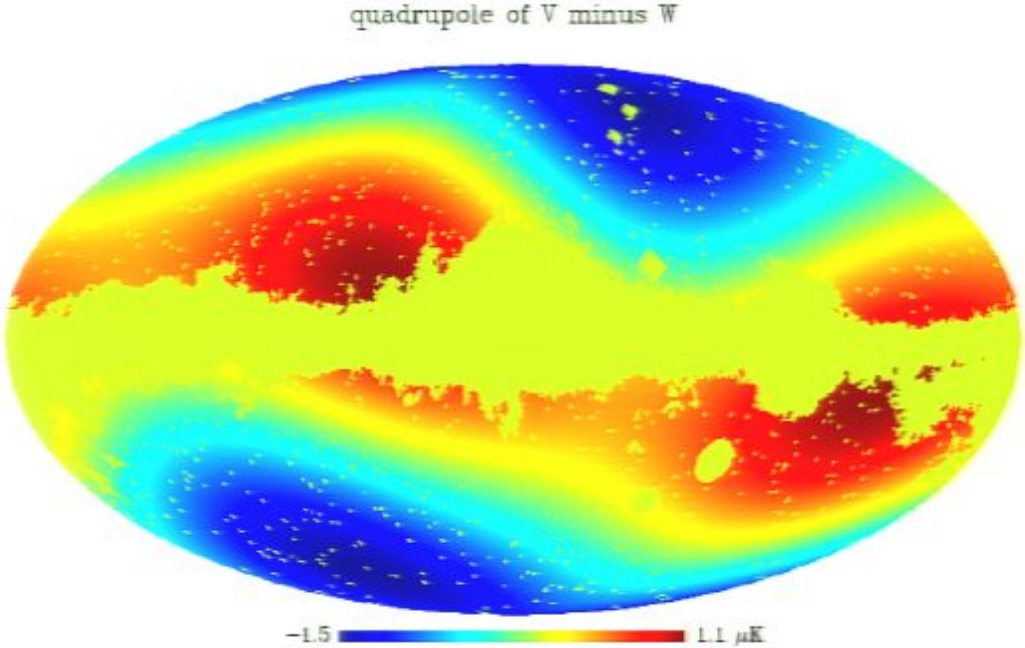

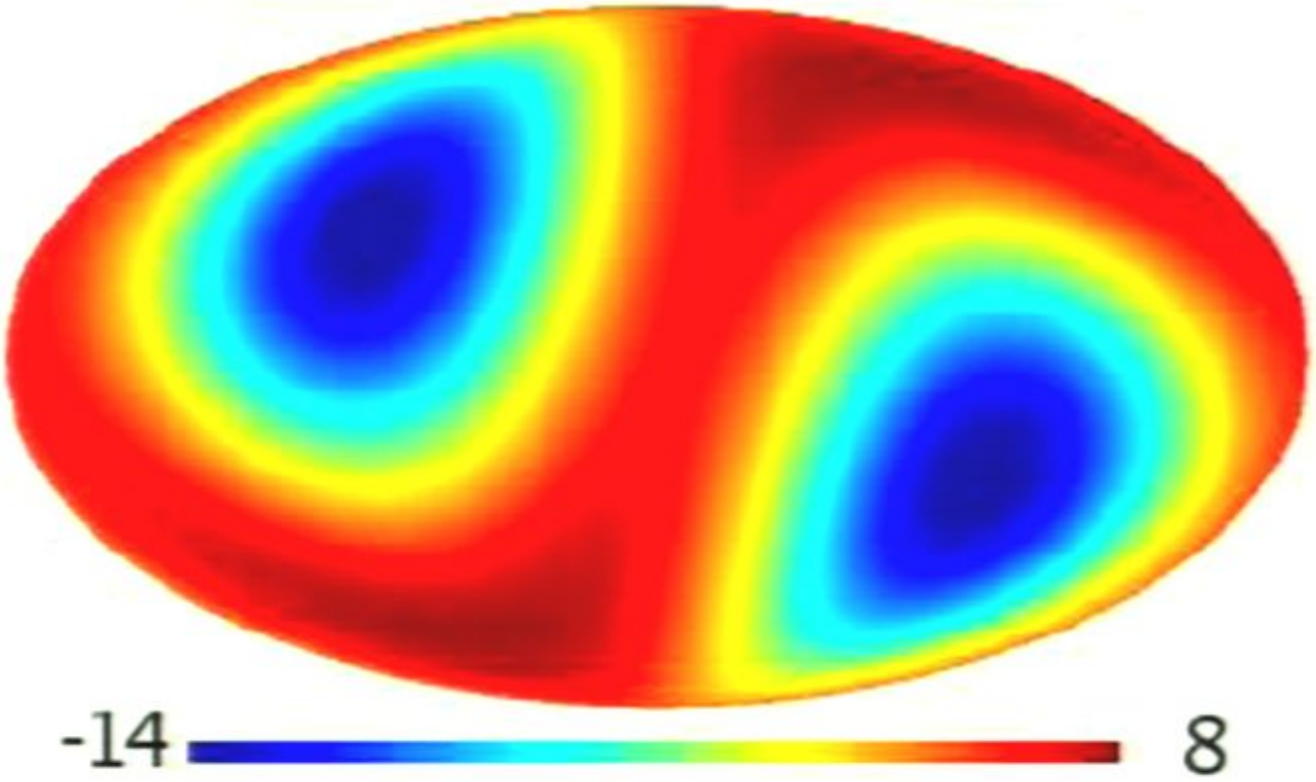

Dust emission model of Diego et al 2009

Quadrupole maps of Q-V (left),Q-W (right) & V-W (bottom)

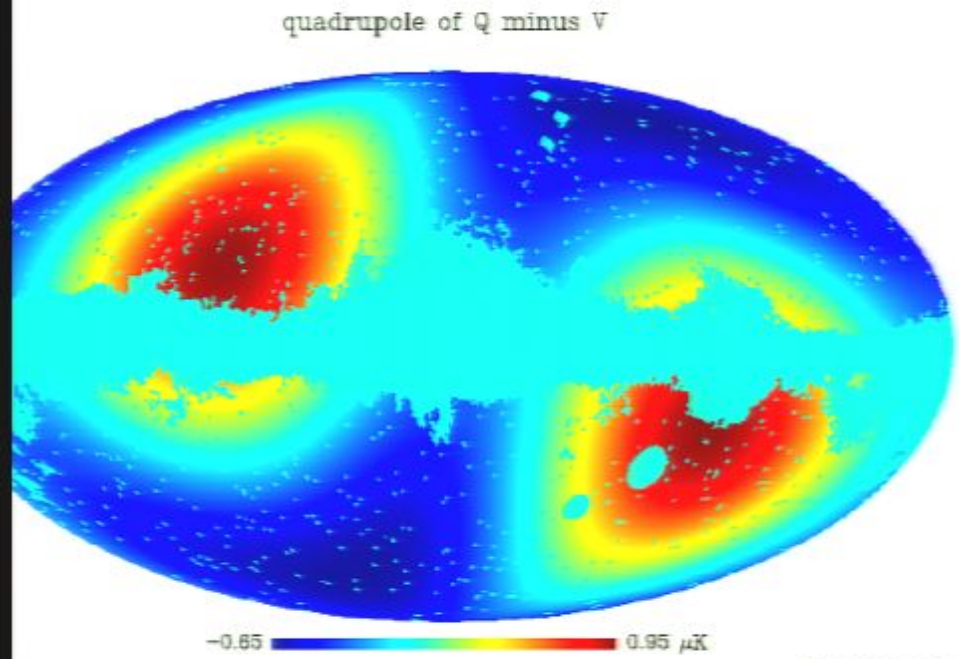

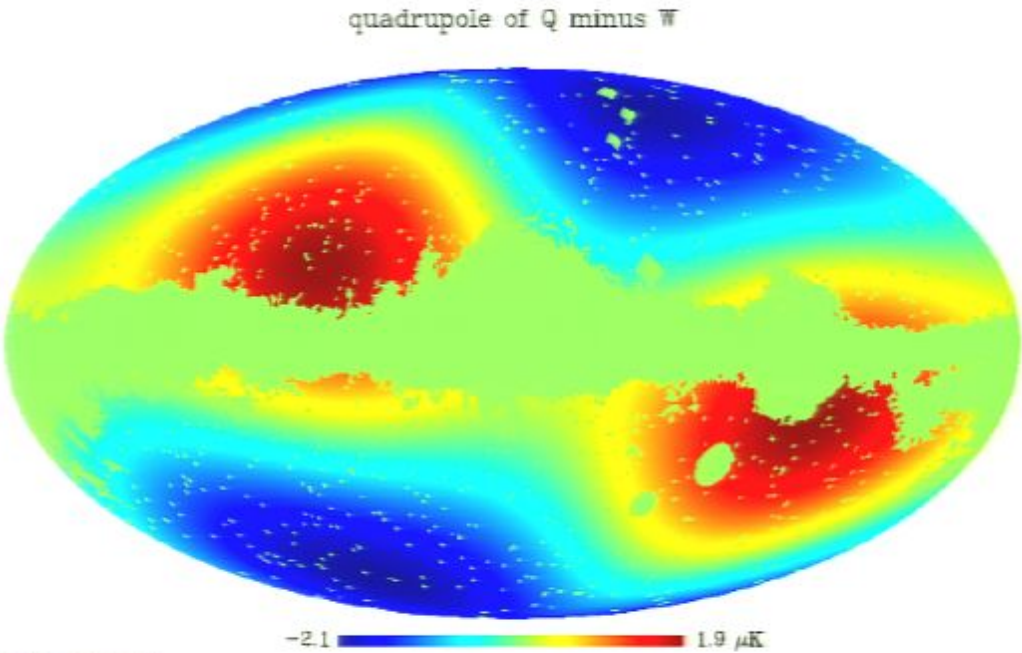

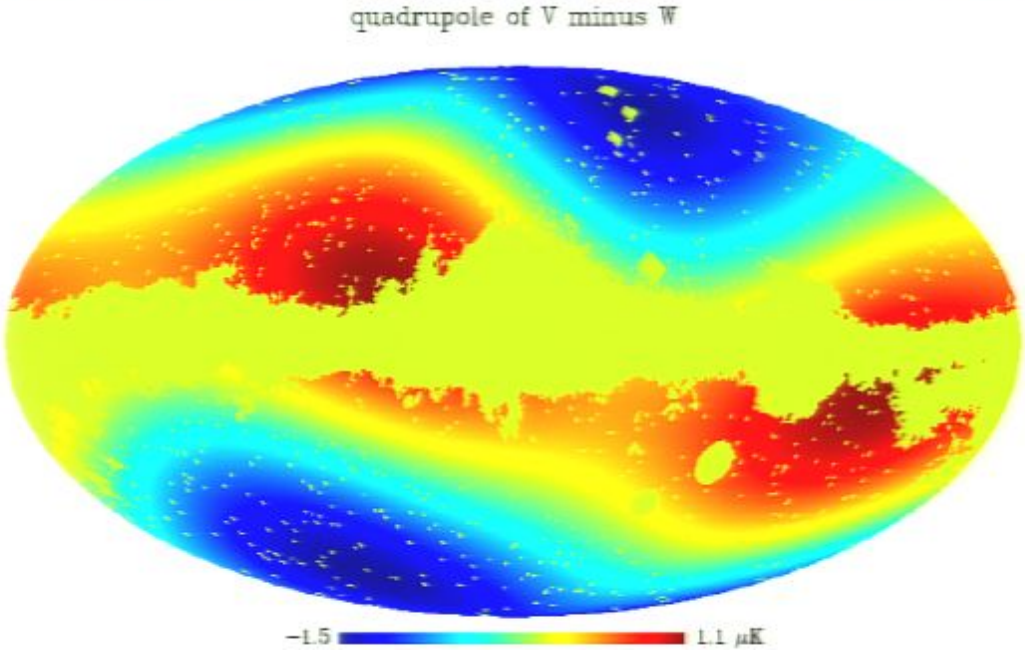

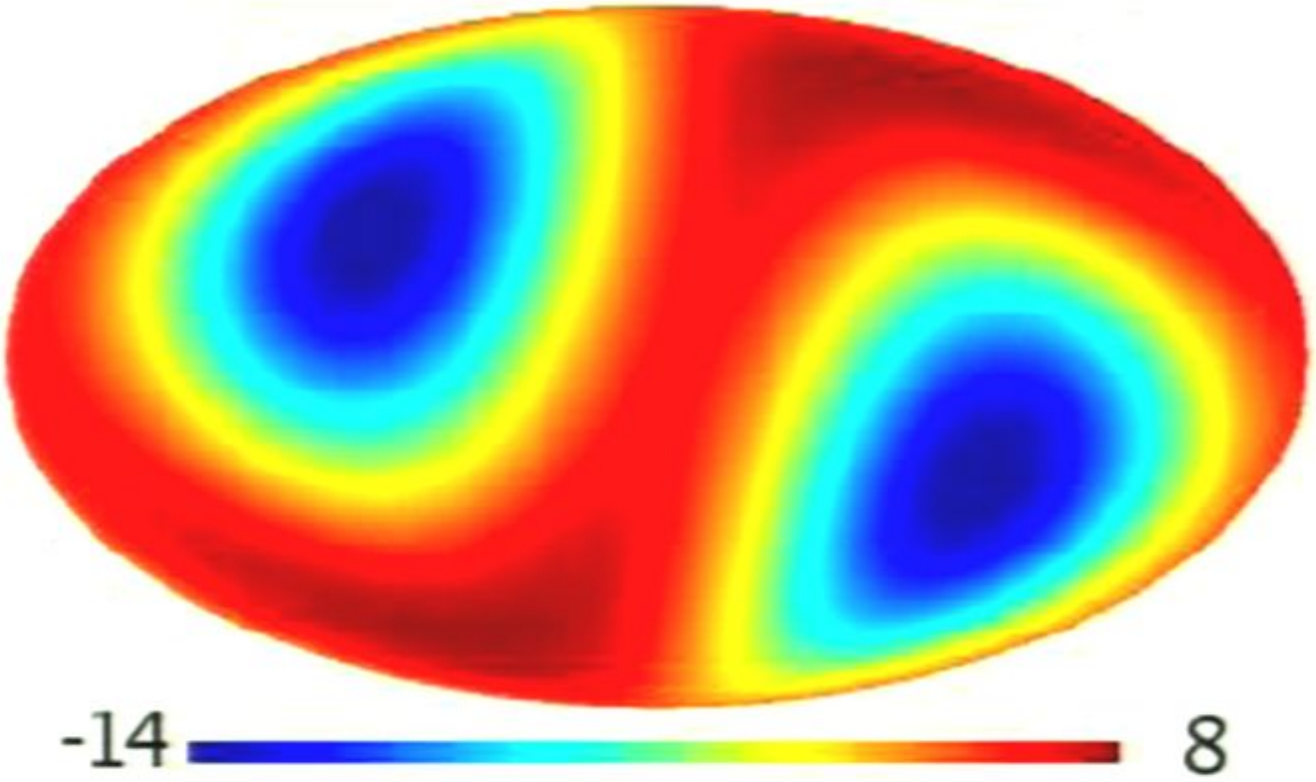

Dust emission model of Diego et al 2009

CONCLUSION

Two WMAP anomalies: the near absence of SZ effect and the presence of a few micro-K non-black body signal in the anisotropy

The first problem may be with the clusters of galaxies.

The 2nd problem affects all scales including the 1st acoustic peak. It only affects two sky quadrants. The ecliptic plane is in these quadrants.

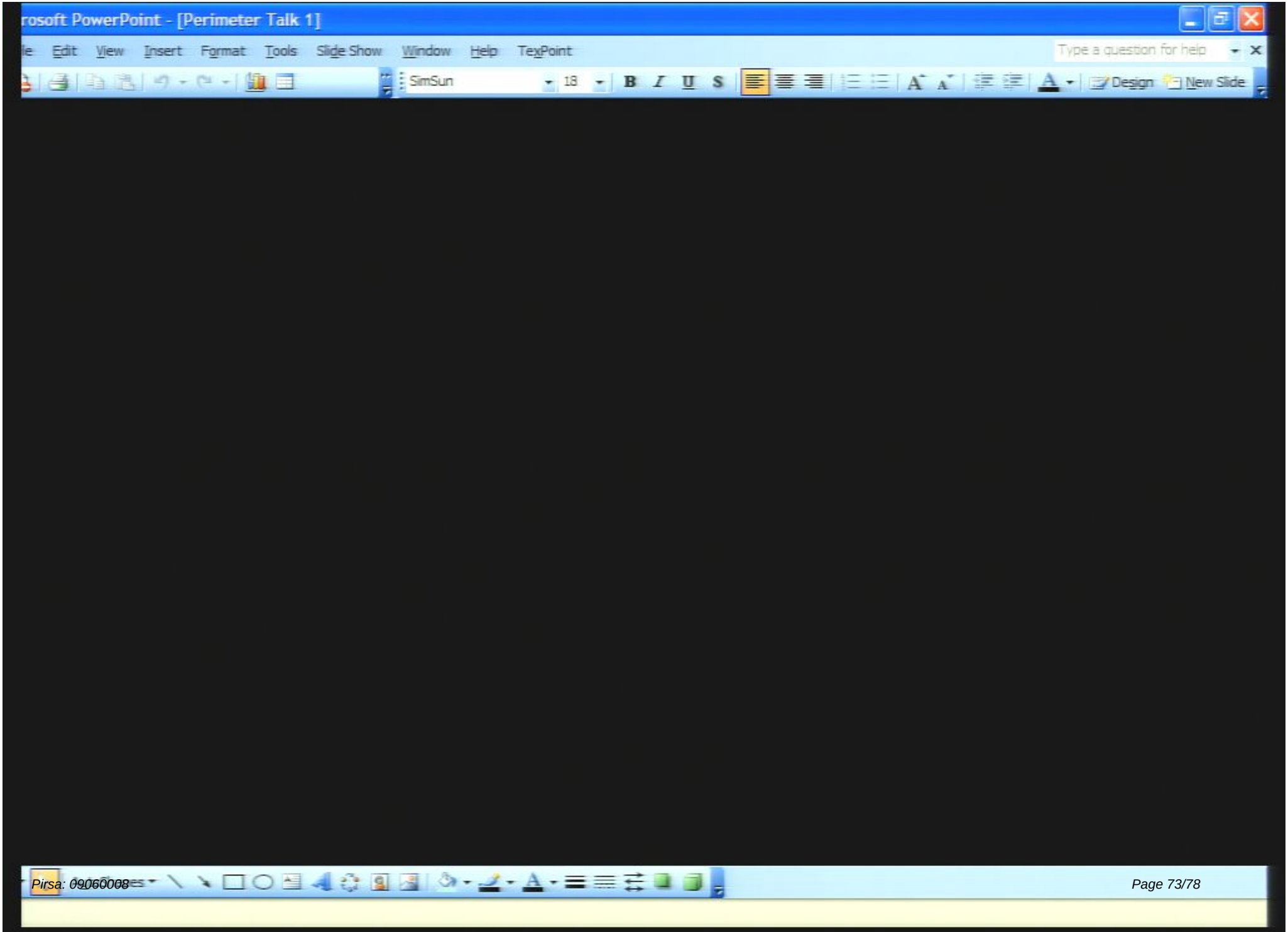
rosoft PowerPoint - [Perimeter Talk 1]
Edit View Insert Format Tools Slide Show Window Help TexPoint
Type a question for help
SimSun
18
Design
New Slide

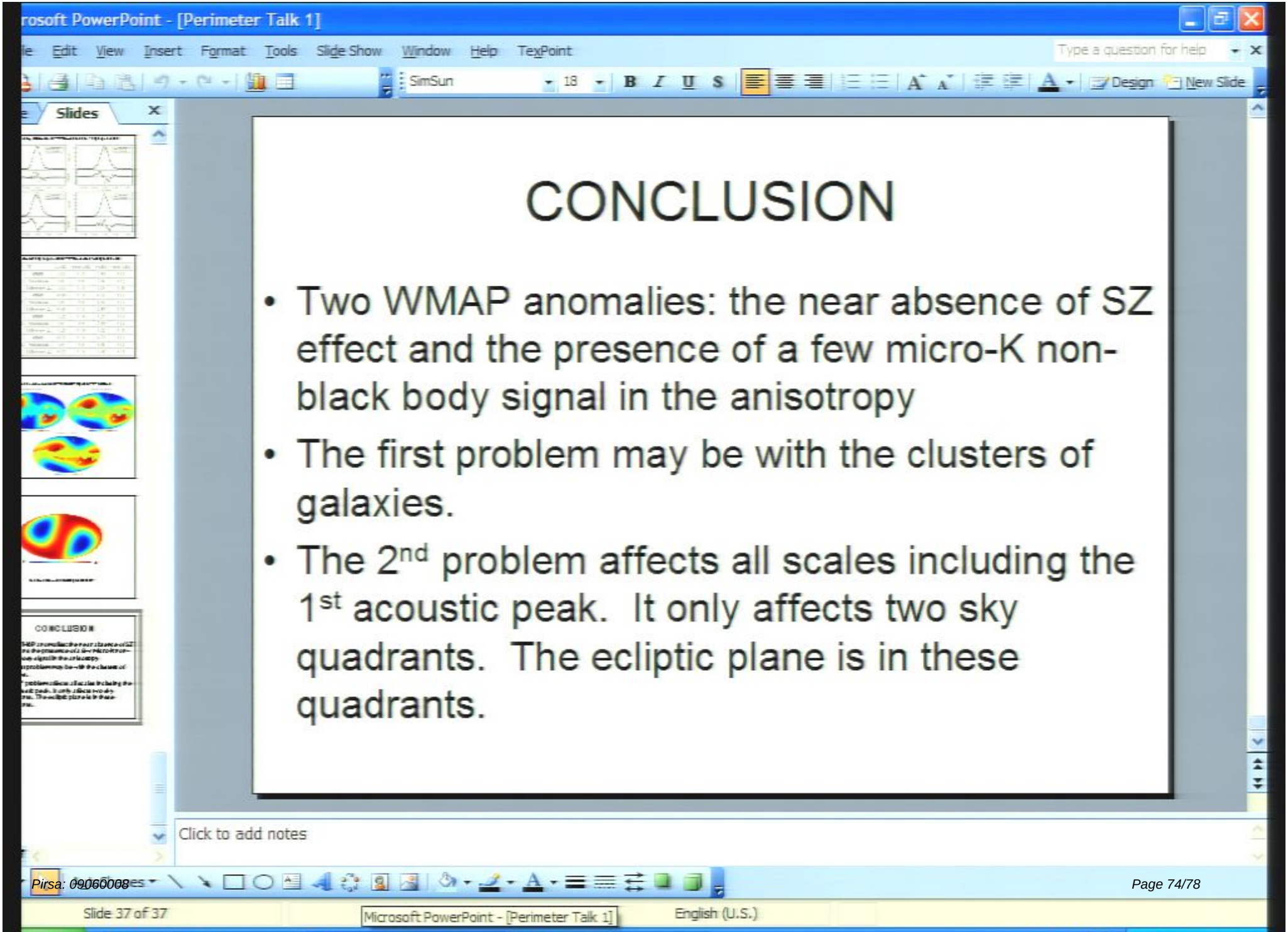
rosoft PowerPoint - [Perimeter Talk 1]
Edit View Insert Format Tools Slide Show Window Help TexPoint
Type a question for help
SimSun 18
Design New Slide
Slides
CONCLUSION
• Two WMAP anomalies: the near absence of SZ effect and the presence of a few micro-K non-black body signal in the anisotropy
• The first problem may be with the clusters of galaxies.
• The 2nd problem affects all scales including the 1st acoustic peak. It only affects two sky quadrants. The ecliptic plane is in these quadrants.
Click to add notes
Slide 37 of 37
Microsoft PowerPoint - [Perimeter Talk 1]
English (U.S.)

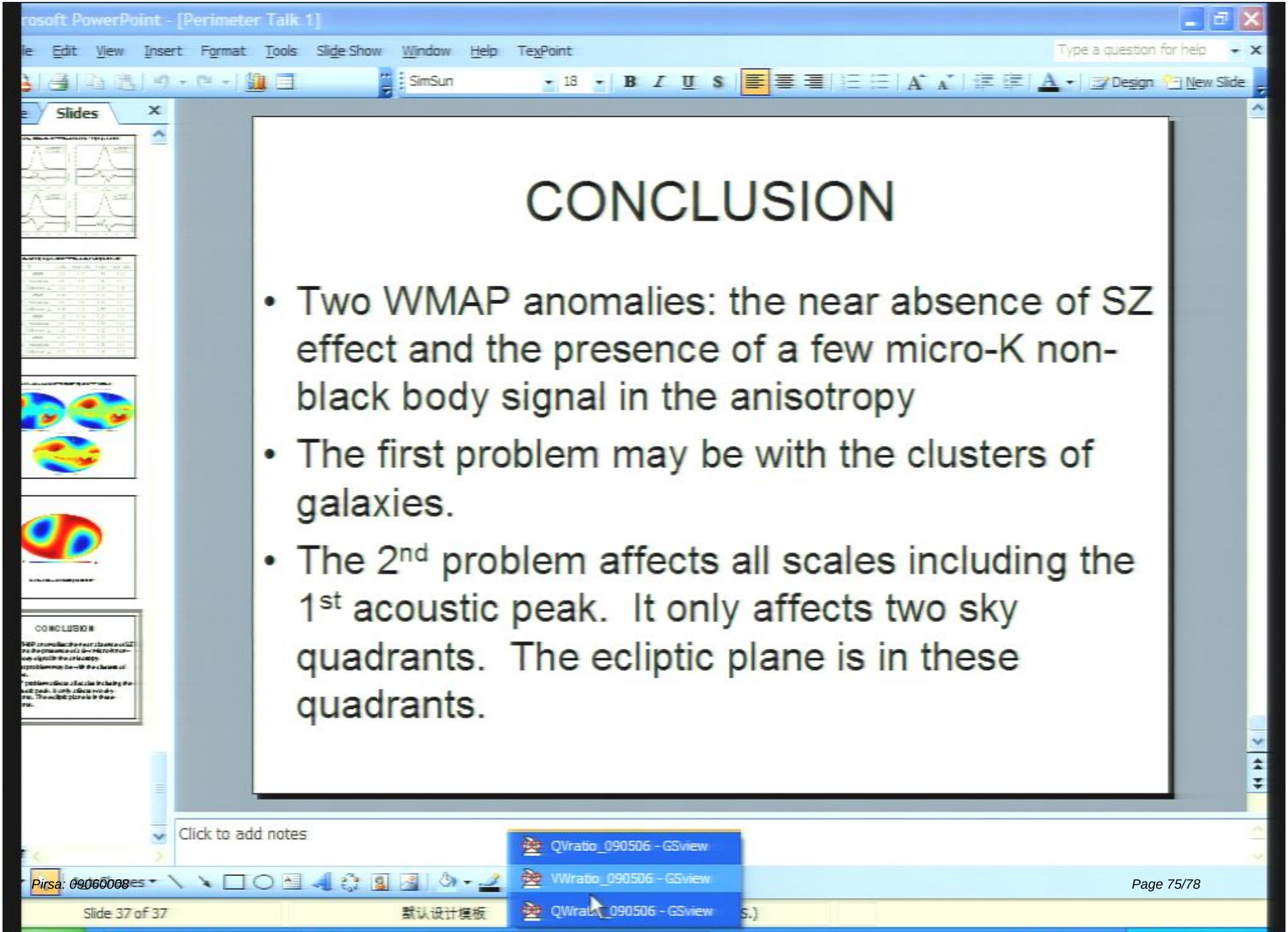
rosoft PowerPoint - [Perimeter Talk 1]
Edit View Insert Format Tools Slide Show Window Help TexPoint
Type a question for help
SimSun 18
Design New Slide
Slides
CONCLUSION
• Two WMAP anomalies: the near absence of SZ effect and the presence of a few micro-K non-black body signal in the anisotropy
• The first problem may be with the clusters of galaxies.
• The 2nd problem affects all scales including the 1st acoustic peak. It only affects two sky quadrants. The ecliptic plane is in these quadrants.
Click to add notes
QVratio_090506 - GSview
VWratio_090506 - GSview
QWratio_090506 - GSview
Slide 37 of 37
默认设计模板

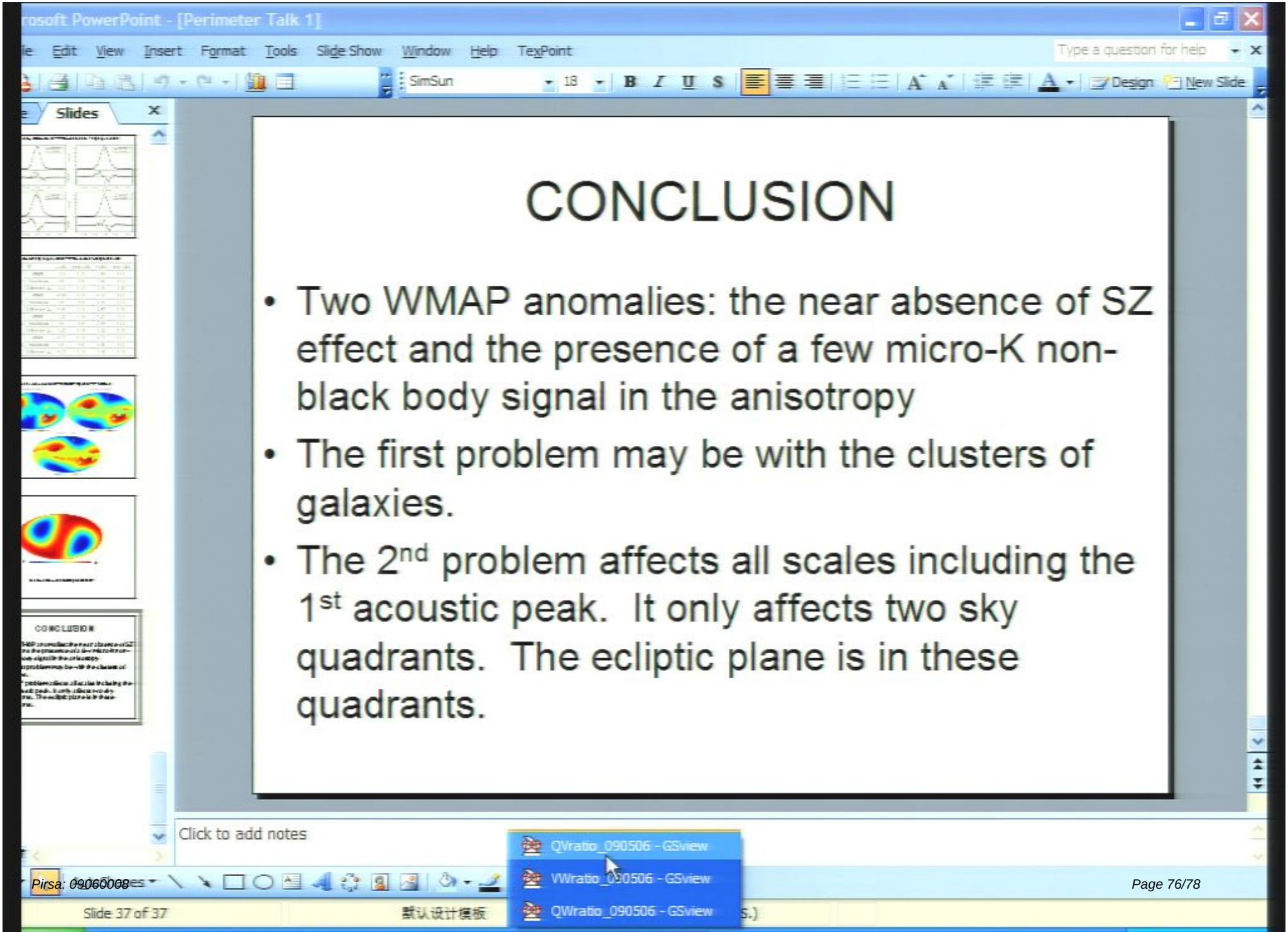
Microsoft PowerPoint - [Perimeter Talk 1]
File Edit View Insert Format Tools Slide Show Window Help TexPoint
Type a question for help
SimSun 18
Design New Slide
Slides
CONCLUSION
• Two WMAP anomalies: the near absence of SZ effect and the presence of a few micro-K non-black body signal in the anisotropy
• The first problem may be with the clusters of galaxies.
• The 2nd problem affects all scales including the 1st acoustic peak. It only affects two sky quadrants. The ecliptic plane is in these quadrants.
Click to add notes
QVratio_090506 - GSview
VWratio_090506 - GSview
QWratio_090506 - GSview
Slide 37 of 37
默认设计模板

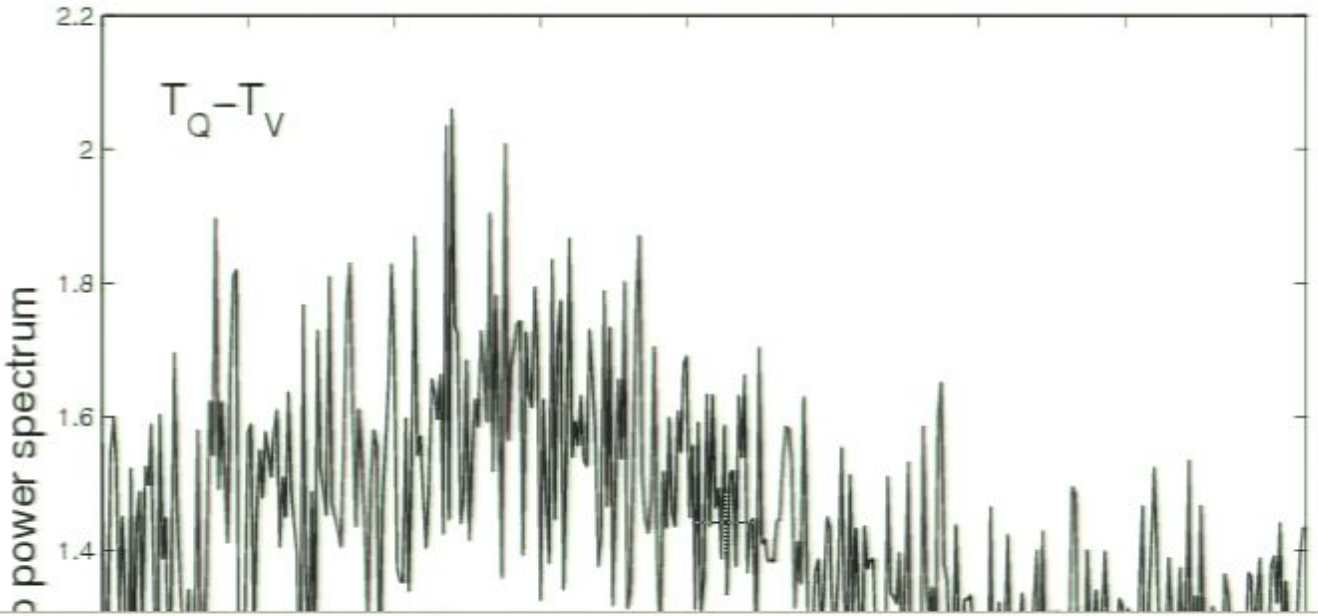
2.2
2
1.8
1.6
1.4
$T_Q - T_V$
power spectrum

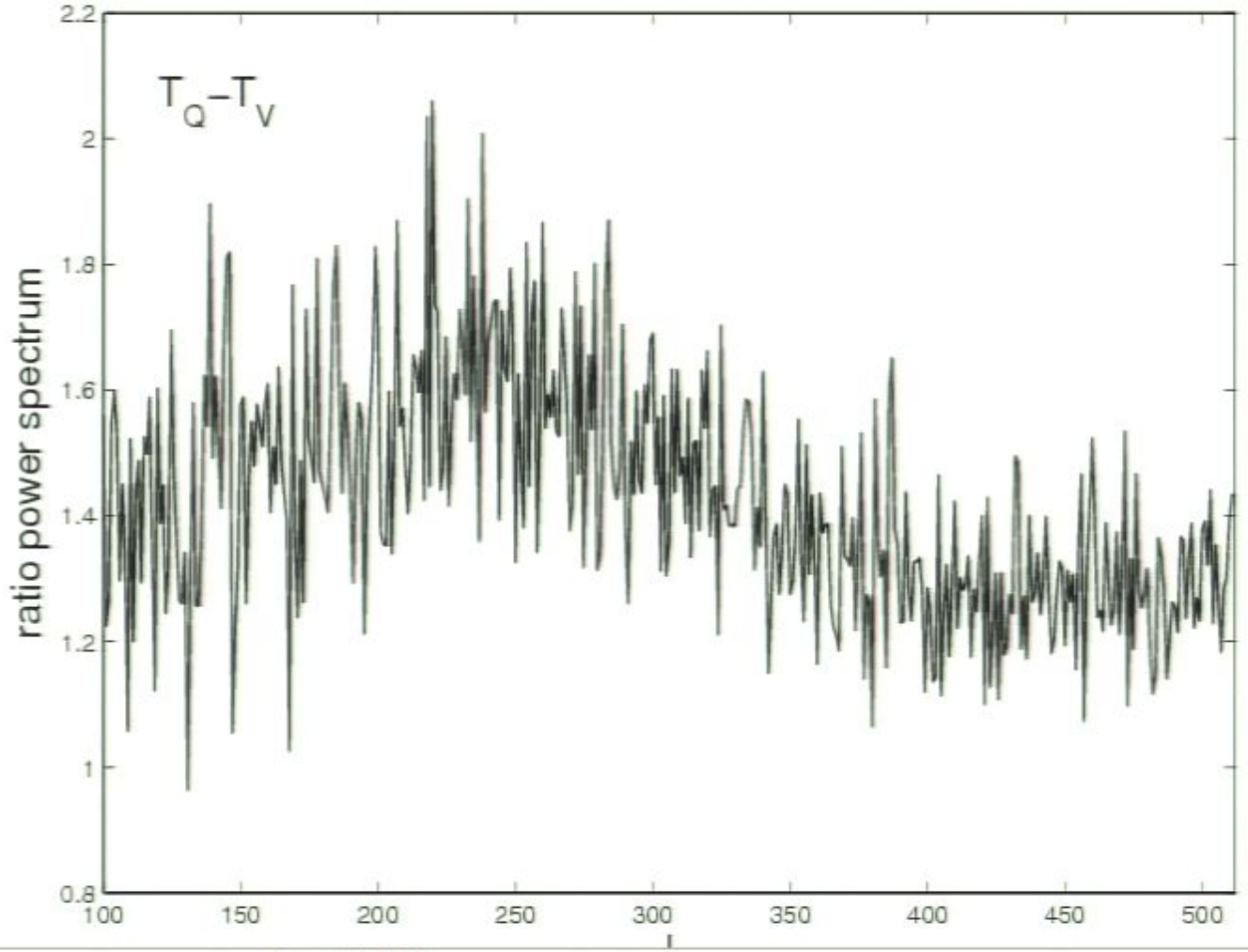
$T_Q - T_V$
ratio power spectrum
2.2
2
1.8
1.6
1.4
1.2
1
0.8
100
150
200
250
300
350
400
450
500